2010

ELECTROSPRAY IONIZATION MASS SPECTROMETRY FOR THE CHARACTERIZATION OF COVALENT AND NONCOVALENT POLYNUCLEAR PLATINUM COMPOUNDS INTERACTING WITH BIO-MOLECULES

John Mangrum
Virginia Commonwealth University

College of Humanities and Sciences

Virginia Commonwealth University

This is to certify that the Dissertation prepared by John Bradley Mangrum entitled "Electrospray Ionization Mass Spectrometry for the Characterization of Covalent and Noncovalent Polynuclear Platinum Compounds Interacting with Bio-Molecules" has been approved by his committee as satisfactory completion of the dissertation requirement for the degree of Doctor of Philosophy

_____

Dr. Nicholas P. Farrell, Research Director, College of Humanities and Science

_____

Dr. Everett E. Carpenter, Committee Chairman, College of Humanities and Science

_____

Dr. Scott Gronert, Committee Member, College of Humanities and Science

_____

Dr. Vladimir A. Sidorov, Committee Member, College of Humanities and Science

_____

Dr. Robert M. Tombes, Committee Member, College of Humanities and Science

_____

Dr. Scott Gronert, Department Chairman, College of Humanities and Science

_____

Dr. Fred M. Hawkridge, Dean, College of Humanities and Science

_____

Dr. Douglas F. Boudinot, Dean of Graduate Studies

_____

Date

Electrospray Ionization Mass Spectrometry for the Characterization of Covalent and Noncovalent Polynuclear Platinum Compounds Interacting with Bio-Molecules

A dissertation submitted in partial fulfillment of the requirements for the degree of Doctor of Philosophy at Virginia Commonwealth University

By
John Bradley Mangrum
B.S., Longwood University, Farmville, Virginia
May, 2000

Director: Dr. Nicholas P. Farrell
Professor
Department of Chemistry

Virginia Commonwealth University
Richmond, Virginia

March 15, 2010

Acknowledgments

I would like to thank my advisor, Dr. Nicholas P. Farrell, for his guidance and support during my graduate research. I want to thank him for taking the time to listen to my numerous research ideas, no matter how far off course they might have taken me. His dedication in the field of cancer research is motivational and inspiring.

I want to express my sincere thanks to the entire Farrell research group, both past and present, for their support and friendship. We all joined the group with one commonality, that being a genuine interest in research to cure cancer. It has been a pleasure and I cannot think of a group of more motivated and talented individuals to have been a part of.

I would like to thank the members of my committee: Dr. Carpenter, Dr. Gronert, Dr. Sidorov, and Dr. Tombes, for their continued support and helpful insights in guiding me along in my research endeavors.

A very special thank you is needed for the entire office staff. You often do not get the recognition you deserve, but without you, this place would cease to function. A heartfelt thank you goes to Rinnie Brown. I have enjoyed all the coffee sessions that turn into half hour conversations that start with, "you know what else is wrong with….." Thanks to Dr. Fenn for anecdotes on life during our drive home.

I gratefully acknowledge my parents Roger and Cathy Mangrum for their continued support and guidance throughout my education. They continue to inspire me each day in search of my goals. I would also like to thank my brother Tracy, for his support and those random late night phone calls. To my Grandmother, thank you for being such a special part of my life. Also, thank you to all my friends and family members for all they have done over the years.

I would not be at this point in my life if it were not for the love and support of Monica Atkinson. She has constantly been my biggest supporter in everything I do. I look forward to spending the rest of our lives together and this dissertation is dedicated to her.

Table of Contents

List of Figures

List of Schemes

List of Abbreviations and Symbols

µL	microliter
µm	micrometer
A	adenine (nucleobase)
Å	angstrom
Bo	field strength of magnet in Tesla
bp	base pair
C	cytosine (nucleobase)
C	coulombs
°C	degrees Celsius
C	coding strand
c,c	cis,cis
CD	circular dichroism
$CE_{50\%}$	collision energy for 50% dissociation
CID	collision induced dissociation
cm	centimeter
CPPS	cell penetrating peptide
CRM	charge residue model
Da	dalton
DC	direct current
DDD	Dickerson-Drew Dodecamer
DLT	dose limiting toxicity
DNA	Dideoxyribonucleic Acid
DPPA	1,2-dipalmitoyl-sn-glycero-3-phosphate
DPPS	1,2-dipalmitoyl-sn-glycero-3-phospho-L-serine
ds	double stranded DNA
e	charge of an electron
E_{com}	Kinetic energy
E_{lab}	kinetic energy lab frame of reference
ESI	elctrospray ionization
eV	electron volt
FTICR-MS	Fourier transform ion cyclotron resonance mass spectrometry
FWHM	full width half maximum
G	guanine (nucleobase)
GAG	glycosaminoglycan
HSA	human serum albumin
HMG	high mobility group
HS	heparan sulfate
HSPG	heparan sulfate proteoglycan
ID	inner diameter
Ids	intensity of double stranded DNA
IEM	ion evaporation model

Iss	intensity of single stranded DNA
ITC	isothermal calorimetry
k	Boltzman constant
kb	kilobase
kDa	kilodalton
kHz	kilohertz
kV	kilovolt
Leff	Effective length of flight tube
M	molar
m/z	mass-to-charge ratio
mc	mass of collision gas
m_i	mass of an ion
min	minute
mM	millimolar
mm	millimeter
MS	mass spectrometry
ms	milliseconds
MS/MS	tandem mass spectrometry
MWCO	molecular weight cut off
NC	noncoding strand
NMR	nuclear magnetic resonance
OD	outer diameter
PCR	polymerase chain reaction
PNA	peptide nucleic acid
ppm	parts per million
QTOF-MS	quadrupole time of flight mass spectrometer
r.f.	radio frequency
r-excite	excitation radius
ss	single stranded DNA
STR	short tandem repeat
T	thymine (nucleobase)
t	time
t_m	melting temperature
t,t	trans,trans
v	velocity of an ion
vc	cyclotron motion
vp-p	voltage peak to peak
z	charge of an ion

Abstract

ELECTROSPRAY IONIZATION MASS SPECTROMETRY FOR THE CHARACTERIZATION OF COVALENT AND NONCOVALENT POLYNUCLEAR PLATINUM COMPOUNDS INTERACTING WITH BIO-MOLECULES

By
John B. Mangrum, Ph.D.

A dissertation submitted in partial fulfillment of the requirements for the degree of Doctor of Philosophy at Virginia Commonwealth University

Virginia Commonwealth University, 2010

Director: Dr. Nicholas P. Farrell
Professor
Department of Chemistry

Polynuclear platinum compounds represent a new class of potential platinum anticancer therapeutics. Derived from the most widely used platinum anticancer drug, cisplatin, these novel compounds are distinct in their interactions with bio-molecules. The effectiveness of platinum anticancer agents is influenced by three pharmacological factors: (i) their resistance to deactivating sulfur nucleophiles, (ii) the ability to gain cellular entry and efficient cellular uptake, and (iii) the ability to form stable and specific complexes with DNA. BBR 3464, the first multinuclear platinum compound to reach phase II clinical trials, has created a new approach to cancer drug design. Large, highly charged platinum compounds have been shown to

form favorable covalent and noncovalent interactions with bio-molecular structures. Compounds such as BBR 3464, form an immediate pre-association with anionic structures on biomolecules before covalent attachment. To better characterize these interactions, a new set of compounds was designed that exclusively interacts via electrostatic associations and hydrogen bonding.

The investigation of noncovalent complexes between DNA, proteins, and peptides with a variety of synthetic and biological relevant structures has become increasingly more common with the coupling of electrospray ionization and mass spectrometry (ESI-MS). Mass spectrometry has been useful to the drug design community by allowing the rapid and accurate characterization of drug binding sites. In the first project we have explored the use of collision induced dissociation (CID) to map the potential binding sites of noncovalent polynuclear platinum compounds of varying size and charge with an antisense oligonucleotide of the Bcl-2 sequence. In the second project, the gas-phase dissociation and stabilizing effects of these polynuclear platinum compounds on duplex DNA were determined. Correlations between the size and charge of associating platinum compounds were determined by comparing the change in gas phase stability under CID conditions. Additionally, the association of these new types of noncovalently binding polynuclear platinum compounds was investigated with model cell surface structures such as anionic heparan sulfate and phospholipids.

Chapter 1:

Platinum and Cancer Biology Background

1.1. Emergence of Platinum as an Anticancer Agent

The anti-cancer therapeutic cisplatin or *cis*-[$PtCl_2(NH_3)_2$], first synthesized in 1845, was serendipitously shown to first inhibit the mitosis of bacteria in the lab and then shortly afterwards found to possess anti-tumor activity in 1969.[1] The development of cisplatin has been well documented. Upon gaining clinical approval in 1978, it has shown remarkable utility in a variety of human carcinomas, such as ovarian, breast, bladder, head, and neck.[2] Testicular cancer cases that once were fatal, have shown a >90% success rate in treatment.[3] With the increasing successes of cisplatin, many platinum based compounds were constructed and tested for improvements of the anti-cancer effectiveness. In 2006, it was reported that over 3000 platinum complexes had been tested for improvements and/or alternatives to cisplatin in the treatment of cancer.[4] However, only 28 (roughly 1%) have shown enough activity to warrant entry into clinical trials.[4] Currently only two other platinum based therapies have been approved for the treatment of human cancers, carboplatin and oxaliplatin.[5] See figure 1.1.

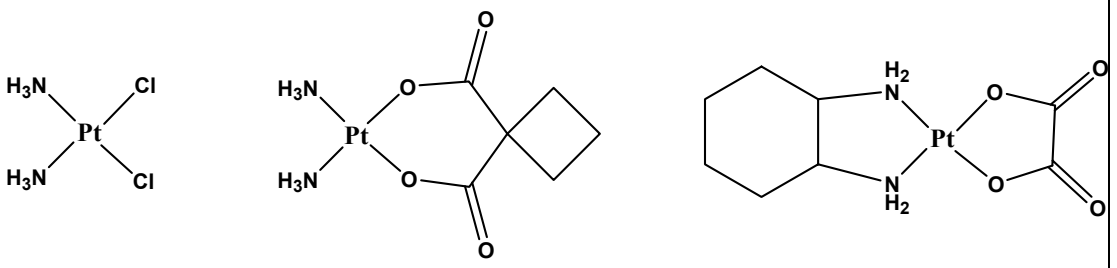

Figure 1.1. FDA approved platinum compounds for the treatment of cancer

1.2 Binding of Platinum Complexes to Biomolecules

The cytotoxicity of platinum drugs is primarily affected by three pharmacological factors: 1.) cellular uptake and efflux, 2.) the frequency and resulting structure of target adducts (DNA), and 3.) the metabolic profile resulting from reactions with sulfur containing proteins and peptides. Although cisplatin has been used with much success for more than 30 years, the exact biochemical mechanism of action is still relatively ambiguous. A series of structure-activity relationship rules that define the favorable characteristics a successful therapeutic should possess was suggested by Cleare and Hoeschele in 1973[6-8]. Those rules are broadly defined as: (a) possess a zero net charge (b) contain two leaving groups or one bidentate leaving group (c) have chloride leaving groups or similar liagands (d) leaving groups oriented in the *cis*-configuration (e) no hydroxy or hydroxo ligands as it increases toxicity and (f) have inert non-leaving groups such as amines.

Platinum compounds induce tumor damage by the stimulation of apoptosis. This process is mediated by the activation of signal transduction pathways that lead to the death receptor

mechanisms.[9] The currently accepted mode of action for cisplatin is that the compound induces cytotoxicity via binding to nuclear DNA which may activate a variety of signalling pathways such as p53, Bcl-2, caspases, and MAPK to name a few. Additionally, disruption of transcription and replication mechanisms also exist.[4]

The anti-cancer properties of cisplatin results from the displacement of the two *cis* chloride ligands and subsequent replacement with aquo ligands, which readily undergo substitution resulting in platination of the biological targets. (See Figure 1.2)

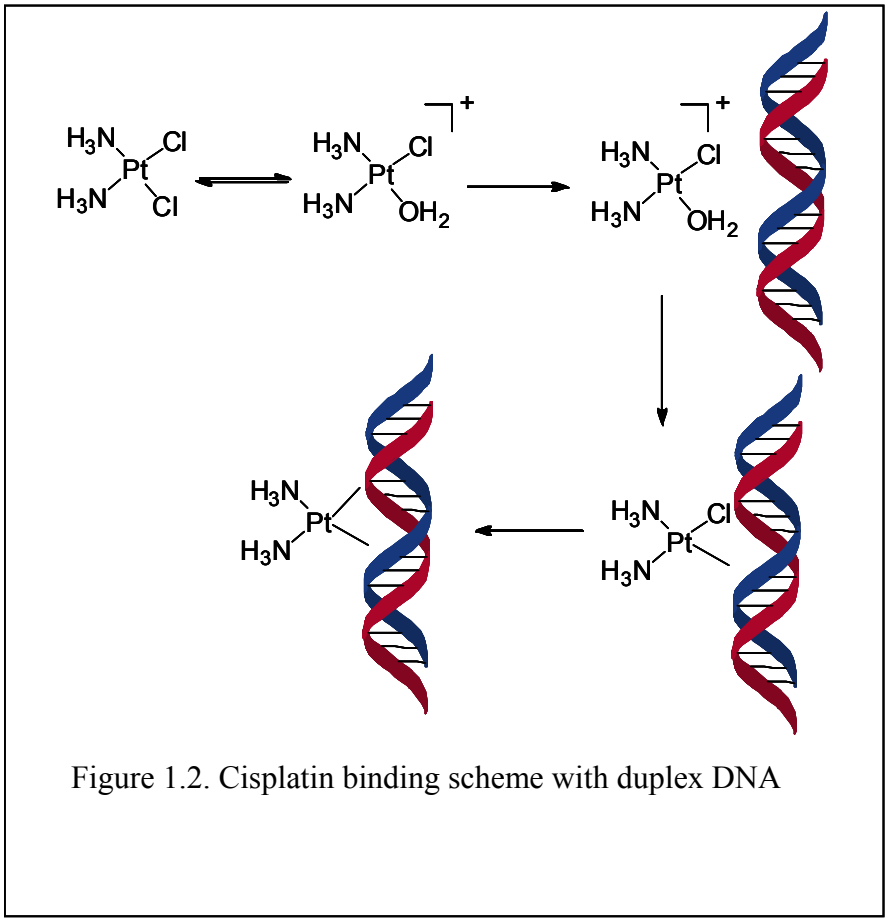

Figure 1.2. Cisplatin binding scheme with duplex DNA

Displacement of chloride ligands is hindered in physiological conditions due to the high concentration of chloride in blood, approaching 100mM. This enables cisplatin to reach the outer cellular surface still as a neutral molecule which helps promote cellular translocation. Once inside the cell the chloride concentration drops to approximately 4-20mM, which is low enough for the hydrolysis of cisplatin to occur.[10-12]

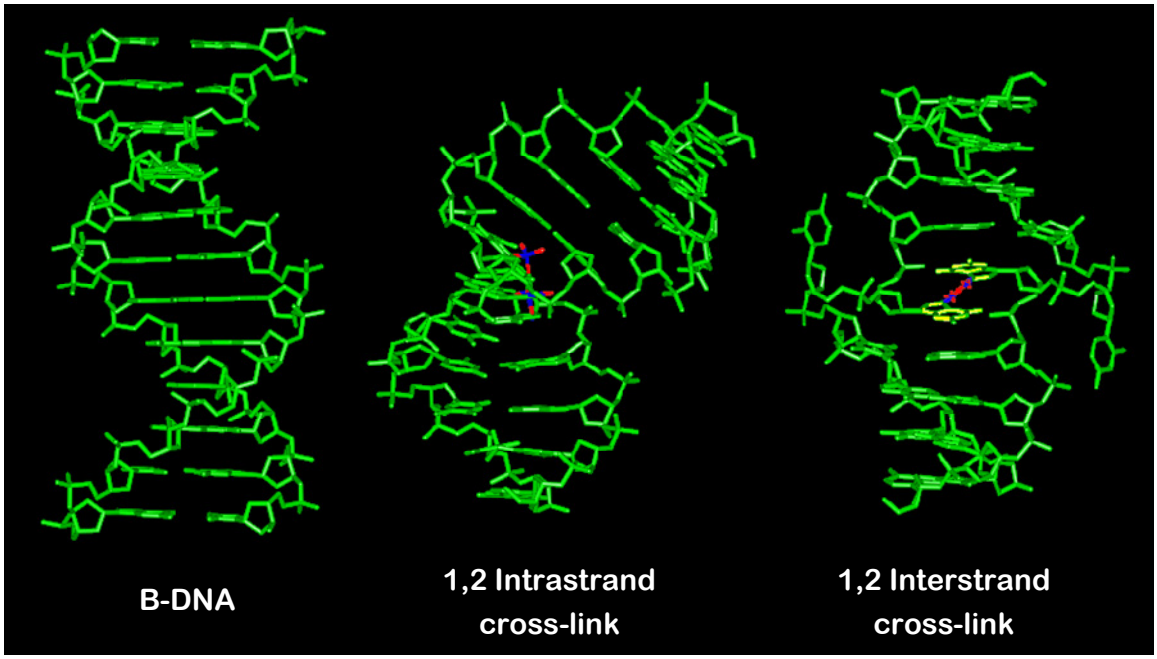

Figure 1.3 DNA distortion upon cisplatin covalent modification[2]

The accepted mechanism by which cisplatin exerts its anti-cancer activity begins with a specific DNA binding profile and follows with a cascade of cellular protein recognition interactions. As seen in the binding scheme figure 1.3, cisplatin forms primarily bifunctional intrastrand adducts

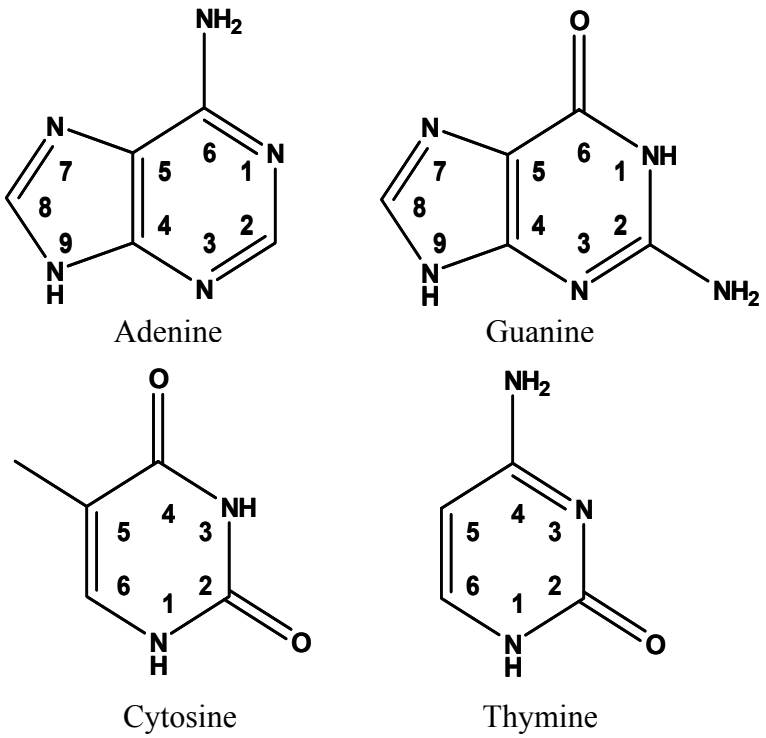

Figure 1.4. Structures of DNA nucleobases. The purine N7 site is the preferential binding site of Pt based

between two adjacent guanine (G) nucleosides, and to a much lesser extent between guanine and adenosine (GA) nucleosides.[13] The end result is platinum bound to the electron dense N7 site of the guanine nucleosides. A much less common binding profile between cisplatin and DNA occurs with interstrand crosslinks with guanine and cytosine (C) and the formation of 1,3 intrastrand crosslinks between G-x-G nucleosides.[13] The formation of the GG intrastrand

crosslinks results in a large bending of the DNA, which subsequently can be recognized by High Mobility Group Proteins (HMG) preventing the normal repair mechanisms from occurring. [14, 15] The 1,2-GG intrastrand binding causes the helix to bend toward the major groove (~ 40-80º) with an unwinding of the helix of around 20-30º.[2] This distortion which is recognized by the HMG binding domain proteins prevents the DNA replication and transcription and ultimately leads apoptosis.[2]

The extensive use of platinum drugs such as cisplatin, is limited due to intrinsic resistance by certain human cancer cell lines or the acquired resistance following initial treatment.[16] The development of acquired resistance is believed to occur through one or more processes: reduced uptake into cancer cells; increased tolerance to the DNA cisplatin interaction; more efficient DNA repair; and cisplatin deactivation via elevated levels of glutathione.[17, 18]

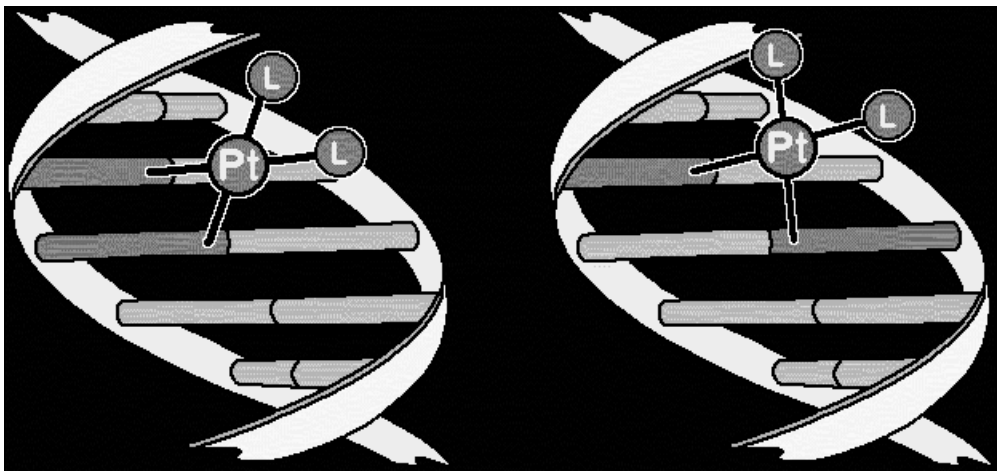

Figure 1.5. The 1,2 Intrastrand and 1,2 Interstrand crosslinks formed between DNA and Cisplatin

The use of cisplatin is also associated with dose-related side effects in addition to the intrinsic and acquired resistance mentioned above.[16, 19] The main dose limiting toxicity (DLT) of cisplatin is nephrotoxicity at 60-120 mg/m^2.[4]

In efforts to lower the side effects and increase the cytotoxicity in cisplatin resistant cancer cells, newer variations of the platinum diamine [Pt(NH_3)$_2$]center have shown success. One such compound that was designed to lower the side effects is carboplatin[16], diammine[1,2-cyclobutane-dicarboxyylato]platinum(II) (see figure 1). Carboplatin has very little to no associated nephrotoxicity and reduced oto-, neuro-, and gastrointestinal toxicities.[19, 20] The DLT for this compound at around 900 mg/m^2 is myelosuppression, bone marrow toxicity.[6] As such, the FDA approved carboplatin in 1989 and is currently sold by Bristol Myers-Squibb for the treatment of advanced ovarian carcinoma.[6, 21] As seen in figure 1.1, carboplatin is structurally different from cisplatin in the fact that the labile chloride ligands are replaced with the more structurally stable chelate ring which also improves solubility. As such, the carboplatin should possess a slower binding profile with proteins and other deactivating bio-molecules. The third mono-platinum compound to be granted FDA approval was oxaliplatin or trans-L-diaminocyclohexaneoxalatoplatinum (II).[6,21]. (see figure 1.1) Oxaliplatin is thought to circumvent some of the associated cisplatin resistance because the large hydrophobic DACH ligand aids in inhibition of DNA transcription.[6, 23-25] The maximum DLT for Oxaliplatin is 200 mg/m^2 with a reported increase in neuropathy.[4] Oxaliplatin is currently marketed by Sanofi-Synthelabo for the treatment of advanced colon carcinomas.[6]

1.3 Polynuclear Platinum Complexes

In 1989, Farrell and coworkers reported a di-nuclear platinum compound comprised of two cisplatin centers bridged with aliphatic diamines of varying length, n = 4,5, & 6.[26] This new class of "multi-nuclear" compounds increased DNA binding over that of cisplatin, as was measured through the inhibition of Eco R1 endonuclease activity.[26] These di-nuclear complexes were expanded to include *trans* platinum centers with only one chloride leaving group and varying charge from 1+ to 3+.[6] Polynuclear platinum anticancer drugs appear to redefine the structure-activity rules for platinum chemotherapy drugs that Cleare and Hoeschele (see section 1.1.2) determined for cisplatin.[6]

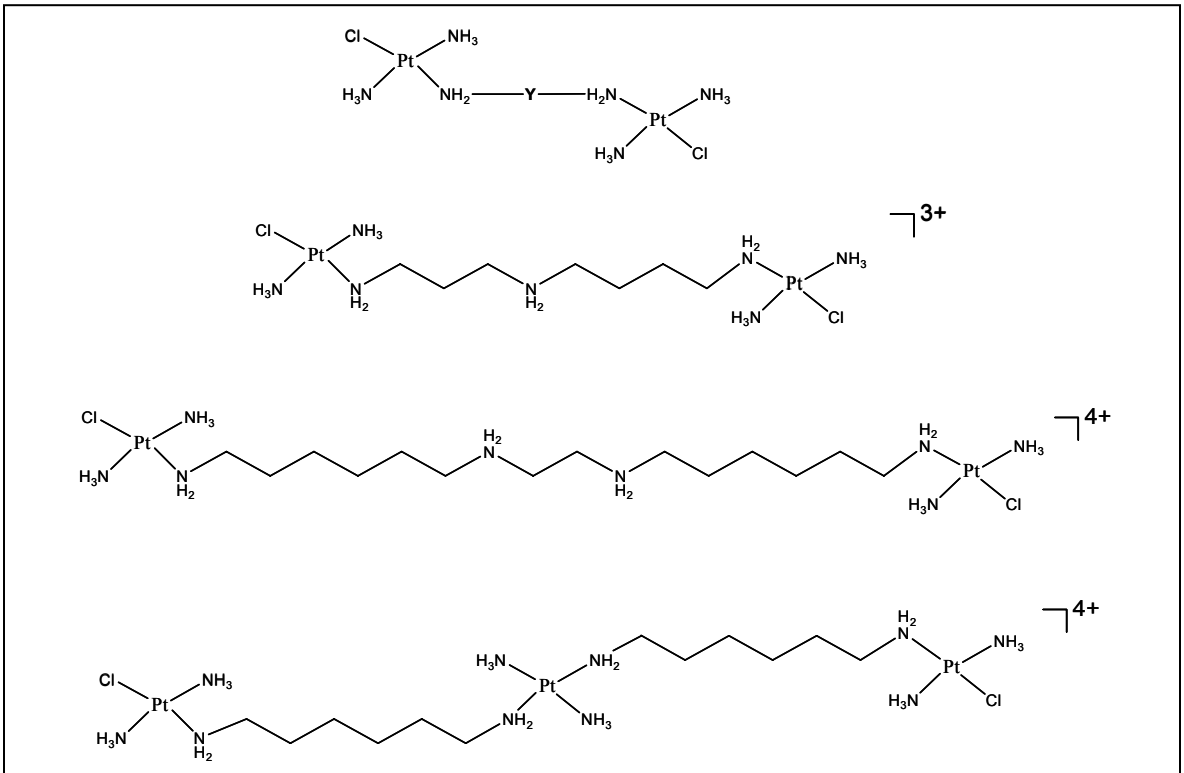

Figure 1.6. Polynuclear platinum compounds where (Y) represents the charged flexible central linker. Examples include: spermine, spermidine, or trans-platinum diamine-dihexane

The basic structure for the polynuclear complexes is seen in figure 1.6. This new motif contains two or more platinum coordination spheres linked with a variety of flexible linkers. The addition of a charged central platinum moiety increases the overall charge of the compound, but also adds additional hydrogen bonding character. This has been shown to add potency over di-nuclear complexes with di-amino hexane linkers.

By having two monofunctional platinum coordination spheres separated by a greater distance, the compounds are still able to bind DNA in a bifunctional manner, but now possess the ability to span several nucleobases, creating different DNA distortions as compared to mononuclear compounds.

As seen in figure 1.7, the polynuclear platinum compound BBR 3464 is capable of forming 1,4 and 1,6 interstrand cross-links, even 1,5 intrastrand crosslinks. The polynuclear motif exhibits a distinctive mode of action, which is different than that of the mononuclear platinum compounds. This dissimilar binding action is believed to be responsible for the effectiveness of BBR 3464 in cisplatin resistant cell lines.[27] In fact, the DNA adducts formed by BBR 3464, are not structurally recognized by antibodies commonly associated with cisplatin adducts or the high mobility group proteins[27-30] It has been reported that BBR 3464 binds to DNA with a frequency of crosslink formation of approximately 20% of the time, which is roughly three times the occurrence of the mononuclear cisplatin.[27, 28] The frequency of interstrand adduct formation is influenced by the geometry of the platinum centers as well as the hydrogen bonding capacity of the central linker group.[6] Increasing the hydrogen bonding character of the linker results in a decrease in the percentage of interstrand crosslink formations.[6]

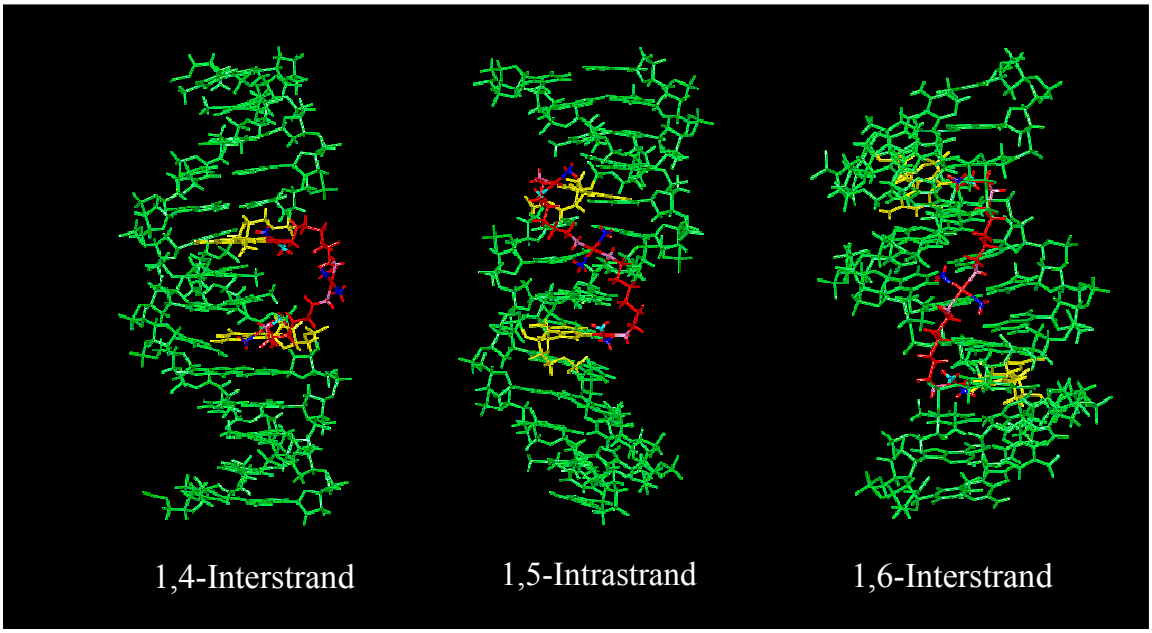

Figure 1.7. BBR 3464 crosslinks formed with DNA

The cationic nature of these polynuclear complexes gives rise to an electrostatic attraction to the anionic phosphate backbone of DNA. In fact, a preassociation prior to the covalent modification of DNA has been identified for BBR 3464[31], as well as other polynuclear compounds, such as a dinuclear platinium species with a 4,4′ -dipyrazolymethane (dpzm) linker by Wheate and Collins.[32] For the BBR 3464, it was determined that the nature and structure of the 1,4 cross link was possibly dictated by the initial preassociation of the central linker in or around the minor groove.[31]

1.4 NonCovalent Polynuclear Platinum Complexes

As was discovered for the covalent binding polynuclear complexes, the preassociation of the central tetraamineplatinum moiety directed the orientation of the DNA interaction.[31] In efforts to determine the nature of these preassociation events, a series of polynuclear platinum complexes were synthesized that have the *trans* labile chloro ligands substituted for an ammonia or a primary amine ligand. See figure 1.8 This exchange results in polynuclear platinum compounds that possesses a high charge (4+ to 8+) and interacts with biomolecules exclusively through electrostatic and hydrogen bonding interactions. It has been shown that the electrostatic interaction of these compounds induce a conformation change in canonical DNA sequences in the B→A and B→Z.[33] Increased cellular uptake in A2780 human ovarian tumor cells has been shown for AH 44 and AH 78.[34] Results show that when compared with the 4+ BBR 3464, the uptake is increased approximately double for the 6+ AH 44 and up to five times higher for the 8+ AH 78.[34] The results indicate that there are two possible reasons for the increase: the increase in overall charge 6+ to 8+ and/or the addition of the dangling hexamine. In addition to cellular uptake, studies of these compounds on the cytotoxicity in a panel of ovarian carcinoma cell lines reveal they are not as toxic as the covalent polynuclear compound, but demonstrate toxicity comparable to cisplatin nonetheless.[34]

One of the three pharmacological factors that determine therapeutic efficacy is how compounds interact with DNA. These noncovalent compounds have recently been shown to present a new distinct third mode of DNA binding in contrast to the two longstanding modes of DNA interaction, intercalation and groove binding.[35] Crystallographic datum of AH 78 with a double stranded dodecamer (Dickerson-Drew) reveal an interaction that can neither be classified as intercalation or groove binding; instead the three square planar tetra am(m)ine Pt(II) coordination spheres form a bidentate "phosphate clamp" with the phosphate oxygen.[35] The single phosphate oxygen accepts two hydrogen bonds, one from each of the *cis* oriented am(m)ines.[35] The interaction appears to be represented by two distinct binding modes: backbone tracking which follows along the backbone of one strand and groove spanning which crosses over the minor groove interacting with both strands.[35] (See figure 1.9)

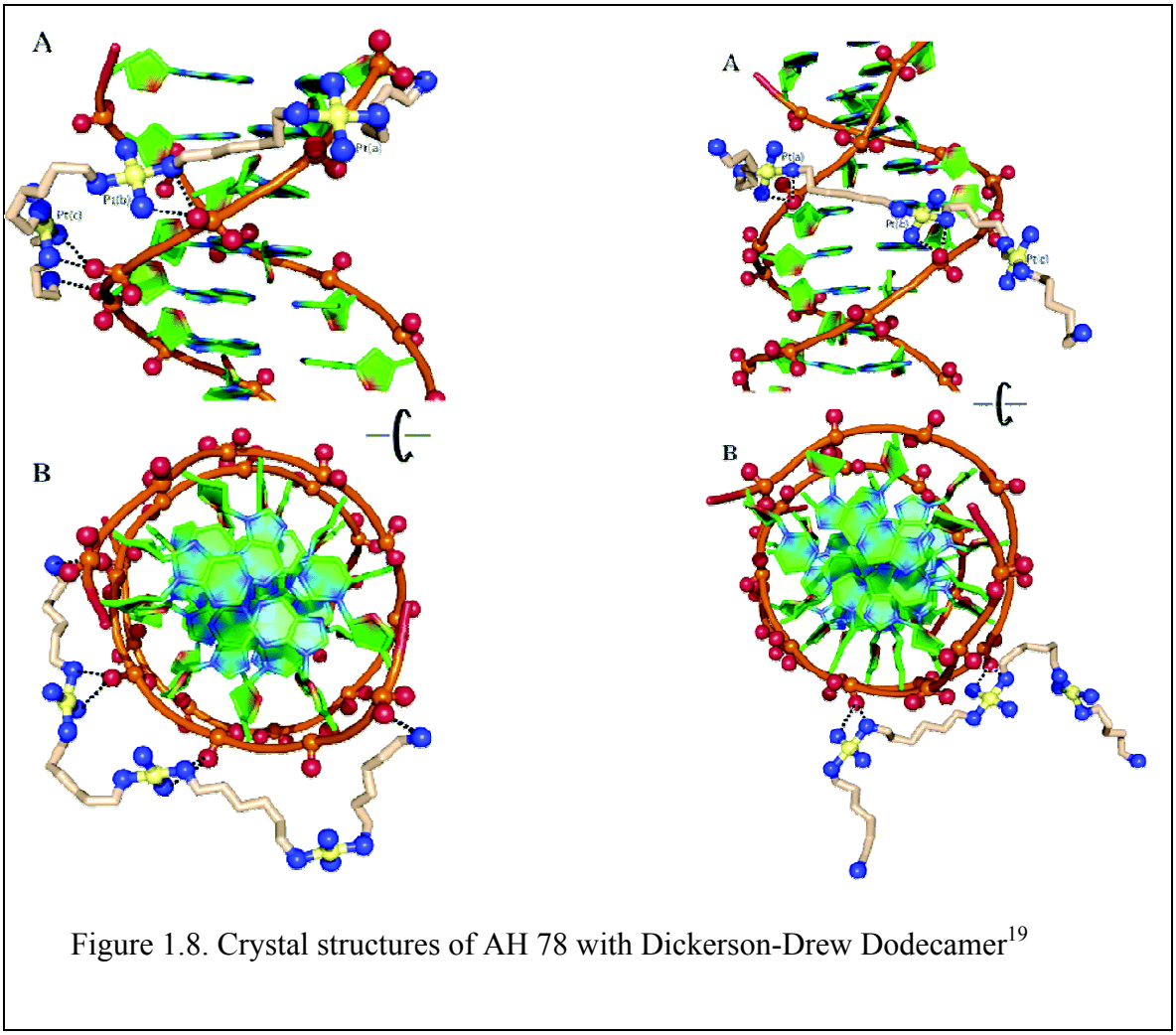

Figure 1.8. Crystal structures of AH 78 with Dickerson-Drew Dodecamer[19]

In the backbone tracking motif, AH 78 associates with four out of five consecutive phosphates along the single stranded backbone of the helix, utilizing six hydrogen bonds to stabilize the structure.[35] The addition of the flexible linker between the platinum coordination spheres allows the compound to form "phosphate clamps" with the am(m)ines of two platinum coordination spheres and the phosphate oxygens across the minor groove.[35] This binding motif stabilizes the duplex with four hydrogen bonds.[35] The binding to the oxygens appears to be selective for the

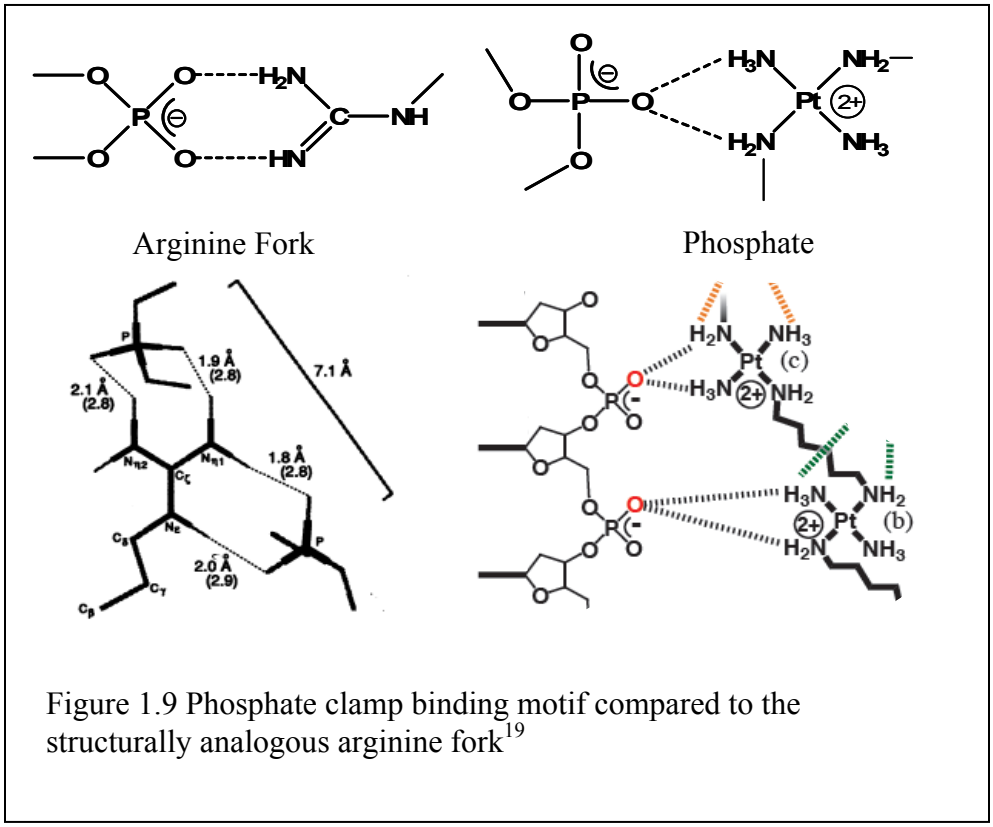

Figure 1.9 Phosphate clamp binding motif compared to the structurally analogous arginine fork[19]

phosphate oxygen and no strong apparent interactions with other oxygens along the strands. This is the first such "phosphate clamp" style binding motif aside from the guanidinium salt bridges found in peptide-biomolecule interactions via arginine residues. see Figure 1.10. The basic Y-shaped planar fork formed by the guaninidium group of the arginine forms interactions with a variety of biological systems such as the acidic carboxylates found in the side chains of aspartic and glutamic acids and post-translational modifications such as phosphorylation and sulfation.[22] The interactions between the basic guaninidium group of the arginine and acidic groups of neighboring biomolecules are important for processes such as the stabilization of protein structure, membrane transport, and enzymatic catalysis.[22, 36-38]

Project Overview

The research discussed in this dissertation focuses on obtaining a better understanding of the interactions of novel polynuclear platinum compounds with a variety of biomolecules that represent viable model systems in which anticancer therapeutic compounds encounter. The use of mass spectrometry to investigate these platinum anticancer compounds with DNA is demonstrated in Chapters 3 and 4. The potential of cell surface heparan sulfate to act as a transport vehicle for these compounds is explored via stability studies in Chapter 5. Additional research carried out during my graduate education is described in the appendix.

1.5 References

1. Rosenberg, B.; VanCamp, L.; Trosko, J. E.; Mansour, V. H., Platinum compounds: a new class of potent antitumour agents. *Nature* **1969,** 222, (5191), 385-6.

2. Jamieson, E. R.; Lippard, S. J., Structure, Recognition, and Processing of Cisplatin-DNA Adducts. *Chem Rev* **1999,** 99, (9), 2467-98.

3. Burdette, S., trans-Platinum reporting for duty. *Chem Biol* **2006,** 13, (5), 465-7.

4. Pasetto, L. M.; D'Andrea, M. R.; Brandes, A. A.; Rossi, E.; Monfardini, S., The development of platinum compounds and their possible combination. *Crit Rev Oncol Hematol* **2006,** 60, (1), 59-75.

5. Farrell, N., *Met Ions Biol Syst* **2004,** 42, 251-296.

6. Wheate, N. J.; Collins, J. G., Multi-nuclear platinum drugs: a new paradigm in chemotherapy. *Curr Med Chem Anticancer Agents* **2005,** 5, (3), 267-79.

7. Cleare, M. J. H., J.D., *Plat. Met. Rev.* **1973,** 17.

8. Cleare, M. J. H., J.D., *Bioinorg. Chem.* **1973,** 2.

9. Boulikas, T.; Vougiouka, M., Cisplatin and platinum drugs at the molecular level. (Review). *Oncol Rep* **2003,** 10, (6), 1663-82.

10. Ahmad, S.; Isab, A.; Ali, S., Structural and mechanistic aspects of platinum anticancer agents. *Transition Metal Chemistry* **2006,** 31, (8), 1003-1016.

11. Reedijk, J., New clues for platinum antitumor chemistry: kinetically controlled metal binding to DNA. *Proc Natl Acad Sci U S A* **2003,** 100, (7), 3611-6.

12. McGowan, G.; Parsons, S.; Sadler, P. J., Contrasting chemistry of cis- and trans-platinum(II) diamine anticancer compounds: hydrolysis studies of picoline complexes. *Inorg Chem* **2005,** 44, (21), 7459-67.

13. Barnes, K. R.; Lippard, S. J., Cisplatin and related anticancer drugs: recent advances and insights. *Met Ions Biol Syst* **2004,** 42, 143-77.

14. Rice, J. A.; Crothers, D. M.; Pinto, A. L.; Lippard, S. J., The major adduct of the antitumor drug cis-diamminedichloroplatinum(II) with DNA bends the duplex by approximately equal to 40 degrees toward the major groove. *Proc Natl Acad Sci U S A* **1988,** 85, (12), 4158-61.

15. Jordan, P.; Carmo-Fonseca, M., Cisplatin inhibits synthesis of ribosomal RNA in vivo. *Nucleic Acids Res* **1998,** 26, (12), 2831-6.

16. Wong, E.; Giandomenico, C. M., Current status of platinum-based antitumor drugs. *Chem Rev* **1999,** 99, (9), 2451-66.

17. Kelland, L. R., Preclinical perspectives on platinum resistance. *Drugs* **2000,** 59 Suppl 4, 1-8; discussion 37-8.

18. Baird, R. D.; Kaye, S. B., Drug resistance reversal--are we getting closer? *Eur J Cancer* **2003,** 39, (17), 2450-61.

19. Hartmann, J. T.; Lipp, H. P., Toxicity of platinum compounds. *Expert Opin Pharmacother* **2003,** 4, (6), 889-901.

20. Monn, S. T. M.; Schurch, S., Investigation of metal-oligonucleotide complexes by nanoelectrospray tandem mass spectrometry in the positive mode. *Journal of the American Society for Mass Spectrometry* **2005,** 16, (3), 370-378.

21. Cassidy, J., Review of oxaliplatin: an active platinum agent in colorectal cancer. *Int J Clin Pract* **2000,** 54, (6), 399-402.

22. Schug, K.; Lindner, W., Using electrospray ionization-mass spectrometry/tandem mass spectrometry and small molecules to study guanidinium-anion interactions. *International Journal of Mass Spectrometry* **2005,** 241, (1), 11-23.

23. Rixe, O.; Ortuzar, W.; Alvarez, M.; Parker, R.; Reed, E.; Paull, K.; Fojo, T., Oxaliplatin, tetraplatin, cisplatin, and carboplatin: spectrum of activity in drug-resistant cell lines and in the cell lines of the National Cancer Institute's Anticancer Drug Screen panel. *Biochem Pharmacol* **1996,** 52, (12), 1855-65.

24. Raymond, E.; Faivre, S.; Woynarowski, J. M.; Chaney, S. G., Oxaliplatin: mechanism of action and antineoplastic activity. *Semin Oncol* **1998,** 25, (2 Suppl 5), 4-12.

25. Schmidt, W.; Chaney, S. G., Role of carrier ligand in platinum resistance of human carcinoma cell lines. *Cancer Res* **1993,** 53, (4), 799-805.

26. Farrell, N. P.; De Almeida, S. G.; Skov, K. A., Bis(platinum) complexes containing two platinum cis-diammine units. Synthesis and initial DNA-binding studies. *Journal of the American Chemical Society* **1998,** 110, (15), 5018-5019.

27. Billecke, C.; Finniss, S.; Tahash, L.; Miller, C.; Mikkelsen, T.; Farrell, N. P.; Bogler, O., Polynuclear platinum anticancer drugs are more potent than cisplatin and induce cell cycle arrest in glioma. *Neuro Oncol* **2006,** 8, (3), 215-26.

28. Brabec, V.; Kasparkova, J.; Vrana, O.; Novakova, O.; Cox, J. W.; Qu, Y.; Farrell, N., DNA modifications by a novel bifunctional trinuclear platinum phase I anticancer agent. *Biochemistry* **1999,** 38, (21), 6781-90.

29. Kasparkova, J.; Zehnulova, J.; Farrell, N.; Brabec, V., DNA Interstrand Cross-links of the Novel Antitumor Trinuclear Platinum Complex BBR3464. *Journal of Biological Chemistry* **2002,** 277, (50), 48076-48086.

30. Zehnulova, J.; Kasparkova, J.; Farrell, N.; Brabec, V., Conformation, recognition by high mobility group domain proteins, and nucleotide excision repair of DNA intrastrand cross-links of novel antitumor trinuclear platinum complex BBR3464. *J Biol Chem* **2001,** 276, (25), 22191-9.

31. Hegmans, A.; Berners-Price, S. J.; Davies, M. S.; Thomas, D. S.; Humphreys, A. S.; Farrell, N., Long Range 1,4 and 1,6-Interstrand Cross-Links Formed by a Trinuclear Platinum Complex. Minor Groove Preassociation Affects Kinetics and Mechanism of Cross-Link Formation as Well as Adduct Structure. *J. Am. Chem. Soc.* **2004,** 126, (7), 2166-2180.

32. Wheate, N. J.; Collins, J. G., A ^{1}H NMR study of the oligonucleotide binding of [(en)Pt(mu-dpzm)2Pt(en)]Cl4. *J Inorg Biochem* **2000,** 78, (4), 313-20.

33. Qu, Y.; Harris, A.; Hegmans, A.; Petz, A.; Kabolizadeh, P.; Penazova, H.; Farrell, N., Synthesis and DNA conformational changes of non-covalent polynuclear platinum complexes. *Journal of Inorganic Biochemistry. The Ninth International Symposium on Platinum Compounds in Cancer Chemotherapy* **2004,** 98, (10), 1591-1598.

34. Harris, A. L.; Yang, X.; Hegmans, A.; Povirk, L.; Ryan, J. J.; Kelland, L.; Farrell, N. P., Synthesis, Characterization, and Cytotoxicity of a Novel Highly Charged Trinuclear Platinum Compound. Enhancement of Cellular Uptake with Charge. *Inorg. Chem.* **2005,** 44, (26), 9598-9600.

35. Komeda, S.; Moulaei, T.; Woods, K. K.; Chikuma, M.; Farrell, N. P.; Williams, L. D., A Third Mode of DNA Binding: Phosphate Clamps by a Polynuclear Platinum Complex. *J. Am. Chem. Soc.* **2006,** 128, (50), 16092-16103.

36. Schmidtchen, F. P.; Berger, M., Artificial Organic Host Molecules for Anions. *Chemical Reviews* **1997,** 97, (5), 1609-1646.

37. Rensing, S.; Schrader, T., The First Synthetic Receptor for the RGD Sequence. *Organic Letters* **2002,** 4, (13), 2161-2164.

38. Best, M. D.; Tobey, S. L.; Anslyn, E. V., Abiotic guanidinium containing receptors for anionic species. *Coordination Chemistry Reviews* **2003,** 240, (1-2), 3-15.

Chapter 2:
Methods to investigate noncovalent interactions between polynuclear platinum compounds and biomolecules

2.1 Electrospray Ionization

Electrospray ionization mass spectrometry (ESI-MS) has become an essential tool in the process of drug discovery, playing a key role in the development of new therapeutics.[1] The utility of ESI-MS toward studying noncovalent interaction between biomolecules was first demonstrated in 1991 with the work of Ganem et al.[2]

Electrospray ionization (ESI) is characterized as a soft ionization technique that allows the gentle introduction of labile, as well as large, nonvolatile molecules into the gas phase.[3] Applying a potential difference of several thousand volts (~1-4 kV) between the ESI needle and the capillary inlet on the mass spectrometer, a spray of highly charged droplets is formed.[3-5] The ionization process produces single and multiple charged ions of either positive or negative nature from an aqueous solution in relation to applied polarity.[4, 5] The majority of the work presented in this dissertation involves negative electrospray ionization and therefore this description will detail the application of the negative ionization process.

Electrospray Ionization occurs as a potential drop or difference is created between the source needle and the mass spectrometer inlet, Figure 2.1.[3, 4, 6] The generation of the electric field between the two electrodes (~2-3mm) results in the formation of an inverted conical spray, termed the Taylor cone.[7] The Taylor cone is comprised of micron sized droplets (~2-3 μm in diameter) of similarly charged solvent and analyte moieties that are then introduced into the mass spectrometer.[3, 6, 8-11]

Within the Taylor cone, the solute molecules have an overall negative charge which is the result of using slightly basic ESI solutions, which aid in the deprotonation of the analyte. As the molecules of solvent/analyte pass through the heated mass spectrometer inlet, they desolvate, resulting in the density of charges in the droplet to increase. Desolvation occurs until the Rayleigh limit, at which time, the coulombic repulsions from the excess of negative charges within the droplet are equal the overall surface tension resulting in a coulombic explosion due to droplet instability, and thus produces subsequent smaller droplets.[8, 12]

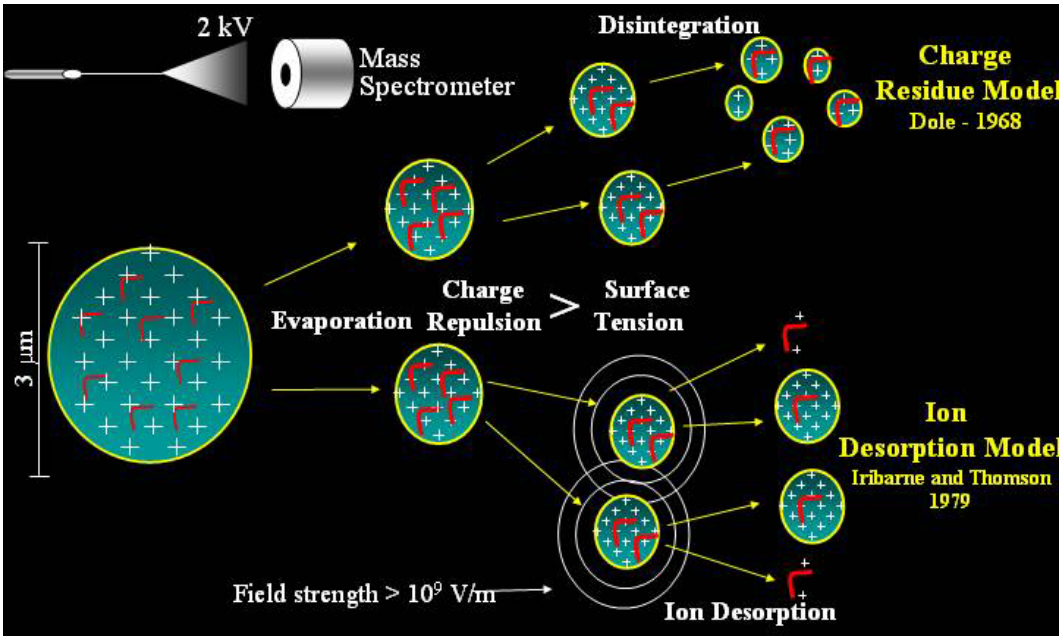

Figure 2.1. Schematic representation of two generally accepted methods of the electrospray ionization (ESI) process.

Production of electrospray droplets in the ESI process is not fully understood. However, two models are widely accepted. Dole proposed the charged residue model (CRM)[13], which involves the cascade of coulombic eruptions which proceed until the droplets contain only one solute

molecule and a select number of charges. The excess solvent shell continues to vaporize leaving the solute ion with single or multiple charges.[8, 12, 13] The second model proposed by Iribarne and Thompson is termed the ion evaporation model (IEM).[8, 12, 14] This model also begins with the production of multiple droplets through the coulombic explosions, however the IEM process continues only until the radii of the droplets become small enough so that the overall charge density located on the surface of the droplet is high enough that the solute molecules inside the droplet are deprotonated/protonated by the presence of hydroxyl/protons on the surface.[3, 14] Molecules of varying degrees of deprotonation/protonation can be brought into the gas-phase by the presence of the strong electrostatic potential on the surface of the droplets as a way to remove the excess of charge surrounding the droplet.[8, 13]

ESI is not tolerant of high salt or detergents in the spray solution. Therefore, for all the experiments in this dissertation, an in-line microdialysis chamber was constructed to decrease the presence of any interfering salts. The dialysis chamber has been described at length by Hannis et al.[15] Briefly, a 13,000 molecular weight cut off (MWCO) hollow regenerated cellulose fiber, SpectroPor was installed between two 190 µm OD x 80 µm ID fused silica tubing, Polymicro. The dialysis fiber is placed in a 20 mM ammonium acetate filled chamber. The sample of interest is dissolved in 10 mM ammonium acetate and injected via syringe at 3 µL/min and recollected. Using this type of set up, approximately 99% desalting efficiency has been achieved.[15] The NH_4^+ displaces the Na^+ or K^+ adducts bound to the anionic sites of the biomolecules and during the desolvation phase in electrospray the NH_4^+ leaves as NH_3. Depicted in figure 2.2 are ESI-MS spectra of a 13-mer oligonucleotide acquired directly from a vial and the same oligonucleotide acquired after dialysis through the chamber.

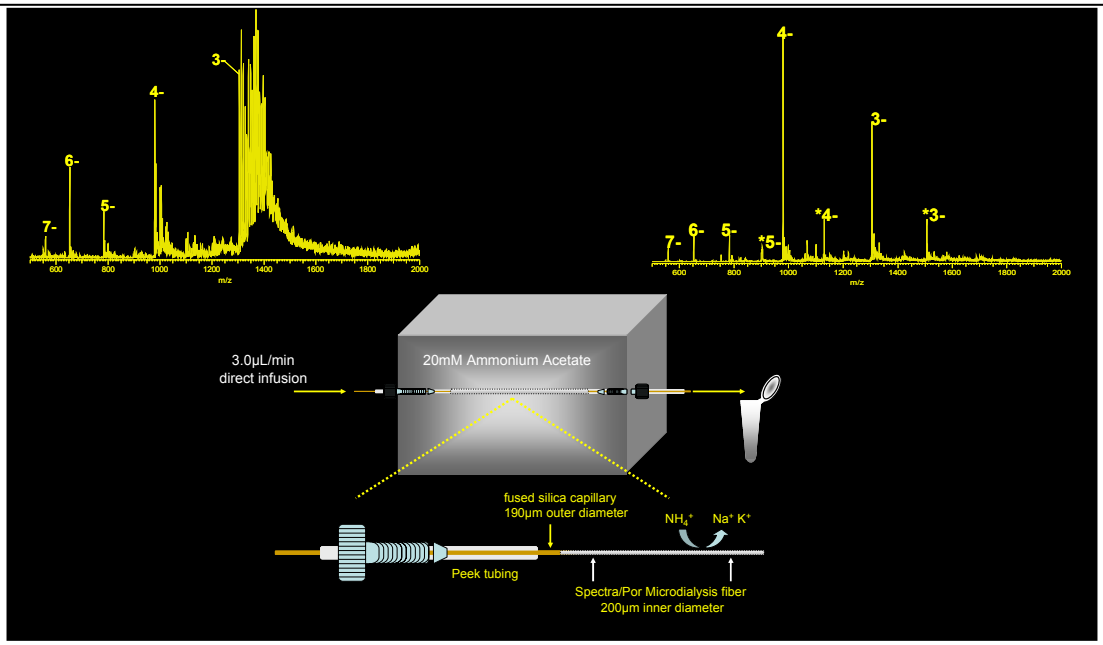

Figure 2.2. Micro-dialysis chamber illustrating pre and post dialysis spectra

2.2 Quadrupole Time of Flight Mass Spectrometry (QTOF-MS)

The experiments for this research were conducted on a QTOF-2 Waters/Micromass (Milford, MA) equipped with a modified micro-electrospray ionization source. Time of flight instruments, such as the one schematically illustrated in figure 2.3, can be thought of as a triple quadrupole with the last quadrupole replaced with an orthogonal reflecting time of flight mass analyzer.[16] The particular instrument from Waters/Micromass utilizes a hexapole (r.f. only hexapole ion guide)/quadrupole/hexapole arrangement.

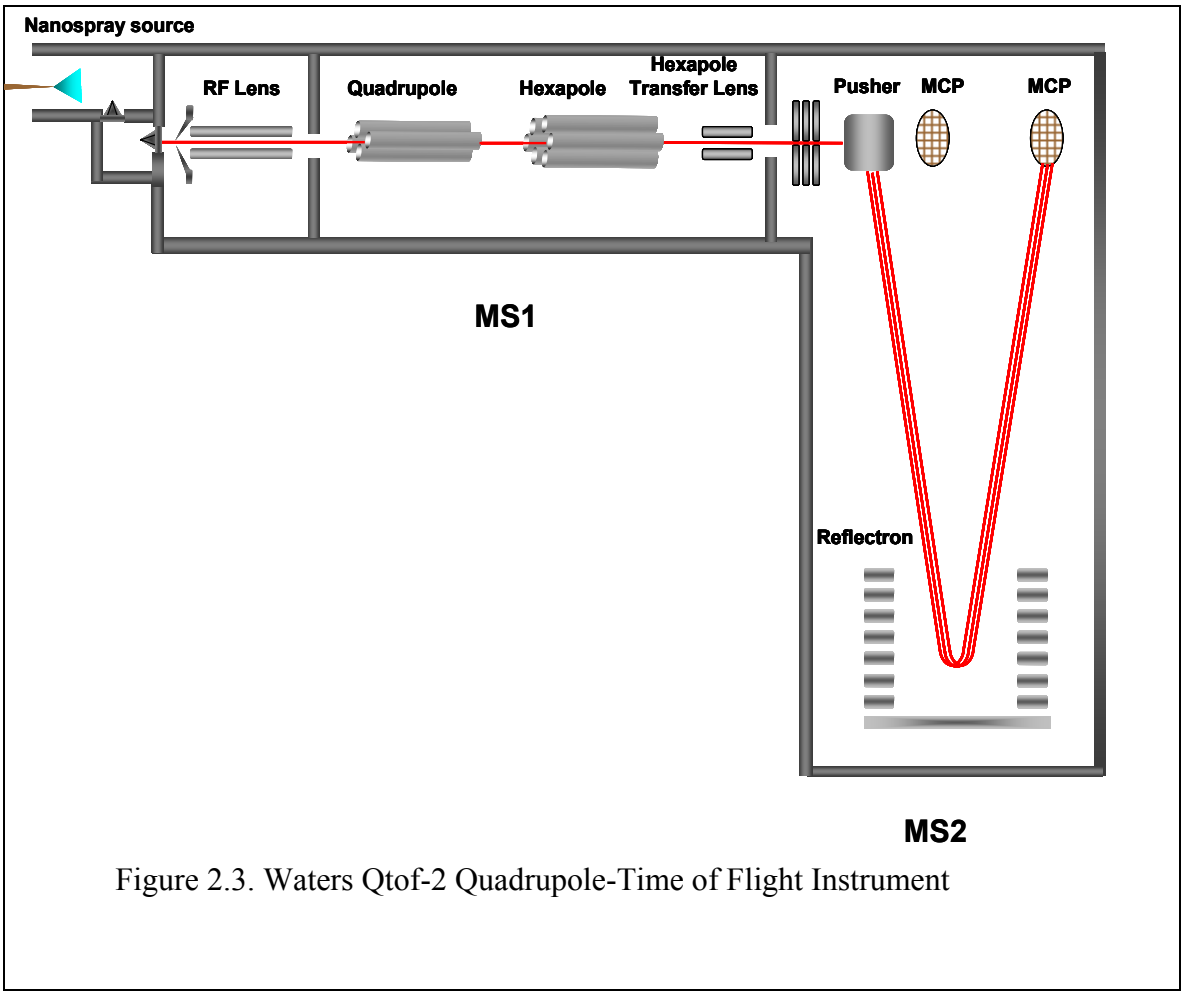

Figure 2.3. Waters Qtof-2 Quadrupole-Time of Flight Instrument

Time of flight instruments operate on the principle that ions of different mass-to-charge (m/z) have characteristically different velocities. The potential energy of the ion is converted to kinetic energy upon acceleration. The relationship of m/z to velocity is as follows:

$$zeE = 1/2mv^2 \qquad \text{(eqn. 2.1)}$$

where the kinetic energy of an ion (½ mv ^{2}) is equal to the potential energy (zeE) where an accelerating electric field (E) is available between the accelerator plates. The velocity of that ion is therefore:

$$v = \left(\frac{2zeE}{m}\right)^{1/2} \text{ or } \quad v = \sqrt{\frac{2zeE}{m}} \qquad \text{(eqn. 2.2)}$$

Any two ions of the same charge, but different masses, will have different velocities under the same experimental conditions.

Since it is impractical to measure the velocity of an ion, we consider the time = t, it takes for an ion to travel a fixed distance = L_{eff}.

$$t = \frac{L_{eff}}{\sqrt{2eU_{acc}}}\sqrt{m/z} \qquad \text{(eqn. 2.3)}$$

Ions with a smaller m/z reach the detector before those of a higher m/z value, as the higher m/z ions have a much lower velocity and therefore a longer time spent in the flight tube.

$$t = C\sqrt{(m/z)} \qquad \text{(eqn. 2.4)}$$

Quadrupole times of flight instruments with orthogonally positioned reflectrons are able to acquire fairly high resolution data, ~ 10,000 at full width half-maximum (FWHM). The instrument resolution is given by equation 2.5 where m = detected peak mass and Δm is the FWHM of the detected peak.

$$R_{FWHM} = \frac{m}{\Delta m} \qquad \text{(eqn. 2.5)}$$

In full scan mode, the ions generated through the ESI process are focused through the MS1 region with the RF hexapole lens and hexapole operating in the RF only mode. The RF field results in radial confinement of the ions by creating a potential well between the rods.[16] In addition, the higher pressures inside the MS1 region allow for radial and axial dampening, often referred to as collisional cooling of the ions,[17] thus reducing the energy spread and the overall diameter of the ion packet.[16]

In the MS/MS mode, the quadrupole in MS1 is operated as a mass filter in order to transmit only the parent ions of interest. By applying both the DC and RF voltages to the quadrupole rods, only ions that have stable trajectories at the applied amplitudes of voltages will traverse down the center, while ions of unstable trajectories will be neutralized by coming into contact with the quadruple rods.[17] The stability of ions exposed to RF-DC voltages is governed by the Mathieu equation and visually represented by the Mathieu stability diagram. Upon acceleration of the ion into the hexapole collision cell, it undergoes collision induced dissociation (CID) with neutral argon gas resulting in fragment ions and depending on the applied collision energy possibly remaining parent ions. The maximum amount of translational energy that can be converted to the internal energy is given in equation 2.6.

$$E_{COM} = E_{LAB}\left[m_c / \left(m_c + m_i\right)\right] \qquad \text{(eqn. 2.6)}$$

The kinetic energy (E_{LAB}) of the ion is provided by the applied electric fields in the instrument; (m_i) is the mass of the ion, and (m_c) the mass of the collision gas atom.

Looking at the equation, it is observable how collisions with larger neutral gas ions result in more kinetic energy being converted into internal energy. For our particular instrument set up, argon was chosen as the collision gas over nitrogen. Another factor influencing the CID of ions is the overall charge state of the ion. The efficiency of CID scales in relation to its charge state since the ion possesses a higher kinetic energy due to the effects of the electric fields of the instrument. Therefore an identical molecule of two different charge states, (1+ and 3+) for example, will have very different kinetic energies before CID. The 3+ ion will have three times the kinetic energy and is therefore more likely to dissociate.

At each successful collision of the argon gas with the parent ion, some of the translational energy is converted to internal energy and upon reaching an internal threshold specific to the isolated ion, the ion will fragment. Leaving the collision cell, ions are accelerated into the MS2 region and focused before encountering a pulsed electric field (usually several kHz in frequency) supplied by the pusher plate in the orthogonal direction in relation to the their initial trajectory. Following a final applied acceleration, the ions enter the field-free flight tube where they encounter a series of grid plates or an electrostatic mirror termed the reflectron (figure 2.4).

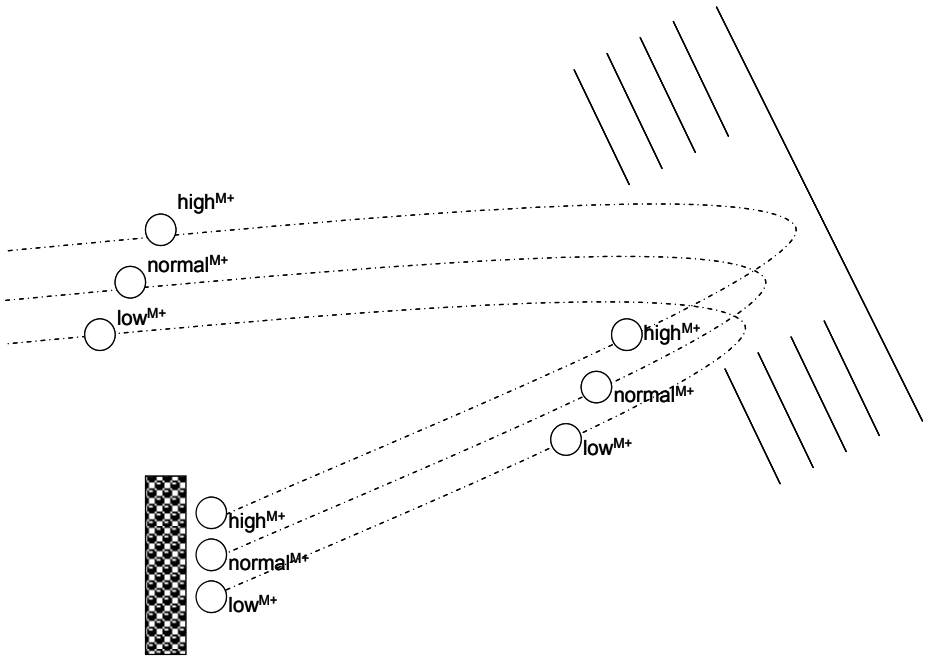

Figure 2.4. Schematic of a V-shaped reflectron depicting ions of differing kinetic energy, but the same m/z values being corrected for increased resolution.[17]

The reflectron results in an increase in instrument resolution as it adjusts the velocities of ions with similar m/z values. Ions of similar mass that might be separated in space due to differences in kinetic energy enter the reflectron at different times. The reflectron electrostatic grid plates apply a decelerating potential to the ions. So ions of higher kinetic energy (faster ions) enter the reflectron and penetrate deeper into the grid plates than the lower kinetic energy (slower ions). The same electric field that decelerated the ions coming in, now accelerates the ions out of the reflectron back to their original velocity. Since the ions with lower kinetic energy penetrate less, they leave the reflectron first followed by the higher kinetic ions which penetrated deeper into the reflectron, thus increasing its path length. However, despite the fact that the ions of lower kinetic energy (slower) left the reflectron first, the ions of higher kinetic energy (faster) have time to catch up and reach the detector as one packet of ions rather than spread out spatially.

2.3 Mass Spectrum Peak Identification

The process of electrospray ionization results in the production of multi-charged ions which allows for large biomolecules to fall within the working range of most mass spectrometers. The resultant x-axis for mass spectrometers is the mass-to-charge ratio which reflects the number of charges a given molecule has obtained or lost during the ionization process. For instance, human serum albumin (HSA) has a molecular weight of ~ 66,000 Da, but with the addition of 25 to 30 protons, results in an m/z ratio that is below 3000 and well within the working range of a variety of mass analyzers.

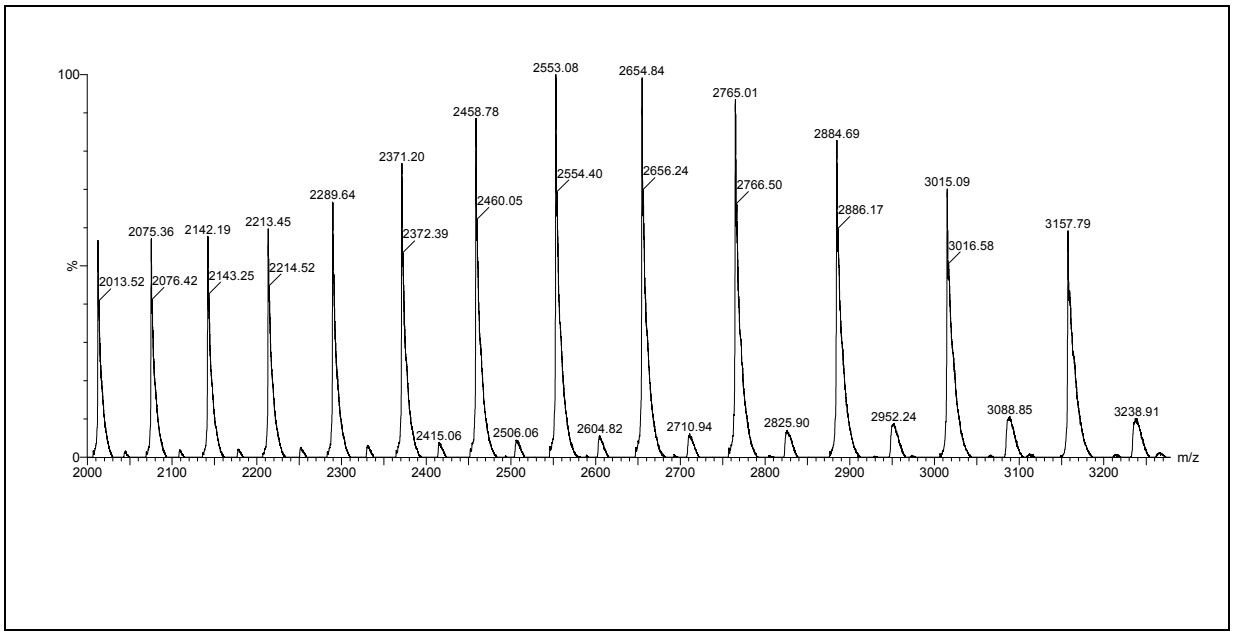

The determination of the m/z value is related to the charge and the type of adduct formed with the molecule. For a molecule of mass (M) it can have (n) number of charges, as well as an additional adduct (m_a)(Na^+, K^+ etc) and is expressed in the equation:

$$m/z = \frac{(M + nm_a)}{n} \qquad \text{(eqn. 2.7)}$$

The interpretation of large biomolecules with multiply charged peaks can be complicated. The use of mathematical algorithms has aided in the determination of intact molecular masses. For this particular software from Waters Corp. the MAXENT or maximum entropy algorithm was used. The deconvoluted mass spectrum of the protein HSA depicted below shows the neutral molecular mass of the intact HSA.

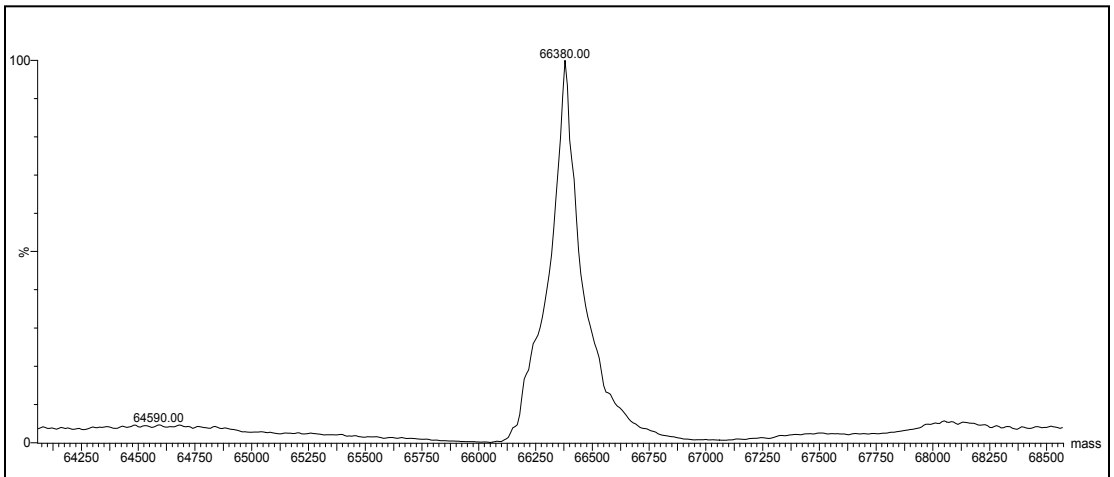

Figure 2.6. Deconvoluted spectra of HSA showing the molecular ion mass determined from the MaxEnt algorithm of the various charge states

Given the mass spectrum in figure 2.5, we can solve for the intact mass by using two adjacent peaks in the spectrum. This is based on the assumption that the two peaks are from the same intact mass and differ by the addition of only one proton. So for the m/z peaks at 2654.84 and 2553.08 we determine the intact mass as follows:

The intact mass can be derived from equation 2.7 since the peak m/z ratios are given and we assume two adjacent peaks are multiply charged ions differing by only one charge. Therefore:

$$2654.84 = \frac{(M + nH^+)}{n}$$

Assuming the lower m/z peak has (n +1) charges we assume:

$$2553.08 = \frac{(M + (n+1)H^+)}{(n+1)}$$

Since the assumption was made that both peaks represent the same mass M = M.

$$n(2654.84) + nH^+ = (n + 1)(2553.08) + (n + 1)H^+$$

$$n(2654.84) = n(2553.08) + 2553.08 + H^+$$

$$n(2654.84\text{-}2553.08) = 2553.08 + H^+$$

$$2654.84n - 2553.08n = 2554.08$$

$$101.76n = 2554.08$$

$$n = 25$$

Putting that back into equation 2.7 gives the intact mass of the analyte:

$$2654.84 = \frac{(M + 25)}{25} \quad \text{so} \qquad 66371 = M + 25$$

$$M = 66346$$

For smaller biomolecules that are examined by mass spectrometry the spectra are not as complex and therefore do not need the rigorous treatment of mathematical algorithms to determine charge state and molecular mass. The difference between isotopically resolved

peaks can be used to determine the overall charge state. The spacing between the peaks is indicative of the charge state: Δm = 1Da is a single charged species, Δm = 0.5 is double charged, Δm = 0.33, and Δm = 0.25 are triply and quadruply charged. For the spectrum

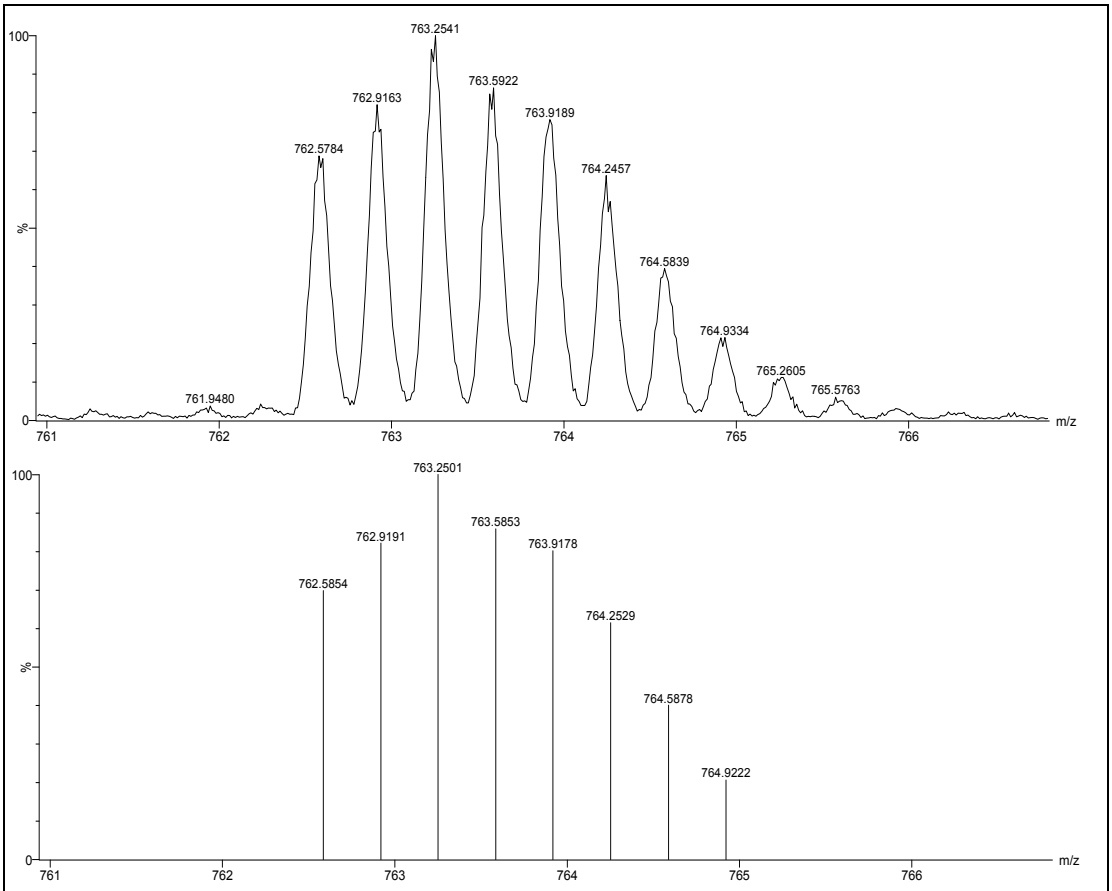

Figure 2.7. ESI-MS of a small peptide illustrating the peak spacing for charge state determination

shown in figure 2.7 of a zinc finger peptide (KGCWKCGKEGHQMKDCTER/Zn) the Δm spacing is 0.33, giving rise to a 3+ peak determination. The overall mass of the zinc finger peptide can then be determined by:

$$M = n[(m/z) - H^{+}] \qquad \text{(eqn. 2.7)}$$

Where n = total number of charges and M = to the neutral mass.

2.4 Fourier Transform Ion Cyclotron Resonance Mass Spectrometry

Fourier Transform Ion Cyclotron Resonance Mass Spectrometry (FTICR-MS), was developed in 1974 by Comisarow and Marshall[18-20] and was based on the fundamental theory of ion cyclotron resonance introduced in the 1930's by Lawrence and Edlefson. Electrospray was first coupled with FTICR-MS in 1989 by Hunt, McLafferty, and coworkers thus allowing researchers the ability to analyze large nonvolatile biomolecules with ultra high resolution.[21] The coupling of ESI with FTICR-MS has proven advantageous because the resulting ions formed typically have a mass-to-charge ratio between 500-2000, which falls within the working mass range of the FTICR-MS.[22]

Figure 2.8 illustrates modified 4.7 Tesla FTICR-MS Ionspec Corporation (Irvine, CA) with superconducting magnet used for all experiments in Chapter 6.[23]

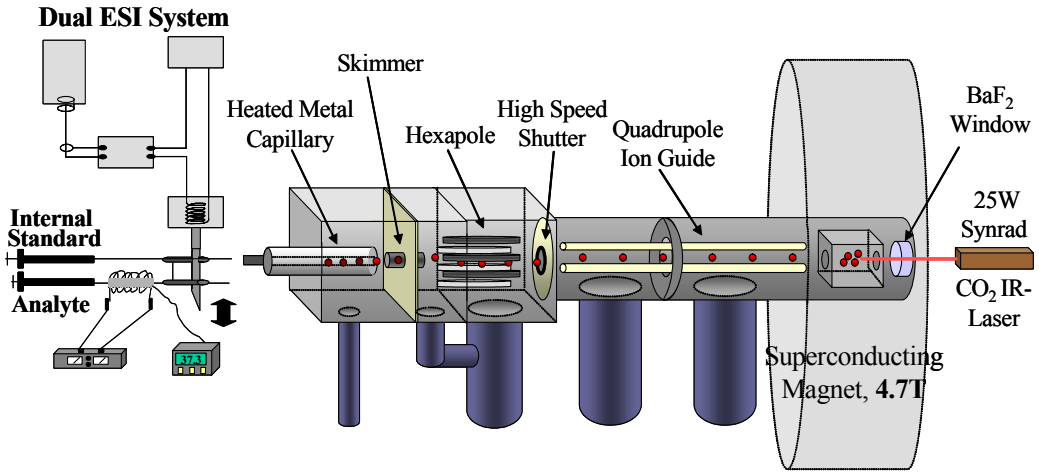

Figure 2.8 Modified Ionspec resistively heated Dual-ESI-FTICR-MS[23]

Ions formed from the ESI process are desolvated in the heated metal capillary region and a small portion sampled by the skimmer cone prior to accumulation in the hexapole.[24] Hexapole accumulation involves applying negative potentials to the hexapole endcaps to confine the ions in the axial direction while also applying an r.f. only potential to confines the ions along the radial direction of the hexapole.[24] The stored ions are removed by applying a negative potential to the entrance endcap and a more positive potential to the exit endcap. This method allows the ions to be electrostatically "dumped" by the opening of a high speed shutter and guided through the low pressure region by an r.f. only quadrupole ion guide prior to axial electrostatic trapping inside the ICR cell.

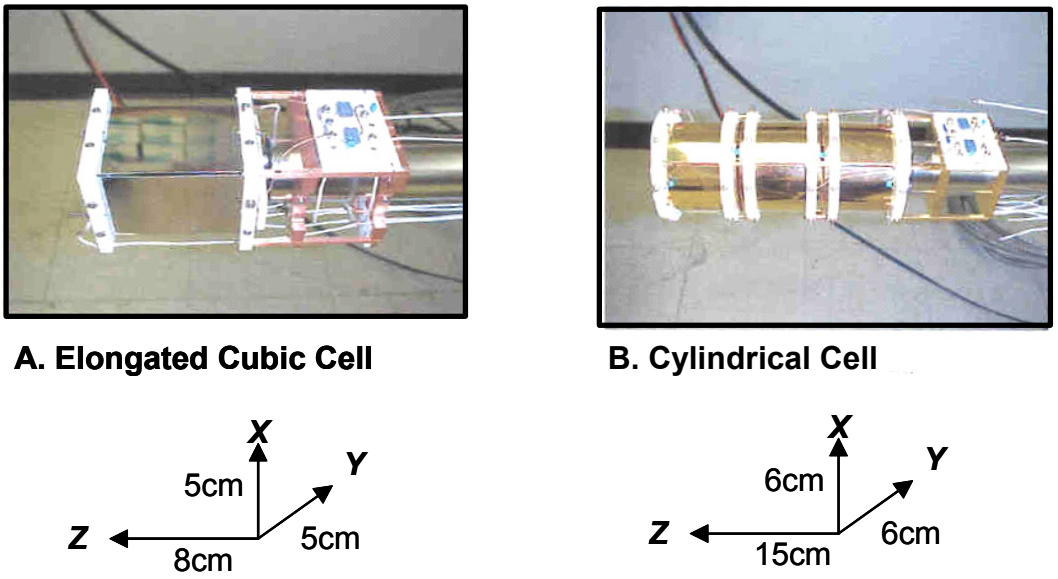

Figure 2.9 ICR cell dimensions for A. Elongated and B. Cylindrical cell types

For the experiments discussed in Chapter 6, a cylindrical ICR cell as shown in Figure 2.9B was used. However, for simplicity in visualization, a cubic Penning ion trap, Figure 2.9A will be discussed. A cubic ion trap consists of six flat stainless steel or gold coated plates arranged with similar operating plates opposing. As shown in Figure 2.9 the six plates consist of two trapping plates (5.1 cm x 5.1 cm), two excitation plates (5.1 cm x 7.7 cm), and two detection plates (5.1 cm x 7.7 cm). In order to obtain a mass spectrum with the FTICR-MS, a sequential series of events must occur within the cell located inside the homogenous region of the superconducting magnet at typical pressures of 1 x 10^{-10} Torr.

FTICR-MS involves using the plates in a sequential program of (1) quenching the ICR cell to remove all ions, (2) trapping of ions, (3) excitation of trapped ions, and (4) detection of the trapped ions. As ions enter the cell, the front trapping plate polarity is lowered to 0V for approximately 2-3 ms to allow ions to freely enter the cell, while the back plate may be set to -5 to -10V for trapping. Once inside the cell, the front trapping plate is brought back to -10V, thus creating a parabolic trapping well. Trapped ions experience a circular ion motion that is termed the Lorentz force, perpendicular to the initial velocity and the field of the magnet.[22, 25] The frequency of this cyclotron motion is represented by equation 2.8,

$$v_c = \frac{zB_O}{2\pi m} \qquad 2.8$$

where the frequency in Hertz of the cyclotron motion v_c is calculated from the ions charge in Coulombs, (z) the field strength of the magnet in Tesla (B_O), and by the mass of the ion in kilograms (m). Assuming the magnetic field strength remains constant, the frequency is thus determined by the ion's mass-to-charge ratio or *m/z*.

The thermal cyclotron radius for a given ion entering the ICR cell is determined by equation 2.9.

$$r_{thermal} = \frac{\sqrt{2mkT}}{zB_O} \qquad 2.9$$

where (m) is the mass of the ion, (k) is the Boltzman constant and (T) is the temperature in Kelvin, (z) is the ion charge in Coulombs, and (B_O) is the magnetic field strength in Tesla.

Following the trapping event and prior to detection, ions are excited to a radius that is substantially larger than the thermal radius described above. The excitation plates, which are parallel to the magnetic field, apply a frequency to the ions and thus alter the ions radius. During this application, a large range of frequencies are scanned at once in a broadband excitation and the trapped ions that are in resonance with the applied r.f. field absorb the energy and thus increase its cyclotron radius while maintaining its cyclotron frequency.[22, 26] This is represented by equation 2.10.

$$r_{post-excite} = \frac{V_{p-P}T_{excite}}{2dB_O} \qquad 2.10$$

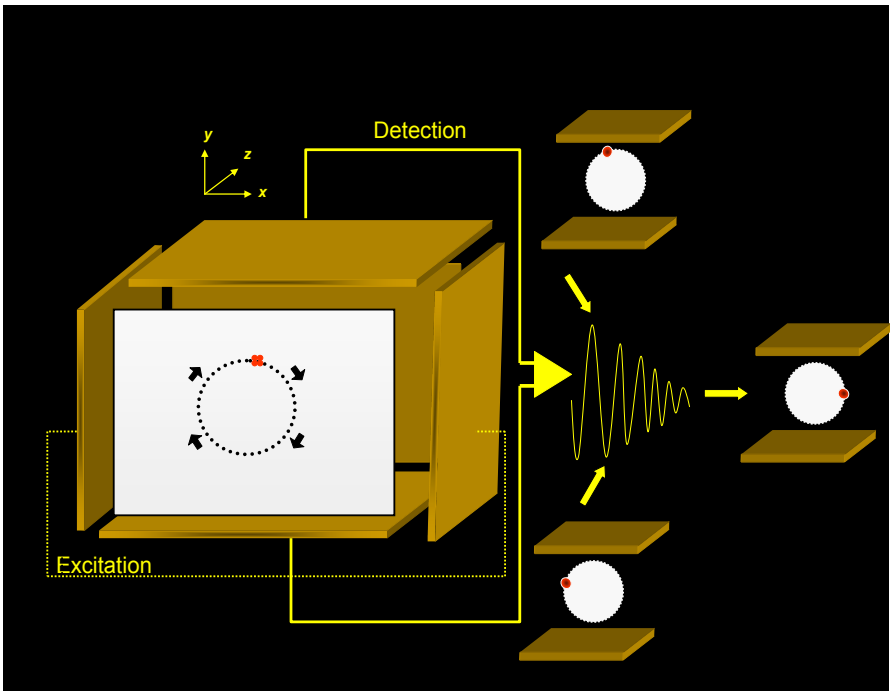

Figure 2.10 Schematic of ICR cell with Detection, Excitation, and trapping plates labeled.

Where ($V_{p\text{-}p}$) represents the potential of the applied r.f. frequency in volts from peak to peak, (d) is the diameter of the ICR or distance between the two plates of the cell in meters.

Once excited to the post-excitation radius, the ions are detected by the two detection plates in parallel with the magnetic field. The detection plates are essentially electrodes and, as the ions are rotating around the cell, they induce an image current by pushing/pulling electrons at the plate interface. As this packet of ions moves away from one plate and toward another it generates a sinusoidal pattern, as depicted in Figure 2.10, which is fast-Fourier transformed into the frequency domain and then subsequently turned to the mass domain by solving equation 2.8.

2.5 Mass spectrometry of biomolecules and metal containing ions

The binding of metal complexes to nucleic acids has been evaluated for more than 20 years.[27] During that time, a variety of techniques including, NMR, ITC, CD, and MS have been used to probe these interactions.[27] Developing an understanding of exactly how these interactions occur is beneficial to the development of new compounds. Noncovalent interactions between anti-tumor, anti-viral, and anti-bacterial compounds with DNA often serve as the precursor to DNA damage or a cascade of interactions that alter the function or act as signaling mechanisms. The use of ESI-MS has been used to study the interactions between DNA and a variety of metals including, transition metals, alkali metals, and even actinide metals.[28]

A number of factors are important when using ESI-MS to investigate the metal-DNA interactions. For instance, the sensitivity of the instrument may be reduced as there is an inherent difficulty in removing the excess metal salts and the disruption of the ion current with the sometimes numerous metal isotopes.[28] Often, an instrument with high resolution is necessary as metal compounds have very complex isotopic distributions. The trinuclear platinum complexes represented in this work are such an example. Finally, metal complexes tend to be more labile during the MS/MS analysis, which make determination of binding sites difficult; therefore enzymatic digestion is often is used.[28]

Using mass spectrometry, Gross and coworkers found that DNA exhibited a different fragmentation profile when its phosphate backbone was complexed with metal ions.[29] It was determined that the addition of metal ions does not change the bonds that are cleaved during the CID process, however, the usual lack of cleavage 3' to thymine is increased in the presence of a bound metal ion.[29]

The multitude of binding opportunities for metal ions with DNA presents a large number of possible interactions with a variety of functional groups and heteroatoms. For instance, Mg^{2+} and K^{+} were shown to have relatively weak electrostatic associations with the phosphodiester backbone of DNA.[29, 30] However, even the weak association was found to play an important role in the stabilization of the secondary and tertiary structures.[30]

A large portion of the research involving metal ions and biomolecules has been focused on the interactions of platinum metals, which is not surprising, given the active role that platinum has played in the treatment for cancer. The interaction of cisplatin with DNA has been extensively studied via ESI-MS[29] and therefore not discussed here. However, some important work looking at the association constants of a $[Pt(NH_3)_4]^{2+}$ with DNA has shown that a rapid interaction occurs that was independent of the location and number of guanine bases.[31] Just as important, the fact that a much larger $[Pt(py)_4]^{2+}$ moiety exhibited less affinity indicated that the size and hydrogen bonding of the ligands with the platinum center may play an important role in the determination of the strength of the interaction.[31]

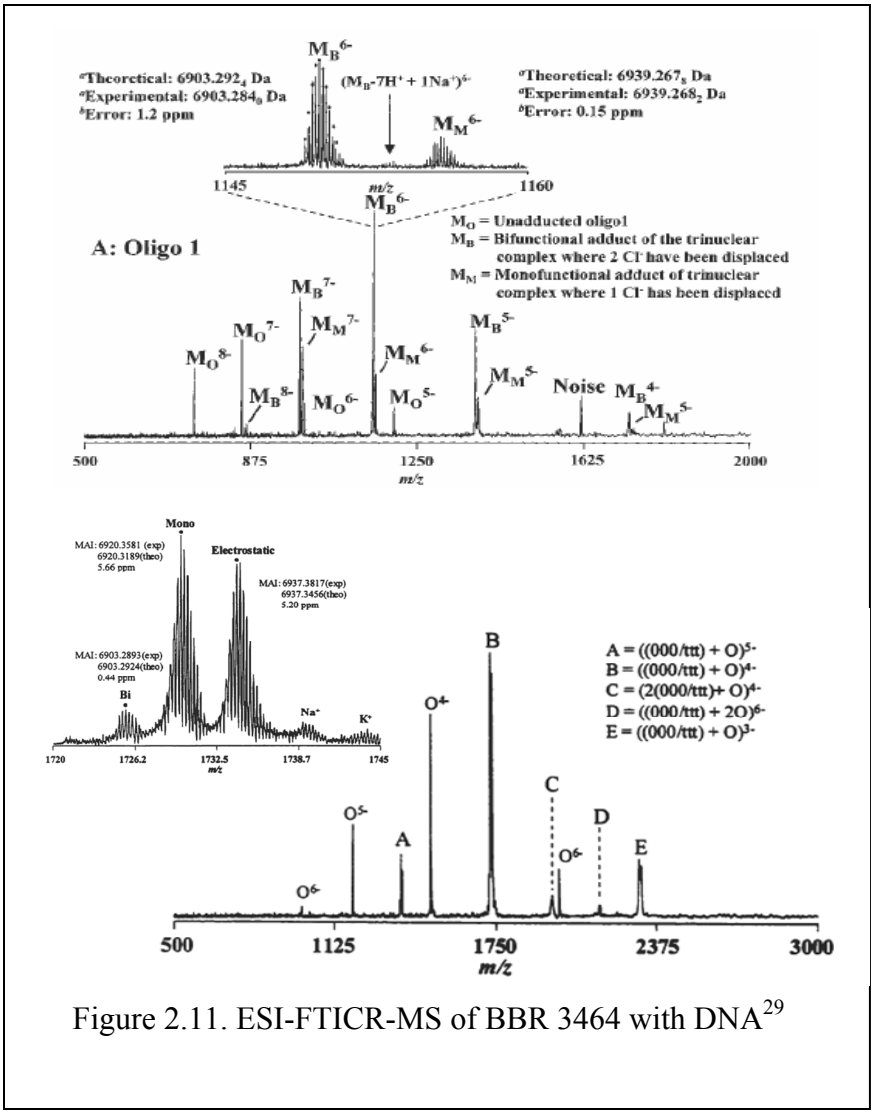

Figure 2.11. ESI-FTICR-MS of BBR 3464 with DNA[29]

The covalent interactions of BBR 3464 with DNA, (figure 2.11) has been investigated using ESI-FTICR-MS, which offers both sensitivity and high resolution.[32] The utility of ESI-MS to preserve the solution structures is seen in the presence of both mono and bi-functional adducts in the interaction of BBR 3464, but also the strong electrostatic association of a AH 44, the noncovalent equivalent compound.[32] (see figure 3.2)

2.6 References

1. Hofstadler, S. A.; Sannes-Lowery, K. A., Applications of ESI-MS in drug discovery: interrogation of noncovalent complexes. *Nat Rev Drug Discov* **2006,** 5, (7), 585-95.

2. Baczynskyj, L.; Bronson, G. E.; Kubiak, T. M., Application of thermally assisted electrospray ionization mass spectrometry for detection of noncovalent complexes of bovine serum albumin with growth hormone releasing factor and other biologically active peptides. *Rapid Commun Mass Spectrom* **1994,** 8, (3), 280-6.

3. Fenn, J. B.; Mann, M.; Meng, C. K.; Wong, S. F.; Whitehouse, C. M., Electrospray ionization for mass spectrometry of large biomolecules. *Science* **1989,** 246, (4926), 64-71.

4. Siuzdak, G., The emergence of mass spectrometry in biochemical research. *Proc Natl Acad Sci U S A* **1994,** 91, (24), 11290-7.

5. Kebarle, P.; Tang, L., From ions in solution to ions in the gas phase - the mechanism of electrospray mass spectrometry. *Analytical Chemistry* **2008,** 65, (22), 972A-986A.

6. Yates, J. R., 3rd, Mass spectrometry and the age of the proteome. *J Mass Spectrom* **1998,** 33, (1), 1-19.

7. Matthias, M., Electrospray: Its potential and limitations as an ionization method for biomolecules. *Organic Mass Spectrometry* **1990,** 25, (11), 575-587.

8. Fenn, J. B., Ion formation from charged droplets: roles of geometry, energy, and time. *Journal of the American Society for Mass Spectrometry* **1993,** 4, (7), 524-535.

9. Whitehouse, C. M.; Dreyer, R. N.; Yamashita, M.; Fenn, J. B., Electrospray interface for liquid chromatographs and mass spectrometers. *Anal Chem* **1985,** 57, (3), 675-9.

10. Yamashita, M.; Fenn, J. B., Electrospray ion source. Another variation on the free-jet theme. *The Journal of Physical Chemistry* **2002,** 88, (20), 4451-4459.

11. Yamashita, M.; Fenn, J. B., Negative ion production with the electrospray ion source. *The Journal of Physical Chemistry* **2002,** 88, (20), 4671-4675.

12. John, B. F.; Matthias, M.; Chin Kai, M.; Shek Fu, W.; Craige, M. W., Electrospray ionization-principles and practice. *Mass Spectrometry Reviews* **1990,** 9, (1), 37-70.

13. Dole, M.; Mack, L. L.; Hines, R. L.; Mobley, R. C.; Ferguson, L. D.; Alice, M. B., Molecular Beams of Macroions. *The Journal of Chemical Physics* **1968,** 49, (5), 2240-2249.

14. Iribarne, J. V.; Thomson, B. A., On the evaporation of small ions from charged droplets. *The Journal of Chemical Physics* **1976,** 64, (6), 2287-2294.

15. Hannis, J. C.; Muddiman, D. C., Characterization of a microdialysis approach to prepare polymerase chain reaction products for electrospray ionization mass spectrometry using on-line ultraviolet absorbance measurements and inductively coupled plasma-atomic emission spectroscopy. *Rapid Communications in Mass Spectrometry* **1999,** 13, (5), 323-330.

16. Igor, V. C.; Alexander, V. L.; Bruce, A. T., An introduction to quadrupole-time-of-flight mass spectrometry. *Journal of Mass Spectrometry* **2001,** 36, (8), 849-865.

17. Gross, J., J. Throck Watson and O. David Sparkman: Introduction to mass spectrometry. Instrumentation, applications, and strategies for data interpretation, 4th ed. *Analytical and Bioanalytical Chemistry* **2008,** 392, (4), 569-570.

18. Marshall, A. G.; Comisarow, M. B.; Parisod, G., Relaxation and spectral line shape in Fourier transform ion resonance spectroscopy. *The Journal of Chemical Physics* **1979,** 71, (11), 4434-4444.

19. Comisarow, M. B.; Marshall, A. G., Fourier transform ion cyclotron resonance spectroscopy. *Chemical Physics Letters* **1974,** 25, (2), 282-283.

20. Melvin, B. C.; Alan, G. M., Frequency-sweep fourier tranform ion cyclotron resonance spectroscopy. *Journal of Mass Spectrometry* **1996,** 31, (6), 588-589.

21. Henry, K. D.; Williams, E. R.; Wang, B. H.; McLafferty, F. W.; Shabanowitz, J.; Hunt, D. F., Fourier-transform mass spectrometry of large molecules by electrospray ionization. *Proc Natl Acad Sci U S A* **1989,** 86, (23), 9075-8.

22. Amster, I. J., Fourier Transform Mass Spectrometry. *Journal of Mass Spectrometry* **1996,** 31, (12), 1325-1337.

23. Mangrum, J. B., Flora, Jason W., Muddiman, C. David, Solution Composition and Thermal Denaturation for the Production of Single-Stranded PCR Amplicons: Piperidine-Induced Destabilization of the DNA Duplex? *American Society for Mass Spectrometry* **2002,** 13, 232-240.

24. Senko, M. W.; Hendrickson, C. L.; Emmett, M. R.; Shi, S. D. H.; Marshall, A. G., External Accumulation of Ions for Enhanced Electrospray Ionization Fourier Transform Ion Cyclotron Resonance Mass Spectrometry. *Journal of the American Society for Mass Spectrometry* **1997,** 8, (9), 970-976.

25. Schweikhard, L.; Marshall, A. G., Excitation modes for Fourier transform-ion cyclotron resonance mass spectrometry. *Journal of the American Society for Mass Spectrometry* **1993,** 4, (6), 433-452.

26. Marshall, A. G.; Hendrickson, C. L.; Jackson, G. S., Fourier transform ion cyclotron resonance mass spectrometry: a primer. *Mass Spectrom Rev* **1998,** 17, (1), 1-35.

27. Urathamakul, T.; Waller, D. J.; Beck, J. L.; Aldrich-Wright, J. R.; Ralph, S. F., Comparison of Mass Spectrometry and Other Techniques for Probing Interactions Between Metal Complexes and DNA. *Inorganic Chemistry* **2008,** 47, (15), 6621-6632.

28. Jennifer, L. B.; Michelle, L. C.; Stephen, F. R.; Margaret, M. S., Electrospray ionization mass spectrometry of oligonucleotide complexes with drugs, metals, and proteins. *Mass Spectrometry Reviews* **2001,** 20, (2), 61-87.

29. Wang, Y.; Taylor, J.-S.; Gross, M. L., Fragmentation of electrospray-produced oligodeoxynucleotide ions adducted to metal ions. *Journal of the American Society for Mass Spectrometry* **2001,** 12, (5), 550-556.

30. Cowan, J., *Inorganic Biochemstry, An Introduction* **1997**, (Wiley-VCH), New York, USA.

31. Carte, N.; Legendre, F.; Leize, E.; Potier, N.; Reeder, F.; Chottard, J.-C.; Van Dorsselaer, A., Determination by Electrospray Mass Spectrometry of the Outersphere Association Constants of DNA/Platinum Complexes Using 20-mer Oligonucleotides and ([Pt(NH3)4]2+, 2Cl-) or ([Pt(py)4]2+, 2Cl-). *Analytical Biochemistry* **2000,** 284, (1), 77-86.

32. Kloster, M. B.; Hannis, J. C.; Muddiman, D. C.; Farrell, N., Consequences of nucleic acid conformation on the binding of a trinuclear platinum drug. *Biochemistry* **1999,** 38, (45), 14731-7.

Chapter 3:
Determination of binding site location of polynuclear platinum complexes along the polyanionic phosphate backbone of DNA

3.1 Introduction

Mass spectrometry has been applied to a variety of different drug discovery approaches.[1] The abbreviated list includes: identification of drug metabolites, drug target identification, drug screening, pharmacokinetics, and the covalent and noncovalent associations with biomolecules.[1]. The usefulness of tandem mass spectrometry (ms/ms) as a tool for the characterization of biopolymers such as DNA, is well established,[2-5] and is based on both the accuracy of measuring parent/product ions and the ability to derive structural information from unimolecular dissociation chemistry.[6] In instances where the nucleic acid is resistant to degradation by enzymatic methods, ms/ms provides an excellent means of obtaining sequence information.[7]

The products produced from the fragmentation of DNA result from cleavage of the phosphate backbone as first described by Grotjhan and co-workers in 1982.[6, 8-10] McLuckey in 1992 devised a nomenclature scheme that resembled that of the naming scheme for peptides and proteins.[11, 12] The nomenclature depicted in figure 3.1 describes the four possible cleavage products in relation to their orientation of the 5′ or 3′ terminus. The notation of *a,b,c*, and *d* describe fragments that contain the 5′ terminus and the *w,x,y,* and *z* notation relates to fragments containing the 3′ terminus. Sequence position is noted with numerical values and (B) represents a nucleobase A,T,G, or C.

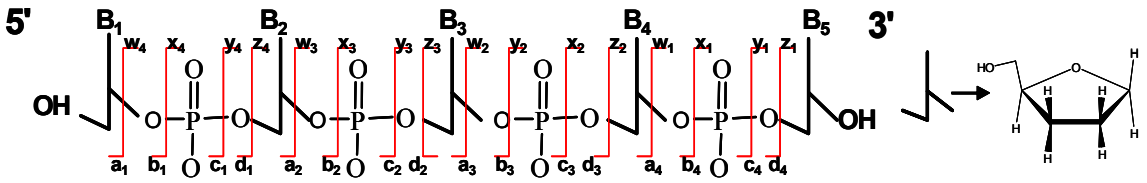

Figure 3.1. McLuckey nomenclature for DNA cleavage.

During the CID process, the phosphate group has a strong effect on the metastable decomposition and CID of the negatively charge nucleotides.[6] For a series of small mono and di-nucleotides, base loss from the 5′ terminus is almost always preferred over base loss from the 3′ terminus.[6] The basicity of the nucleobases also has an impact on whether the resultant fragmentation includes loss of the base as an ion or a neutral.[6] The order of basicity for the nucleobases is $C^- > T^- > A^- > G^-$ when comparing the relative abundances of the BH elimination.[6] Following an exhaustive set of experiments,[13-15] McLuckey was able to establish the following tendencies for single-stranded oligonucleotide fragmentations:

(1) the initial dissociation step results in the loss of a base which can be either charged or neutral depending on the parent ion charge. Low charge state parent ions generally resulted in neutral base loss and higher parent charge resulted in charged bases being formed.

(2) the 3′ terminus is usually disfavored in the loss of a base.

(3) the most important fragmentation step is the subsequent cleavage of the 3′ C-O bond of the sugar from which the base is lost. This generally gives w and a-B type ions irrespective of charge or nature of the base.

(4) lower charge states generally result in more loss of the PO_3^- group and can compete for the loss of the base.

3.2 Platinum Complex-DNA Interactions:

Investigations into the association and dissociation mechanisms of Pt drugs with DNA may potentially lead to a better understanding of how these compounds exhibit their antitumor properties. The soft ionization of electrospray coupled with mass spectrometry has enabled research into the electrostatic outersphere associations between oligonucleotides and two mono-nuclear platinum species: platinum tetram(m)ine $[Pt(NH_3)_4]^{2+}$ and platinum tetrapyridine $[Pt(py)_4]^{2+}$.[16] Tandem mass spectrometry (MS/MS) has proven to be a powerful tool in gathering sequence information from nucleic acids, when there are difficulties in obtaining the data through enzymatic digestion.[7] Initial reports of MS/MS of platinated oligonucleotides date back to 1991 by Martin et al[17] and 1992 with Costello et al.[18] In addition to cleavage of the glycosidic bond of the oligonucleotide, the platinum sphere consistently lost the NH_3 groups. It is noted that the cleavage of the N-glycosidic bond is promoted when cisplatin is bound to the oligonucleotide.[17] Martin et. al. showed that platination helped stabilize the oligonucleotide and results in a significant decrease in fragment ion abundance.[7] Iannitti-Tito performed ms/ms studies on a hexa-oligonucleotide with cisplatin and could not determine a sequence specific fragmentation pattern.[19]

A detailed study of polybasic noncovalent binding complexes with DNA has shown that such interactions can be identified using mass spectrometry.[20] Furthermore, CID has proven to be useful in the illustration of possible fragmentation pathways of an oligonucleotide complexed with polybasic peptides.[20]

3.3 Antisense Therapeutics:

Antisense oligonucleotides offer a promising therapeutic solution to selectively control gene expression in certain cancers. It has been previously shown that when Bcl-2 antisense oligonucleotide therapy is used in conjunction with treatment of cisplatin in MCF-7 breast cancer cells, cell viability decreases.[21] Combination therapies involving cisplatin and Bcl-2 antisense oligonucleotides have also shown some success in other types of cancer. In the bladder cancer cell lines T24R1 and T24R2, the addition of the Bcl-2 antisense oligonucletotide was concluded to reverse cisplatin resistance and amplify the cytoxity of the cisplatin.[22] Recently, Bcl-2 antisense oligonucleotides with cisplatin therapy led up to an 80% cure rate in mice with nasopharyngeal carcinoma.[23]

Antisense oligonucleotides are distinctive in that the chemical composition of the nucleotide can be altered to render it more resistant to nuclease degradation in vivo. Currently, modified oligonucleotides are being investigated in clinical trials for their antisense binding properties. The most successful antisense oligonucleotides involve the modification of the phosphate backbone of the oligonucleotide with a sulfur atom, currently marketed under the name G3139-Genasense®. This modification renders the oligonucleotide more resistant to nuclease degradation, but it also has been shown to increase the cyctoxicity by nonspecific binding to serum proteins. Additionally, it has been shown that modification of DNA with the addition of cationic amino or guanidinum groups is successful in achieving an efficient antisense oligonucleotide.[24] Important as it relates to the research in this dissertation, the increased stabilities of these structures were attributed to a localized region of reduced negative charge on the antisense-guanidinium complex.[24] Even with its success, antisense strategies have their limitations and short comings, such as poor stability and low cellular uptake. It has been

reported that cellular uptake of the oligonucleotide can be < 2% of the initial dose depending on the specific type of oligonucleotide chemical composition and certain cell types.[25-27]

The use of noncovalently bound platinum compounds to provide increased stability allows for a native DNA backbone structure that may result in less cytotoxicity issues. Also, the addition of the highly charged platinum compound may enhance cellular uptake. Our group has recently shown that the use of these highly charged (4+ to 6+) polynuclear platinum compounds successfully stabilized calf thymus DNA by increasing the melting temperature by as much as 20°C.[28] We have also shown that the cellular accumulation of the "noncovalent" polynuclear platinum compound is about 5 times greater than the covalent parent compound BBR 3464 in A2780 human ovarian tumor cell lines.[29]

In this current investigation we have chosen to study the gas-phase stability of the oligonucleotide-platinum complex using electrospray ionization mass spectrometry (ESI-TOF-MS/MS). For the work presented in this chapter we studied a synthetic mimic of the 18-mer oligonucleotide antisense sequence specific for the Bcl-2 mRNA (5`-TCTCCCAGCGTGCGCCAT-3`) currently used in clinical trials by Genta, not containing the modified phosphothiorate oligonucleotide backbone. The synthetic oligonucleotide purchased did not have the modified backbone. Aside from a fundamental interest, this study deals with a model of DNA that is of great interest in antisense gene therapy.

3.4 Experimental:

Experiments were conducted on a Micromass-Waters Qtof-2 mass spectrometer (Milford, MA) equipped with a custom built microspray source. Electrospray source conditions were kept constant with a source temperature of 120°C, capillary voltage of 2.0 kV, cone voltage 38 V, and flow rates of 0.5 µL/min. In tandem mass spectrometry (MS/MS) experiments, collisional energy was varied from 10 eV to 40 eV. The use of translational energy to represent the applied collisional energy in this work was chosen so that comparisons could be made between complexes of differing charge states. The translational energy is the product of the ions charge state and the applied collisional voltage.

The oligonucleotide 5′-TCT CCC AGC GTG CGC CAT-3′ (M= 5411.5 Da) was purchased from Midland Certified Reagents, (Midland, TX) and further desalted in a custom built dialysis chamber using hollow 13,000 molecular weight cut off (MWCO) filters in 20 mM ammonium acetate. The dialysis of the oligonucleotide in ammonium acetate results in displacement of Na^+ and K^+ ions from the anionic backbone and replacement with NH_4^+ ions. During the electrospray desolvation process the NH_4^+ loses a proton and NH_3 is lost as a neutral molecule. The dialyzed oligonucleotides are now relatively salt free making for a cleaner mass spectrum.

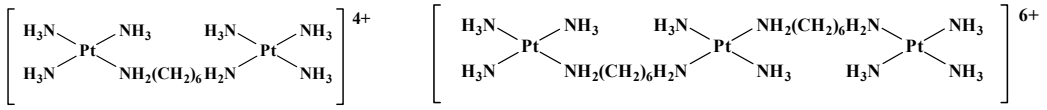

0,0 (n =6)
AH 88

0,0,0 (n =6,6)
AH 44

Figure 3.2. Noncovalent platinum complexes

Oligonucleotides were reconstituted in 18 Ω ohm water and quantified by UV-VIS at 260 nm. Noncovalent polynuclear platinum compounds AH 88 (M = 608 Da) and AH 44 (M = 953 Da) were synthesized in house and purified using HPLC.[28]

A stock solution of 500 uM Pt compound was prepared in 18 Ω ohm water. Oligonucleotides and Pt compounds were mixed in a 1:1 molar ratio and incubated at 37°C for 20 minutes then mixed with electrospray solution to form 50:50 methanol:20 mM ammonium acetate. Full scan and tandem MS/MS data were analyzed using MassLynx 4.0 software.

3.5 Results and Discussion:

Detection of Noncovalent Complexes:

Herein we describe the detection by ESI-TOF-MS of noncovalent complexes between polynuclear platinum anticancer compounds with an antisense oligonucleotide sequence. As we expect these complexes to be negatively charged in solution, all spectra were obtained in negative ionization mode. Figure 3.3 (A) and (B) show the full scan spectra of AH 88 (4+) and AH 44 (6+) electrostatically interacting with the 18-mer oligonucleotide, respectively. Free oligonucleotide, present in each spectra with charge states ranging from four to six negative charges and oligonucleotide:polynuclear platinum complexes with the same four to six negative charge states. The absence of the free platinum compound is expected in the negative ionization mode, as they have a high positive charge and no acidic groups to deprotonate and therefore are unlikely to be detected. Given the high charge and size of these polynuclear platinum complexes, the most abundant stoichiometry observed was 1:1. It should be noted that the much smaller and lesser charged AH 88 (4^+)is capable of forming a 1:2 binding ratio under these conditions with the 18-mer oligonucleotide, but is only represented at approximately 5% of the

relative abundance(see figure 3.3 A). The addition of two AH 88 platinum compounds of this size and charge, presumably still results in the remaining phosphate groups of the oligonucleotide retaining sufficient negative charge for detection. The high charge of AH 44 would most likely result in coulombic repulsions of two platinum compounds on the single strand and is unlikely to exist during the ESI desolvation process, not to say that it cannot exist in solution. It should be noted that the ammonium acetate concentration of 20mM was adequate for

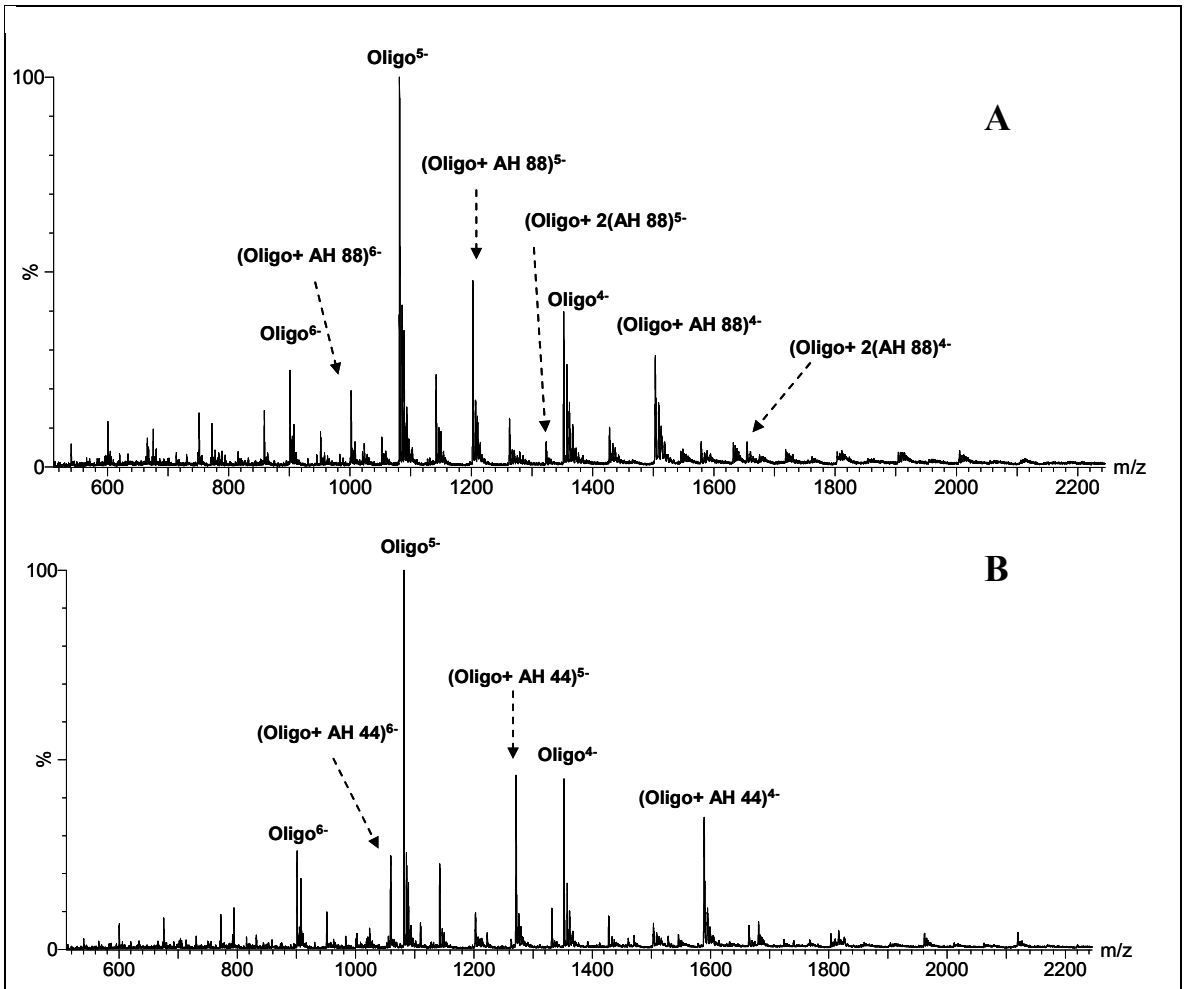

Figure 3.3. Full scan ESI-TOF-MS of 18-mer oligonucleotide 5′- TCT CCC AGC GTG CGC CAT -3′ with (A) AH 88^{4+} and (B) AH 44^{6+}. Most abundant complex peaks correspond to 1:1 stoichiometry for each of the represented charge states.

the detection of these electrostatic complexes. Terrier and co-workers have recently shown that polybasic compounds interacting electrostatically with oligonucleotides are ionic in solution and therefore compete with ammonium ions from the ammonium acetate for phosphate residues.[20] During this research, no effort was made to quantitatively determine the binding affinities of these complexes or reaction rates. Mass spectrometry, while extremely useful, can present problems when comparing complexes of different size and structure due to the differences in ionization potentials, leading to misleading results. In addition, for research in probing electrostatic interactions between complexes, the species represented in solution may not always transfer to the gas phase in the same proportions. Therefore, this study focuses on the gas phase stability of the complexes formed between the novel polynuclear platinum compounds and the phosphates of an oligonucleotide.

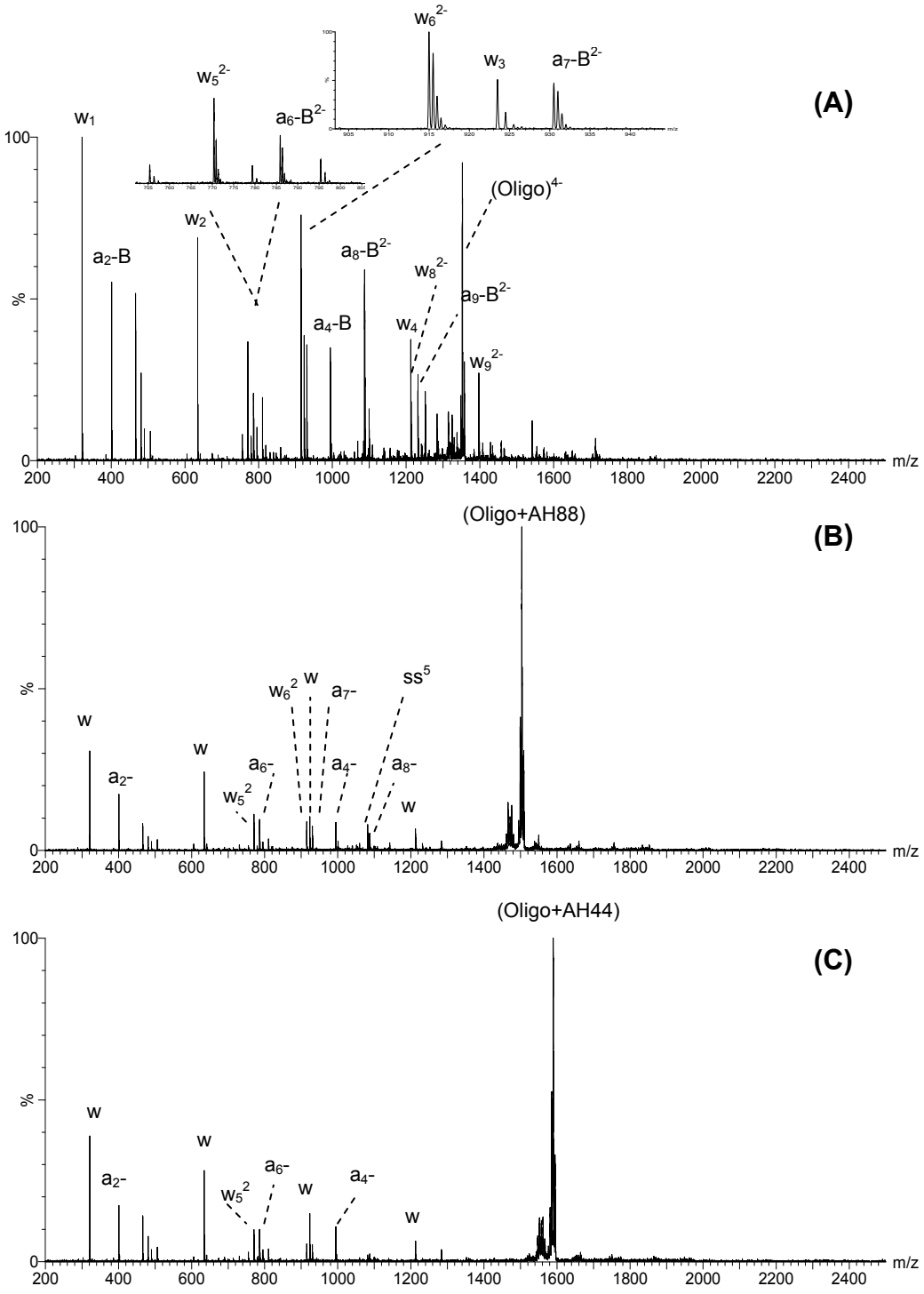

Figure 3.4 ESI-MS/MS spectra of (A) $(Oligo)^{4-}$, (B) $(Oligo+AH\ 88)^{4-}$, (C) $(Oligo+AH44)^{4-}$. Translational energies are (A) 100 eV, (B) 120 eV, and (C) 120 eV.

Collision Induced Dissociation (CID)

Tandem mass spectrometry experiments were done on free oligonucleotide, and then with the electrostatic complexes of oligonucleotide with AH 88 and AH 44. For each system two charge states, the 4- and 5-, were studied in efforts to see how higher charge distributions affected the fragmentation profile. The CID investigations were done at progressively higher translational energies up to the point where the parent ion was completely dissociated or removed from the spectrum. As these samples were introduced into the mass spectrometer in negative ionization mode, the lack of negatively charged polynuclear platinum complexes in the full scan spectra was expected. Tandem mass spectrometry experiments of the "free" oligonucleotides and the complexed oligonucleotides allowed for the determination of an approximate binding location along the phosphate backbone. Using McLuckey nomenclature for oligonucleotide fragmentation, we were able to determine that these polynuclear platinum complexes increase the overall stability of the phosphate backbone along the interior nucleotides and do not alter the dominant fragmentation mechanism of producing *a* and *w* type ions. Additionally, we have used mass spectrometry to rapidly identify the binding site location for a polynuclear platinum compound on the phosphate backbone.

Free Oligonucleotide.

The CID products of the free unbound 18-mer oligonucleotide in Figure 3.4 were representative of covalent bond cleavage of the phosphodiester backbone. Sequence fragment ions produced at the different translation energies were of the a_n-B and w_n type, according to McLuckey nomenclature. As shown in Figure 3.5, the fragmentation of the 4^- free oligonucleotide (A) at m/z 1352 and at 100 eV of translational energy, covers nearly complete fragmentation. The

spectra in Figure 3.4 represents the translational energy at which approximately 50% of the parent ion exists in the spectra.

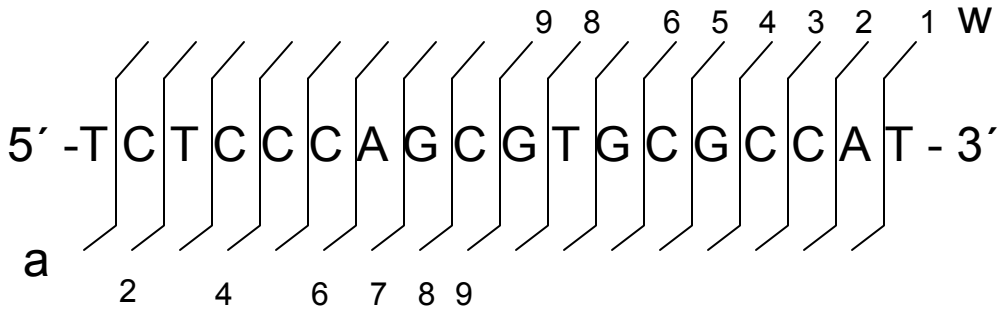

Figure 3.5 McLuckey fragmentation profile of free oligo at 100V of translational energy. Nearly complete fragmentation of the backbone is observed allowing for all peak assignments

The plot of fragment ions illustrates that approximately equal distribution of a-type and w-type ions exists. Nearly complete sequence coverage was achieved with the only fragments that do not appear in the spectra being those from the 3′- side of the thymine base. This correlates well with known DNA fragmentation data in that the 3′- side of the thymine base is not readily seen as a w-type ion. Careful inspection of the data, show peaks at 466 m/z and 481 m/z that are internal fragment ions of the oligonucleotide. These peaks occur at the higher translational energies and are therefore due to the higher energies involved or the possible result of secondary fragmentations. The relative abundances for all the ions produced are displayed in the histogram in Figure 3.6. As is expected, higher translational energies led to more sequence coverage.

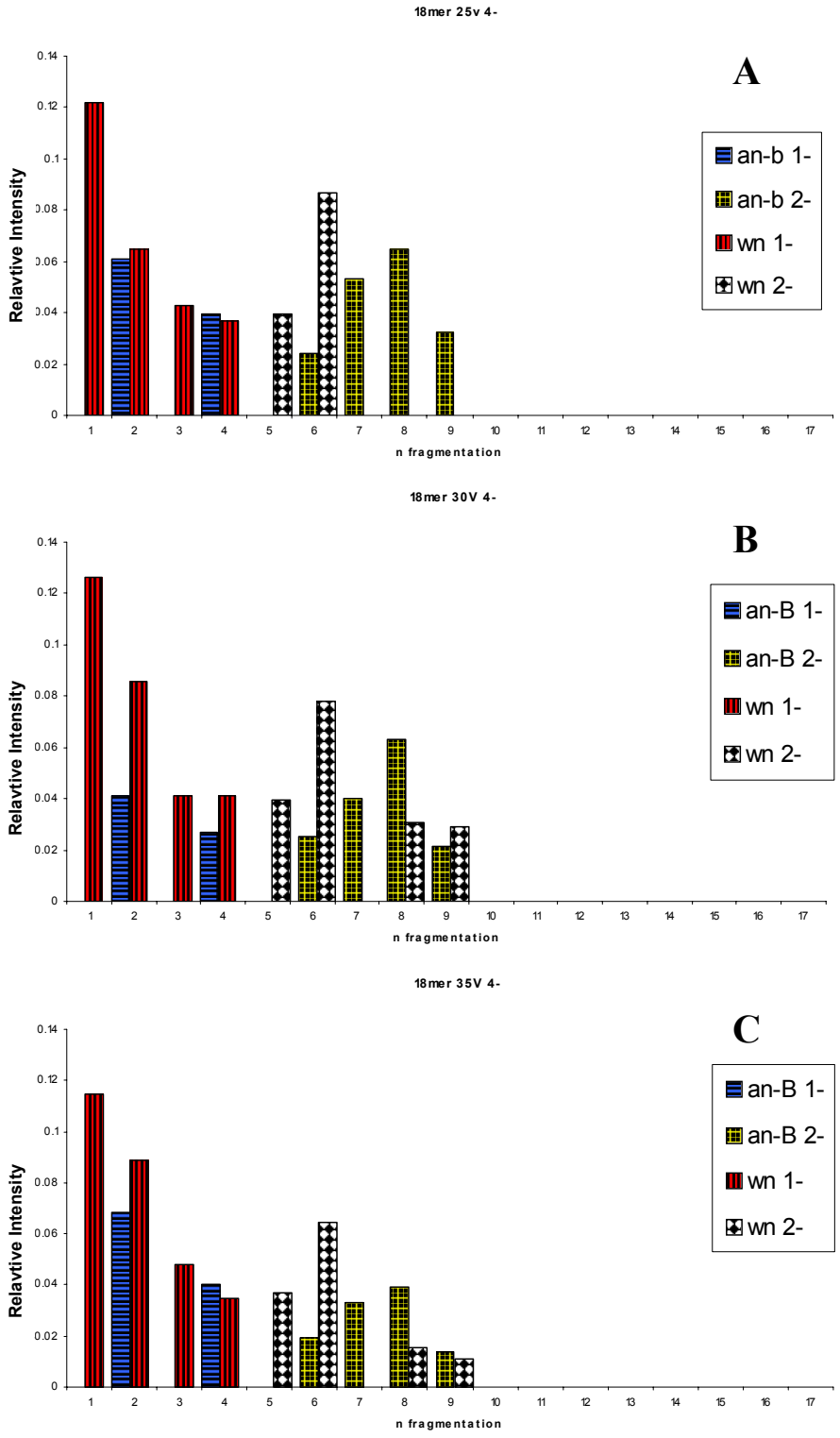

Figure 3.6 Relative intensity plot of free a-B/w-ions of free oligonucleotide at varying translational energy (A) 100 eV, (B) 120 ev, (C) 140 eV. Internal fragments omitted from data.

Polynuclear platinum compound AH 88^{4+}.

In the CID spectrum (Figure 3.5 B) of the (oligo+AH 88)$^{4-}$ at 120 eV translational energy, the product ions produced are still of the a-B and w-type ions. Upon, further review of the spectra, a peak at 1081 m/z appears which would correspond to the 5^{-} intact free 18-mer oligonucleotide. This was unexpected as a shift to lower charge states is normally observed during the CID process as intact molecules lose a charged fragment and therefore shift to a higher mass-to-charge ratio. This fragment ion was produced from the noncovalent dissociation of the AH 88 from the oligonucleotide. It is reasonable to believe that the gas phase interaction of the amines on the platinum compound with the phosphate resulted in a region of neutral charge with a hydrogen bond being formed between the two species. Upon CID, the the hydrogen bond between the phosphate and amines is broken and the proton remains on the platinum moiety. The stabilizing effects of the highly charged cationic platinum complex when noncovalently attached to the 18-mer oligonucleotide over the "free" 18-mer oligonucleotide are seen in the increase in collision energy necessary to induce backbone cleavage of the oligonucleotide.

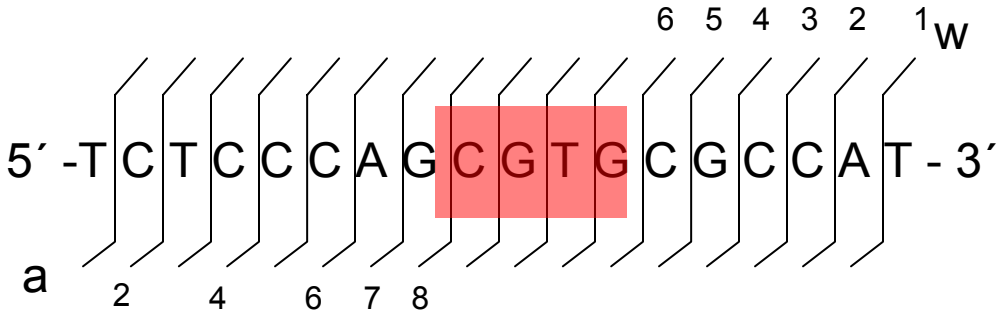

Figure 3.7. CID fragmentation of (oligo+AH88)$^{4-}$ at 120 eV translational energy. Region of enhanced stability highlighted

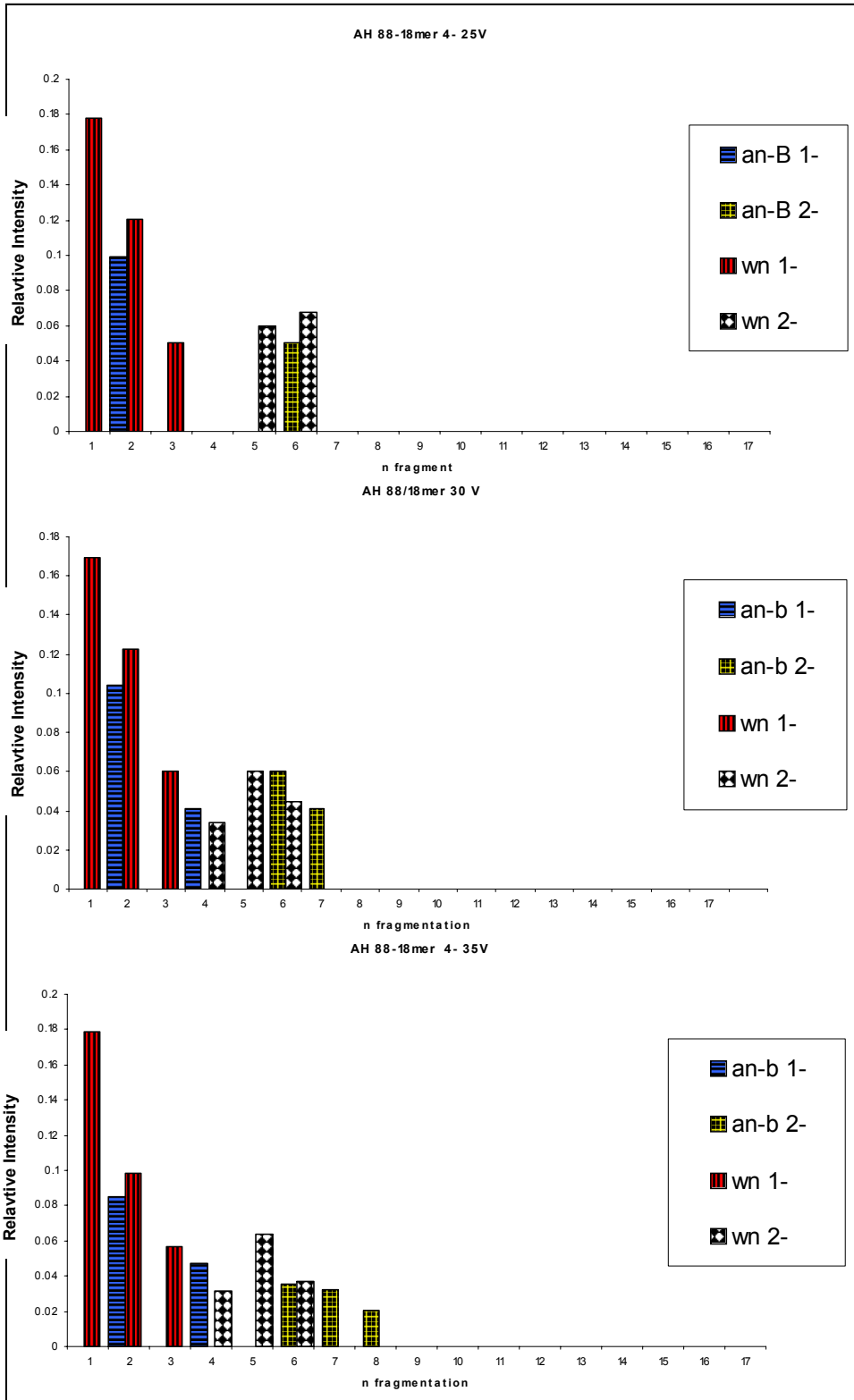

Figure3.8 Relative Intensity plot of the 4- AH 88/18-mer complex a-B/w ions produced by CID of free 18-mer oligonucleotide. (A) 100 eV (B) 120 eV (C) 140 eV translational energy.

Polynuclear platinum compound AH 44^{6+}.

The Figure 3.4 (C) displays the spectrum of (oligo+AH 44)$^{4-}$ Pt complex at 1590 m/z and 120 eV of translational energy. The number and intensity of product ions observed are noticeably less for this translational energy. Unlike the fragmentation for the dinuclear AH 88^{4+}, there is no remaining free oliognucleotide as the result of a noncovalent dissociation pathway. Again, due to the lack of acidic sites, the polynuclear platinum comound does not bear a negative charge and is thus not observed. The increase in overall stability is noticeable in the presence of remaining oligonucleotide/Pt complex in the spectra. Upon further investigation of the sequence coverage

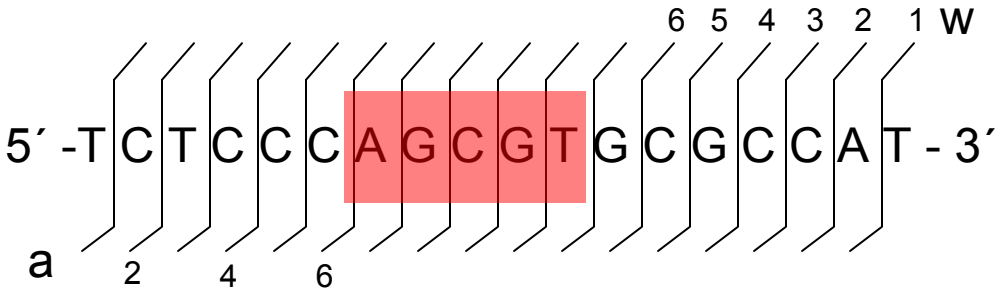

Figure 3.9 Oligo+AH 44 fragmentation profile. The area highlighted in red represents the portion of the oligo that was not identifiable in the spectra. The absence represents the presumed binding site for AH 44.

with the Pt adducts reveals that an intact five-nucleobase stretch in the internal sequence of the bases exists. The increase in collision energy is representative of the increased stability of the phosphate backbone via the hydrogen bonding of the AH 44 trinuclear platinum complex. The location of increased stability represents five potential phosphates for which the Pt adduct may have been located. We know from crystallographic data that our trinuclear complexes are capable of spanning three phosphate groups in a backbone tracking binding motif.[30] This would point to the overall charge of 6+ from the AH 44 neutralizing the five phosphate groups, and thus remain undetected in the spectra. The disappearance of the complex and no free AH 44 or fragments containing the complex indicates that the AH 44 most likely bears no charge within

the complex. The missing portion of the sequence would effectively have zero charge and not be visible in the negative ion spectra. At no point during the CID process were there any observable free oligonucleotide peaks, further illustrating the strong interaction of the AH 44 with the phosphate backbone.

Positive ESI-MS/MS of the 18-mer oligonucleotide with AH 44 and 88 were conducted to determine if an oligonucleotide fragment complexed with the AH 44 could be detected (Data not shown). The results however, failed to provide any detail of binding site location and more importantly, the presence of free AH 44 was not detected either. These results were unexpected as the positive ionization mode should provide a spectrum of the cationic AH 44 and 88. The most plausible explanation is that upon interaction of the AH 44 and 88 with the phosphate backbone a neutral region is formed and because of the stability of the phosphate clamp there is no discernible dissociation.

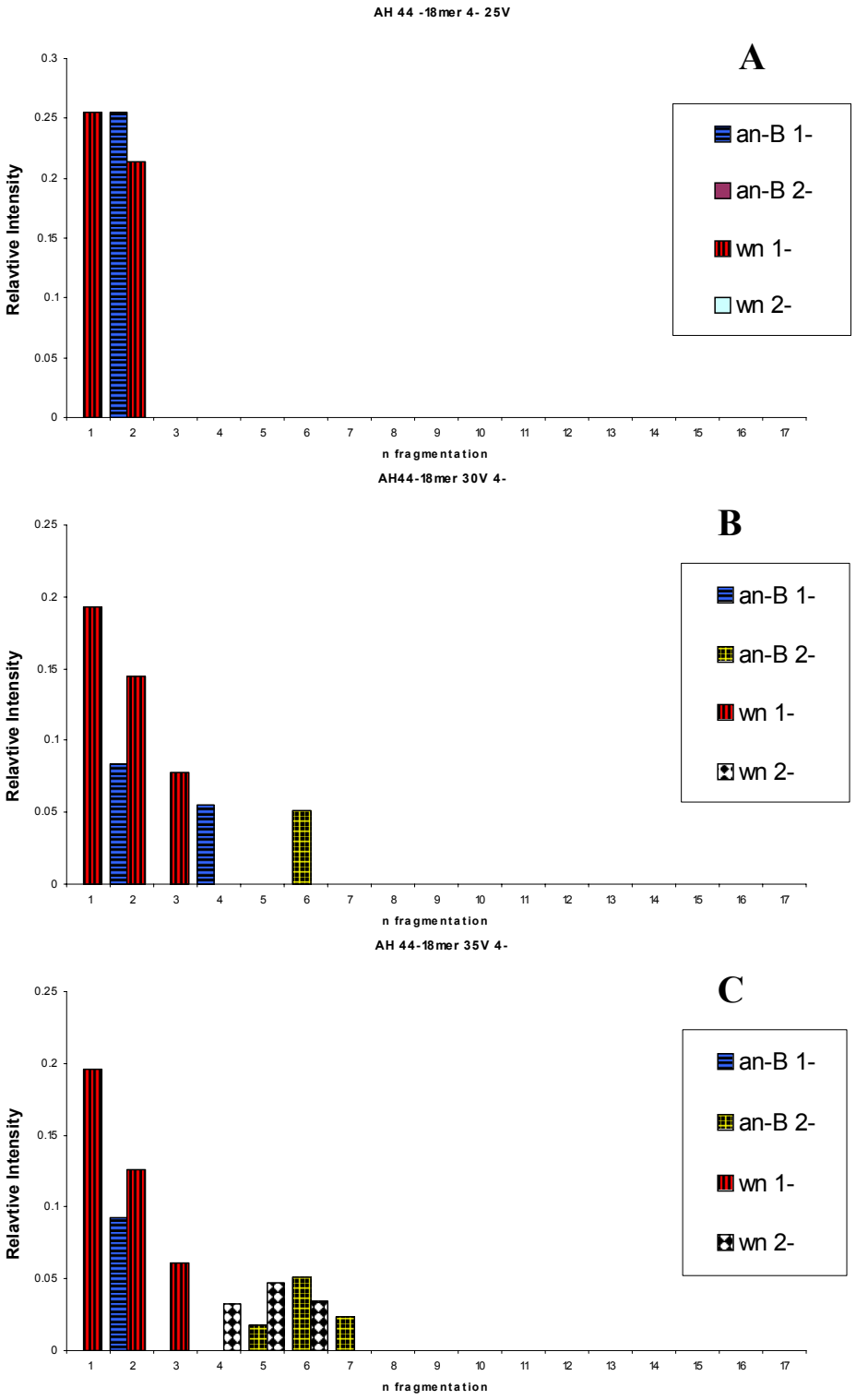

Figure 3.10 Relative Intensity plot of the 4- AH 44/18-mer complex a-B/w ions produced by CID of free 18-mer oligonucleotide. (A) 100 eV (B) 120 eV (C) 140 eV translational energy. Internal fragment ions not included in graphs

Fragmentation pathway for oligonucleotide-polynuclear platinum complexes.

Based on the observed fragmentation patterns and binding site location of these noncovalent complexes, we propose two possible fragmentation pathways occurring in the gas phase, Figure 3.11. Pathway 1A involves the noncovalent dissociation of the platinum moiety from the intact oligonucleotide which is then preceded by pathway 1B where secondary fragmentations result in the production of the a-B and w type ions. As seen in the CID spectra of the $(oligo+AH88)^{4-}$, only a small fraction of the complex exhibits this dissociation pathway, but we feel that it is important to mention.

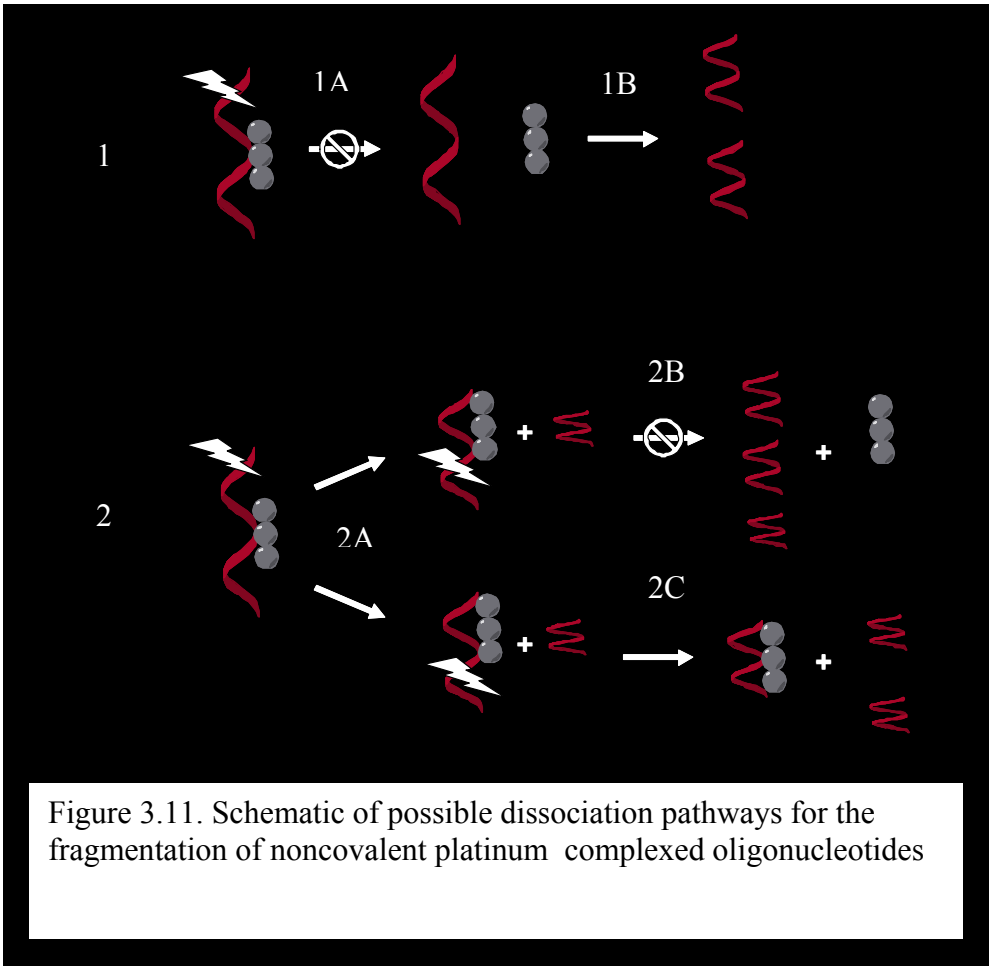

Figure 3.11. Schematic of possible dissociation pathways for the fragmentation of noncovalent platinum complexed oligonucleotides

This pathway is more likely for polybasic compounds that have the ability to carry a negative charge upon dissociation, as the increase in negative repulsion between the oligonucleotide and compound would make noncovalent dissociation favorable. In our case, the platinum species will most likely come off as a neutral, but the possibility still exists. Pathway 2A represents a more favorable dissociation scheme for these highly charged and extremely stable platinum-DNA compounds. First, because these oligo+Pt complexes are so stable, noncovalent dissociation is unfavored and covalent cleavage of the phosphodiester backbone is the primary pathway. As seen in the CID experiments, small singly charged oligonucleotide a-B and w-type fragments dominate the spectra. This is indicative of the cleavages occurring on either side of the stabilized region of platinum binding. As only four available charges are present on either side, we get mainly single charged fragments until we increase the translational energy to 140 eV. Pathway 2B would only be likely to occur if secondary collisions were to noncovalently dissociate the complex from the now smaller oligo fragment + platinum compound. We do not see any evidence of larger sequence ions in the spectra that would correlate to pathway 2B. Lastly, pathway 2C depicts the possibility of secondary collisions cleaving the remaining phosphodiester backbone leaving the remaining platinum bound region unfragmented and undetectable by mass spectrometry as it does not carry a charge.

3.6 Conclusions

The results presented in this work show that the electrostatic interaction between highly charged polynuclear platinum complexes and single stranded oligonucleotides is extremely strong in the gas phase. The high stability of the interactions between the phosphate groups and the platinum complexes was confirmed by the dominant covalent fragmentation pathway observed. Only the

small AH 88^{4+} resulted in a minimal amount of noncovalent dissociation to produce free single stranded oligonucleotide. The increase in size and charge of AH 44^{6+} did not promote the noncovalent dissocation as the stability of the overall complex with the additional hydrogen bonding was greater. Upon inspection of the higher translational energy spectra, it is apparent that the overall complex is losing ~ 17 mass units, which may correspond to the fragmentation of the NH_3 ligands on the platinum compound. Indeed, Schaff and coworkers have identified the loss of NH_3 during the ESI surface collision induced dissociation experiments from both cis and trans dinuclear platinum complexes.[31]

It is noteworthy to illustrate that no peak in the spectrum corresponds to loss of the Pt adduct from the intact oligonucleotide. The lack of coulombic repulsions between the AH compounds and the oligonucleotide create a region of increased stability that must be overcome and therefore the pathway that dominates the CID spectra is the covalent fragmentation of the backbone. The lack of charge between the areas of interaction between the two is further illustrated in the absence of any Pt adducted oligonucleotide fragments. Finally, we have used mass spectrometry as a rapid and efficient means to determine the approximate binding site location of noncovalent polynuclear platinum compounds on an oligonucleotide. This provides a much simpler method of identification in comparison to other tedious methods such NMR and enzymatic cleavage.

3.7 References

1. Alves, S.; Woods, A.; Delvolvo, A.; Tabet, J. C., Influence of salt bridge interactions on the gas-phase stability of DNA/peptide complexes. *International Journal of Mass Spectrometry* **2008,** 278, (2-3), 122-128.

2. Keller, K. M.; Brodbelt, J. S., Charge state-dependent fragmentation of oligonucleotide/metal complexes. *Journal of the American Society for Mass Spectrometry* **2005,** 16, (1), 28-37.

3. Ni, J.; Pomerantz, S. C.; Rozenski, J.; Zhang, Y.; McCloskey, J. A., Interpretation of Oligonucleotide Mass Spectra for Determination of Sequence Using Electrospray Ionization and Tandem Mass Spectrometry. *Analytical Chemistry* **1996,** 68, (13), 1989-1999.

4. Nordhoff, E.; Kirpekar, F.; Roepstorff, P., Mass spectrometry of nucleic acids. *Mass Spectrometry Reviews* **1996,** 15, (2), 67-138.

5. Patrick, A. L., Indirect mass spectrometric methods for characterizing and sequencing oligonucleotides. *Mass Spectrometry Reviews* **1996,** 15, (5), 297-336.

6. Wu, J.; McLuckey, S. A., Gas-phase fragmentation of oligonucleotide ions. *International Journal of Mass Spectrometry* **2004,** 237, (2-3), 197-241.

7. Nyakas, A.; Eymann, M.; Schurch, S., The influence of Cisplatin on the gas-phase dissociation of oligonucleotides studied by electrospray ionization tandem mass spectrometry. *J Am Soc Mass Spectrom* **2009,** 20, (5), 792-804.

8. Grotjahn, L.; Frank, R.; Blocker, H., Ultrafast sequencing of oligodeoxyribonucleotides by FAB-mass spectrometry. *Nucleic Acids Res* **1982,** 10, (15), 4671-8.

9. Cerny, R. L.; Tomer, K. B.; Gross, M. L.; Grotjahn, L., Fast atom bombardment combined with tandem mass spectrometry for determining structures of small oligonucleotides. *Analytical Biochemistry* **1987,** 165, (1), 175-182.

10. Cerny, R. L.; Gross, M. L.; Grotjahn, L., Fast atom bombardment combined with tandem mass spectrometry for the study of dinucleotides. *Anal Biochem* **1986,** 156, (2), 424-35.

11. McLuckey, S. A.; Van Berker, G. J.; Glish, G. L., Tandem mass spectrometry of small, multiply charged oligonucleotides. *Journal of the American Society for Mass Spectrometry* **1992,** 3, (1), 60-70.

12. Roepstorff, P.; Fohlman, J., Proposal for a common nomenclature for sequence ions in mass spectra of peptides. *Biomed Mass Spectrom* **1984,** 11, (11), 601.

13. McLuckey, S. A.; L.Stephenson, J. J.; O'Hair, R. A. J., Decompositions of odd- and even-electron anions derived from deoxy-polyadenylates. *Journal of the American Society for Mass Spectrometry* **1997,** 8, (2), 148-154.

14. Scott, A. M.; Gopalakrishnan, V.; Sohrab, H.-G., Charged <I>vs.</I> neutral nucleobase loss from multiply charged oligonucleotide anions. *Journal of Mass Spectrometry* **1995,** 30, (9), 1222-1229.

15. McLuckey, S. A.; Habibi-Goudarzi, S., Decompositions of multiply charged oligonucleotide anions. *Journal of the American Chemical Society* **2002,** 115, (25), 12085-12095.

16. Carte, N.; Legendre, F.; Leize, E.; Potier, N.; Reeder, F.; Chottard, J.-C.; Van Dorsselaer, A., Determination by Electrospray Mass Spectrometry of the Outersphere Association Constants of DNA/Platinum Complexes Using 20-mer Oligonucleotides and ([Pt(NH3)4]2+, 2Cl-) or ([Pt(py)4]2+, 2Cl-). *Analytical Biochemistry* **2000,** 284, (1), 77-86.

17. Martin, L. B., 3rd; Schreiner, A. F.; van Breemen, R. B., Characterization of cisplatin adducts of oligonucleotides by fast atom bombardment mass spectrometry. *Anal Biochem* **1991,** 193, (1), 6-15.

18. Costello, C. E.; Comess, K. M.; Plaziak, A. S.; Bancroft, D. P.; Lippard, S. J., Fast atom bombardment and high performance tandem mass spectrometry of platinum(II) oligodeoxyribonucleotide fragments. *International Journal of Mass Spectrometry and Ion Processes* **1992,** 122, 255-279.

19. Iannitti-Tito, P.; Weimann, A.; Wickham, G.; Sheil, M. M., Structural analysis of drug-DNA adducts by tandem mass spectrometry. *Analyst* **2000,** 125, (4), 627-33.

20. Terrier, P.; Tortajada, J.; Buchmann, W., A study of noncovalent complexes involving single-stranded DNA and polybasic compounds using nanospray mass spectrometry. *J Am Soc Mass Spectrom* **2007,** 18, (2), 346-58.

21. Basma, H.; El-Refaey, H.; Sgagias, M. K.; Cowan, K. H.; Luo, X.; Cheng, P. W., BCL-2 antisense and cisplatin combination treatment of MCF-7 breast cancer cells with or without functional p53. *J Biomed Sci* **2005,** 12, (6), 999-1011.

22. Hong, J. H.; Lee, E.; Hong, J.; Shin, Y. J.; Ahn, H., Antisense Bcl2 oligonucleotide in cisplatin-resistant bladder cancer cell lines. *BJU International* **2002,** 90, (1), 113-117.

23. Lacy, J.; Loomis, R.; Grill, S.; Srimatkandada, P.; Carbone, R.; Cheng, Y. C., Systemic Bcl-2 antisense oligodeoxynucleotide in combination with cisplatin cures EBV+ nasopharyngeal carcinoma xenografts in SCID mice. *Int J Cancer* **2006,** 119, (2), 309-16.

24. Ohara, K.; Smietana, M.; Vasseur, J.-J., Characterization of Specific Noncovalent Complexes between Guanidinium Derivatives and Single-Stranded DNA by MALDI. *Journal of the American Society for Mass Spectrometry* **2006,** 17, (3), 283-291.

25. Lysik, M. A.; Wu-Pong, S., Innovations in oligonucleotide drug delivery. *J Pharm Sci* **2003,** 92, (8), 1559-73.

26. Wickstrom, E. L.; Bacon, T. A.; Gonzalez, A.; Freeman, D. L.; Lyman, G. H.; Wickstrom, E., Human promyelocytic leukemia HL-60 cell proliferation and c-myc protein expression are inhibited by an antisense pentadecadeoxynucleotide targeted against c-myc mRNA. *Proc Natl Acad Sci U S A* **1988,** 85, (4), 1028-32.

27. Marti, G.; Egan, W.; Noguchi, P.; Zon, G.; Matsukura, M.; Broder, S., Oligodeoxyribonucleotide phosphorothioate fluxes and localization in hematopoietic cells. *Antisense Res Dev* **1992,** 2, (1), 27-39.

28. Qu, Y.; Harris, A.; Hegmans, A.; Petz, A.; Kabolizadeh, P.; Penazova, H.; Farrell, N., Synthesis and DNA conformational changes of non-covalent polynuclear platinum complexes. *Journal of Inorganic Biochemistry* **2004,** 98, (10), 1591-1598.

29. Harris, A. L.; Yang, X.; Hegmans, A.; Povirk, L.; Ryan, J. J.; Kelland, L.; Farrell, N. P., Synthesis, Characterization, and Cytotoxicity of a Novel Highly Charged Trinuclear Platinum Compound. Enhancement of Cellular Uptake with Charge. *Inorg. Chem.* **2005,** 44, (26), 9598-9600.

30. Komeda, S.; Moulaei, T.; Woods, K. K.; Chikuma, M.; Farrell, N. P.; Williams, L. D., A Third Mode of DNA Binding: Phosphate Clamps by a Polynuclear Platinum Complex. *J. Am. Chem. Soc.* **2006,** 128, (50), 16092-16103.

31. Thomas, G. S.; Yun, Q.; Nicholas, F.; Vicki, H. W., Investigation of the <I>trans</I> effect in the fragmentation of dinuclear platinum complexes by electrospray ionization surface-induced dissociation tandem mass spectrometry. *Journal of Mass Spectrometry* **1998,** 33, (5), 436-443.

Chapter 4:

Duplex DNA Stabilization and evidence for phosphate binding

4.1 Introduction

Mass spectrometry is an essential tool in the drug development process, with an indispensable involvement in many of the key steps of identifying new therapeutics, compound purity, toxicology, and pharmacokinetics.[3] The investigation of noncovalent complexes between DNA, proteins, and peptides with a variety of synthetic and biologically relevant structures has become increasingly more common with the coupling of electrospray ionization and mass spectrometry (ESI-MS). Two ways in which investigations into noncovalent associations have benefited from mass spectrometry are: 1. the use of a full scan MS to obtain a relative stoichiometry of the complexes that are present in solution and also make inferences on their relative abundances, and 2. tandem mass spectrometry (MS/MS) or MS^n allows the gas phase stabilities between the two complexes to be examined.[4] Mass spectrometry is an ideal experimental method for the characterization of pure intermolecular interactions because it can be conducted free from any interfering solvent.[5, 6] The first published paper detailing the characterization of noncovalently interacting biomolecules in the gas phase following ESI was reported in 1991 by Ganem et al.[7] Since that time, a review of the literature shows a publication record of ~500 research and review articles dealing with the detection or characterization of noncovalent biomolecular complexes. ESI-MS offers several advantages over traditional methods of noncovalent characterizations[3], such as: (1) the interacting compounds do not have to be modified with special probes or labels. This maintains the native shape or structure of the species to be studied and doesn't alter their binding properties; (2) minimal amounts of sample are needed to perform an analysis, microgram quantities in comparison to milligram amounts for NMR and crystallography; (3)

sample purity is ideal, but not imperative in the study of noncovalent complexes because the data is separated on a mass scale. This ability to detect a mass shift from expected results allows the identification of degradation products or intermediates and gives the researcher the ability to select which products to investigate further.

4.2 Noncovalent Interactions on DNA

Biological events involving DNA interacting with small molecular ligands, metal ions, and proteins, are crucial for the regulation of such processes as transcription and replication. [8] The interactions between the biomolecules may be either noncovalent, and therefore reversible, or irreversible through covalent modifications or coordinative binding with metal complexes.[8]

Duplex DNA with its negative phosphate groups, formation of major and minor grooves, and the planar nucleobase structures, offer numerous possible binding sites for the interaction of noncovalent compounds. These types of interactions involving small molecules are characterized as; (1) electrostatic interactions between the negative phosphate backbone and cationic metal complexes or charged organic molecules, (2) hydrogen-bond interactions between minor/major groove binders, and (3) intercalation, where extended planar ligands insert between adjacent base pairs and associate via π-stacking interactions.[8] Examples are shown in Figure 4.1, as representative structures for minor groove binders and intercalators, respectively. Minor groove binders are generally curved or bent and usually have an associated positive charge. They are able to insert into the minor groove without distorting the shape of the double helix.[5] Minor groove binders, such as the ones shown in Figure 4.1(A) show a sequence specificity for AT-rich regions in duplex DNA. This preference for AT regions is related to three factors: (a) AT regions have more negative electrostatic potential, which are favorable for positively charged

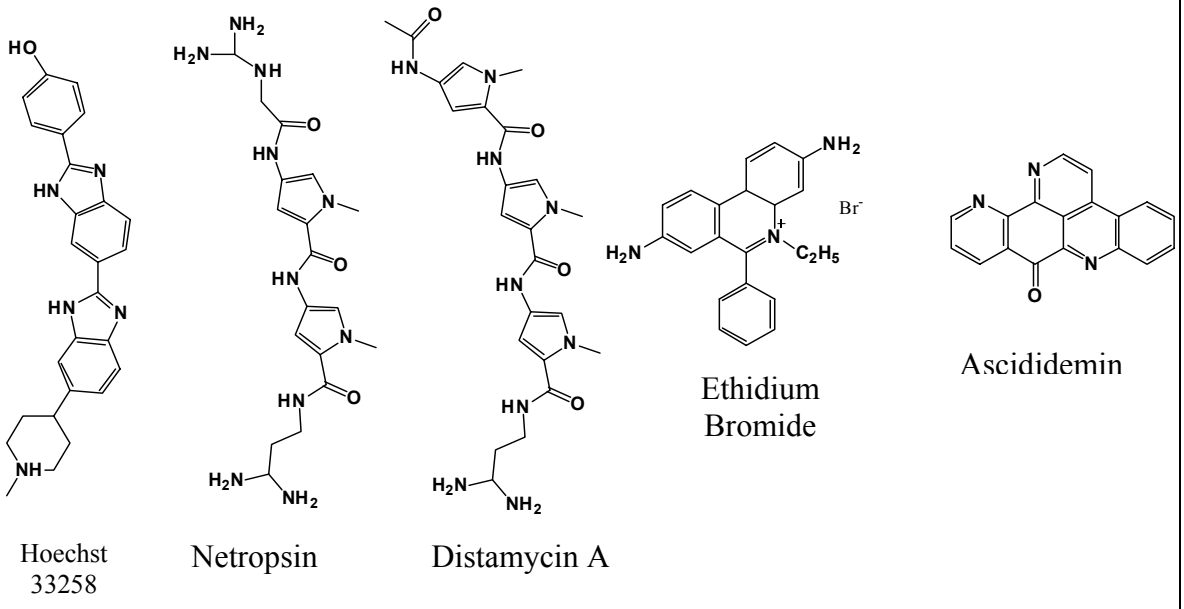

Figure 4.1. Commonly studied minor groove binders and intercalators

compounds; (b) the narrowness of the AT-rich minor groove allows for favorable contacts with the sugar moieties, and (c) GC regions of the duplex have an $-NH_2$ of guanine on the floor of the groove which adds steric hinderance.[5] Intercalators by comparison, are represented by planar aromatic or heterocyclic ring systems that interact with duplex DNA by inserting themselves and stacking between base pairs.[9, 10] Unlike minor groove binders, intercalators perturb the DNA duplex structure as the helix must unwind to form the intercalation site.[5] The consequence of these interactions through hydrogen bonding, van der Waals, hydrophobic and electrostatic forces, can result in an overall stabilizing effect on the DNA.[9, 11, 12]

4.3 Noncovalent polynuclear platinum complexes with DNA

Noncovalent interactions between biomolecules and antitumor complexes play an important role in a therapeutics mechanism of action. In the case of the clinically relevant polynuclear compound, BBR 3464, the covalent binding process is preceded by an initial noncovalent association with the duplex DNA sequence.[2] The presence of a charged moiety in the form of a platinum tetraamine significantly enhances the potency over a neutral linker such as hexane.[2, 13]

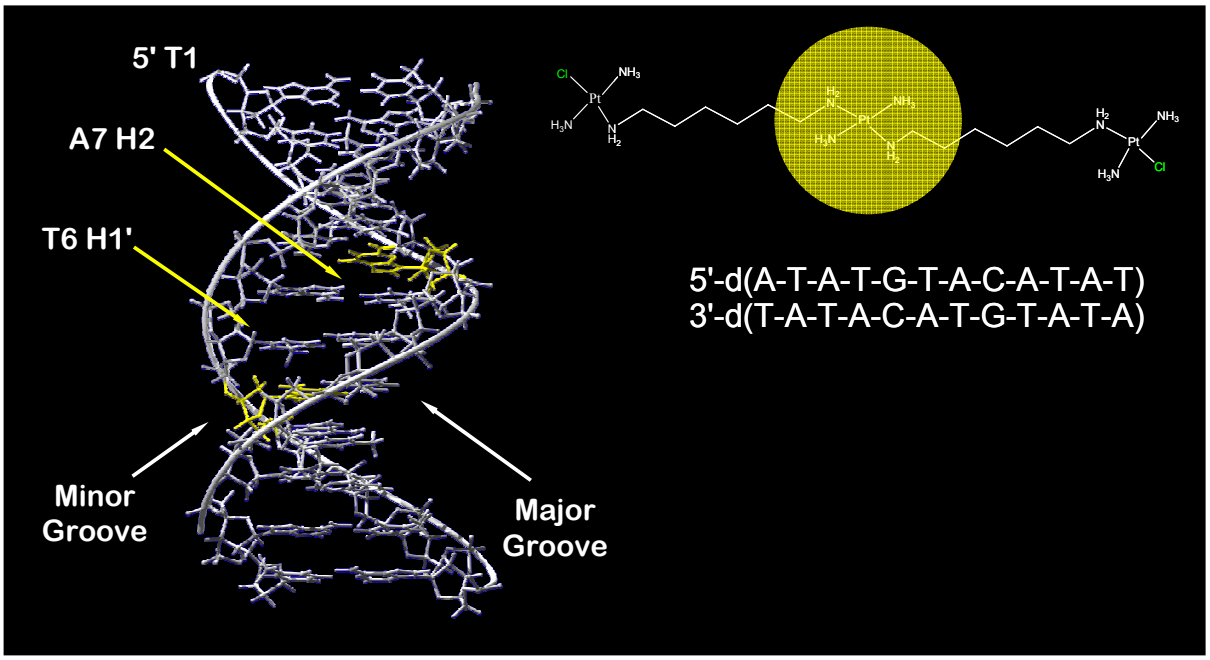

Figure 4.2 Electrostatic interaction of BBR 3464 with duplex DNA [2]

Recently, we have shown that highly charged cationic trinuclear platinum compounds with varied overall charge (+6 to +8), have increased cellular accumulation in A2780 human ovarian tumor cells, by as much as five times their covalent analog BBR 3464, currently in Phase II clinical trials[14]. The surprising increase in cellular accumulation by cells and cytotoxicity may

be due to the unique structure/charge relationship of these compounds. X-ray crystallography has revealed a possible third mode of DNA binding, the "phosphate clamp", involving the +8 trinuclear platinum compound shown in Figure 4.3.[15] The phosphate clamp was shown to form via the three square planar tetra-am(m)ine Pt (II) coordination units using a bidentate coordination preferentially with the O2 phosphate oxygens. Crystallographic data shows two distinct modes of binding to DNA: 1. groove spanning and 2. backbone tracking.[15] This type of $Pt(NH_3)_3$ – phosphate binding is similar to the guanidinium - phosphate moieties found in numerous biological complexes. The focus of this research was to investigate the gas phase stability of oligonucleotides complexed with the "phosphate clamp" DNA binding motif. We used the highly charged +6 trinuclear platinum complex $[\{Pt(NH_3)_3\}_2$-μ-trans-$Pt(NH_3)_2(NH_2(CH_2)_6NH_3)_2$ and the +8 dangling amine (DA) polynuclear platinum complex $[\{trans\text{-}Pt(NH_3)_3\}_2(NH_2)(CH_2)_6(NH_3^+)\}_2$-μ-trans-$Pt(NH_3)_2(NH_2(CH_2)_6NH_2)_2]$ (Figure 4.8). These noncovalent platinum compounds are structurally similar to our clinically relevant, covalent binding BBR 3464, expect for the replacement of the labile chloride ligands with nonlabile ammines and hexane-diamines, respectively. The presence of the additional amine ligands increases the overall charge and hydrogen bonding capabilities of these compounds to the negatively charged phosphate backbone of nucleic acids.

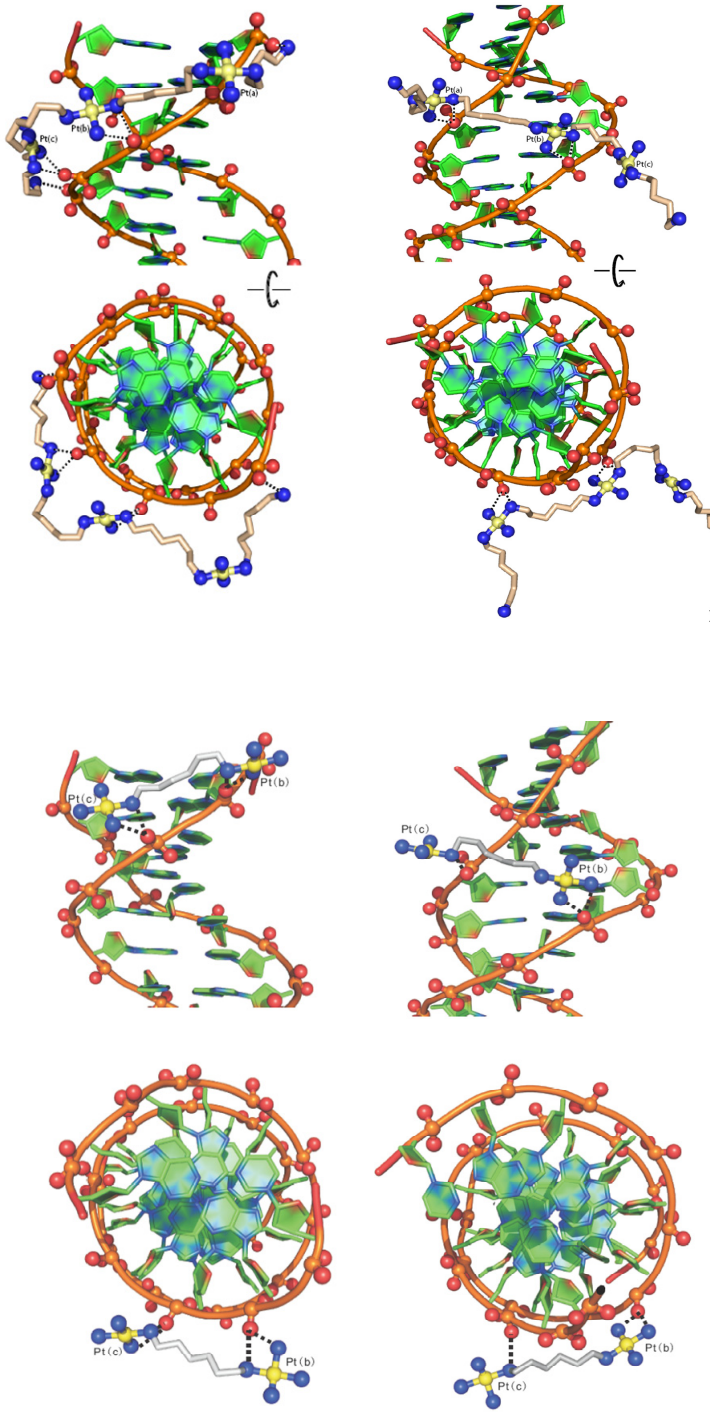

Figure 4.3 X-ray crystal structure of noncovalent platinum complexes forming phosphate clamp interactions with DNA.[15]

4.4 Experimental

Experiments were conducted on a Micromass-Waters Qtof-2 mass spectrometer (Milford, MA) equipped with a custom built microspray source. Electrospray source conditions were kept constant with a source temperature of 120°C, capillary voltage of 2.0 kV, cone voltage 38 V, and flow rates of 0.5 μL/min. In tandem mass spectrometry (MS/MS) experiments, collisional energy was varied from 10 eV to 40 eV. The oligonucleotides 5′-TAG CGC TTT TTC GCG TA -3′ (M= 5167 Da) and 5′- TA CGC GAA AAA GCG CTA -3′ (M= 5212 Da) was purchased from Midland Certified Reagents, (Midland, TX) and further desalted in a custom built dialysis chamber using hollow 13,000 molecular weight cut off (MWCO) filters in 20 mM ammonium acetate. Equimolar solutions of oligonucleotides were annealed in 20mM ammonium acetate at 90º C for 5 minutes and allowed to cool to room temperature. A stock solution of 500 uM Pt compound was prepared in 18 Ω ohm water. Oligonucleotides and Pt compounds were mixed in a 1:1 molar ratio and incubated at 37°C for 20 minutes then mixed with electrospray solution to form 50:50 methanol:20 mM ammonium acetate. Full scan and tandem MS/MS data were analyzed using MassLynx 4.0 software.

4.5. Results and Discussion

Electrospray ionization time of flight mass spectrometry (ESI-TOF-MS) and collision-induced dissociation (CID) were used to investigate the gas phase stability of synthetic oligonucleotides complexed with the highly charged noncovalent polynuclear platinum compound. Investigations into the gas phase stability of duplex DNA-drug complexes have previously been studied for intercalators and minor groove binders[#97][5, 9, 12, 16-18], but this is the first reported gas phase

study of a platinum phosphate clamp style DNA-drug interaction with duplex DNA. As this new binding mechanism represents a novel approach to cancer therapeutics, a systematic study of the different complexes was undertaken. Only recently has the application of mass spectrometry and CID been reported for the characterization of these types of salt bridge interactions, such as those between arginine forks and phosphate groups.[19-23] Shown in Figure 4.4, the nature and orientation of the platinum phosphate clamp is very similar to the arginine forks formed between the guanidinium group of peptides and anionic structures such as phosphates, sulfonates, and carboxylates. Studies by Schug and Lindner have shown that phosphonate and sulfonate functionalized amino acid complexes display a higher rate of complexation when compared to carboxylate functionalized amino acids.[22, 23] Despite the lower propensity to form a guanidinium-carboxylate complex, gas phase CID showed a much higher energy for dissociation in comparison to the phosponate and sulfonate functionalized complexes.[11, 22]

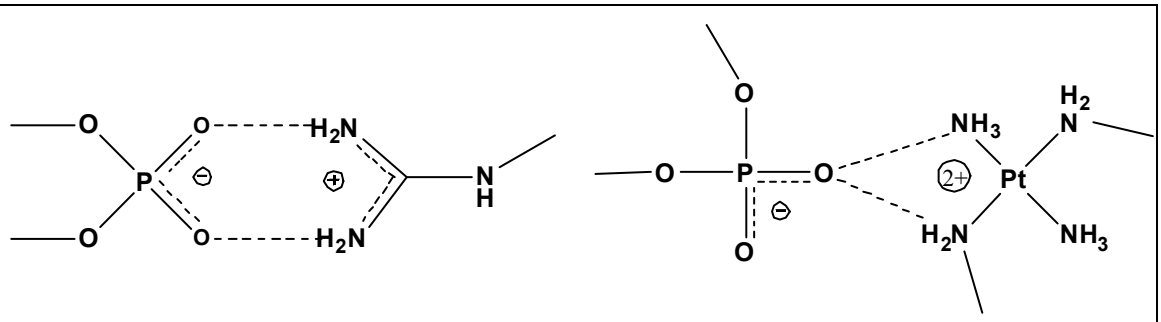

Figure 4.4 Structural similarity of the arginine fork found in nature with the platinum phosphate clamp motif

4.6 CID of DNA-Drug complexes

As mentioned earlier, the interaction of drugs with DNA can be classified in two general categories, intercalators and minor groove binders. In addition to how they interact with DNA, drugs can also be categorized by their dissociation pathway with DNA during the CID process. Rosu and coworkers have formed a general description for this compound specific dissociation pathway[5] The first pathway represented by intercalators results in the loss of the drug as a neutral species upon CID resulting in free duplex DNA remaining. (Figure 4.5) It should be noted that the size and sequence of the duplex DNA can also result in strand separation and therefore free duplex is not always the CID product when dealing with intercalators.[5]

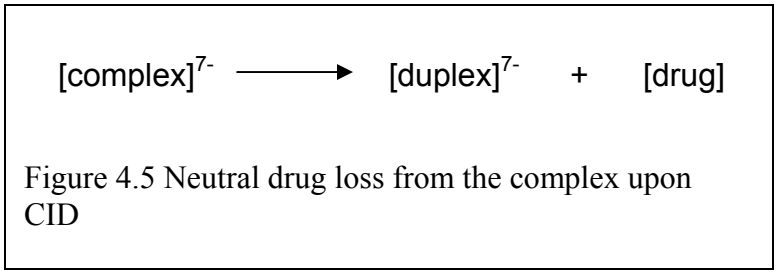

Figure 4.5 Neutral drug loss from the complex upon CID

Figure 4.5 shows the fragmentation pathway in which the DNA-drug complex dissociates with the loss of a negatively charged drug from the complex. These types of pathways depend on the drugs ability to give up a proton to the DNA.

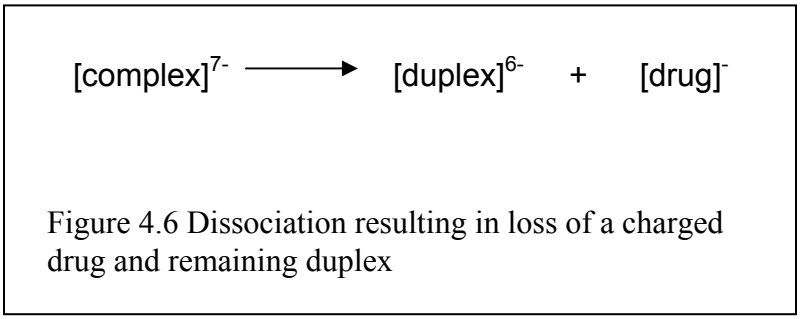

Figure 4.6 Dissociation resulting in loss of a charged drug and remaining duplex

The third and final dissociation pathway, shown in Figure 4.6, results in the separation of the duplex DNA structure into its single strand components, with each strand sharing the available

charge of the intact duplex.[5] The drug molecule generally remains bound to one or both strands upon CID. This type of fragmentation profile is representative of the positively charged intercalator ethidium bromide and **all** minor groove binders.[5] For those compounds characterized by the dissociation pathway in Figure 4.5, the ability to lose the drug as a neutral from this fragmentation pathway also exists and is sometimes seen for the minor groove binders Hoechsts 33258 and 33342.[5] As has been mentioned by Rosu et al, the stability of a DNA-Drug complex can be compared directly to the stability of the DNA duplex alone by comparing the differences in CID energies[5] In addition, they have also determined that key structural differences in the drugs may play a part in the perceived stability increases, such as the ability to form a higher number of hydrogen bonds with the duplex, and overall charge of the drug.[5]

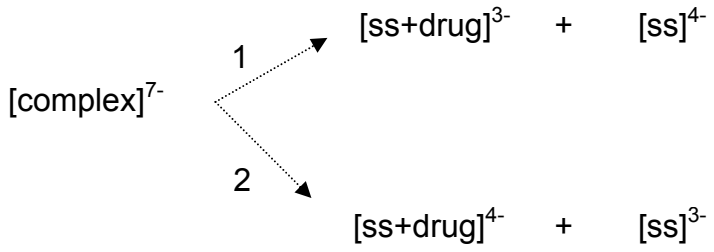

Figure 4.7 Fragmentation pathway exhibited by minor groove binders.

4.7 CID of Duplex DNA-Platinum Complexes

In efforts to investigate the potential effects of the phosphate clamp motif, a series of noncovalent polynuclear platinum compounds were chosen based on their ability to interact with DNA. Figure 4.8 shows the five structurally distinct platinum compounds used in this study, with each compound allowing for comparisons to be made about charge and hydrogen bonding character. The compounds represented above vary in both charge state (4+) for compound (A); (6+) for compounds (B-D); and (8+) for compound (E), and hydrogen bonding character with variation in the central linker.

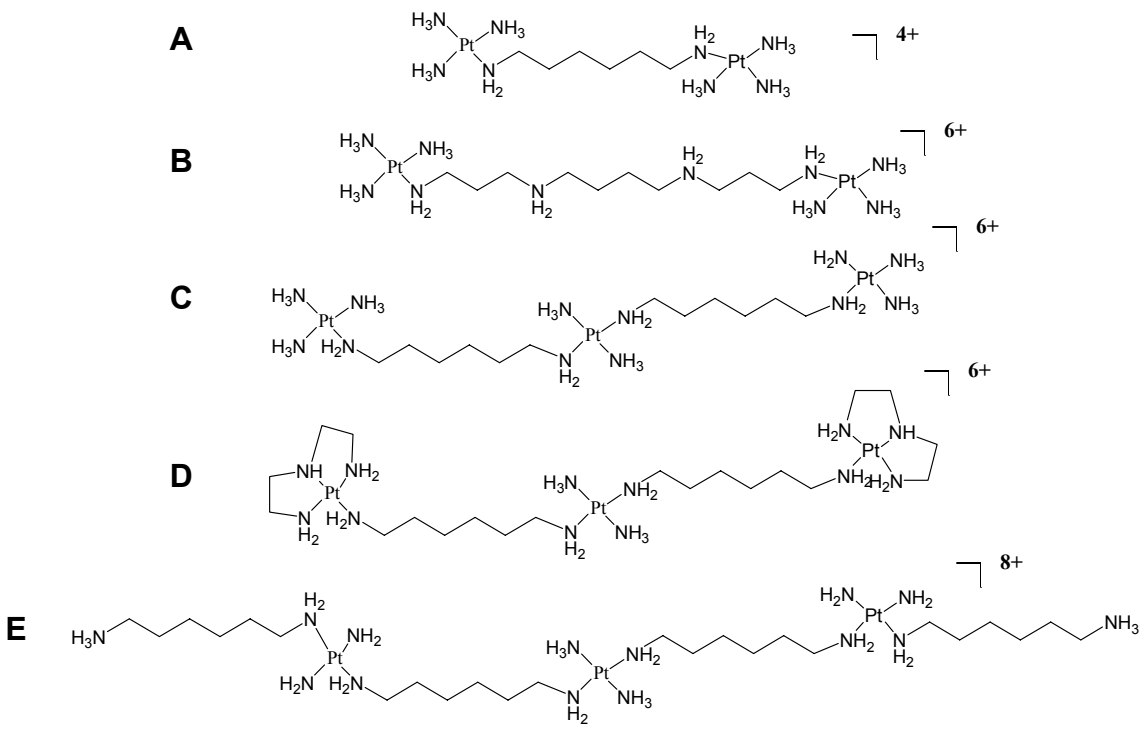

Figure 4.8 Polynuclear platinum compounds. (A) AH 88, (B) AH 59, (C) AH 44, (D) AH 48, and (E) AH 78

It has been established that the presence of a central platinum moiety plays a critical role in the pre-association with biomolecules.[2] Compounds (B-D) all possess a high 6+ charge, but differ in their potential to interact with the duplex DNA. Compound (B) AH 59, is a dinuclear compound separated by a charge spermine linker. Compound (C) AH 44 and compound (D) AH 48 are both trinuclear compounds with a central platinum moiety, but differ in the two outer platinums with the presence of dien in AH 48. The rationale in comparing (C) and (D) is that the dien structures should limit the ability to form the phosphate clamp and therefore result in a weaker interaction. Additionally, the comparison with a known minor grove binder, Hoechst 33258, was used to determine if these compounds altered the fragmentation pattern.

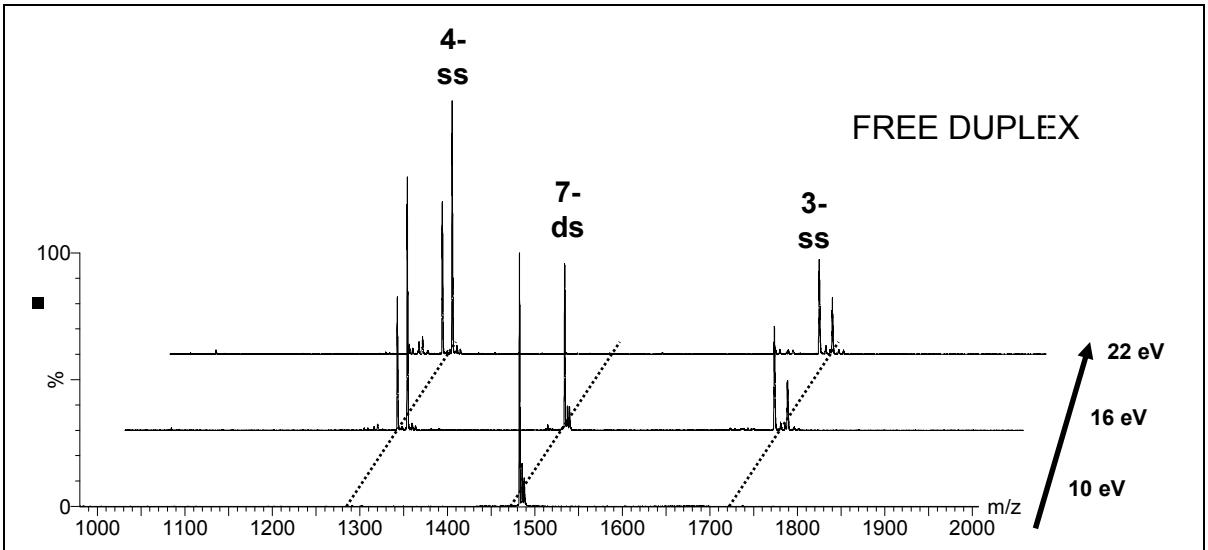

Figure 4.9 Free 17-mer duplex CID at increasing collisional energy

Figure 4.9, represents the 7- charge state of the free 17-mer duplex at increasingly higher collisional voltages with the 16V of collisional energy representing the $CE_{50\%}$ which is roughly the point at which 50% of the duplex remains intact. Upon CID of the 7- charge state at 1482

m/z, strand separation with the seven available charges being distributed among them is seen. Due to the high charge state chosen for the CID, there is no covalent backbone cleavage observed as the higher charge aids in the coulombic repulsion of the two strands. As a result, the duplex separates into the 3- and 4- single strand constituents. This is consistent with the described mechanism of duplex dissociation as described above by Rosu.[5]

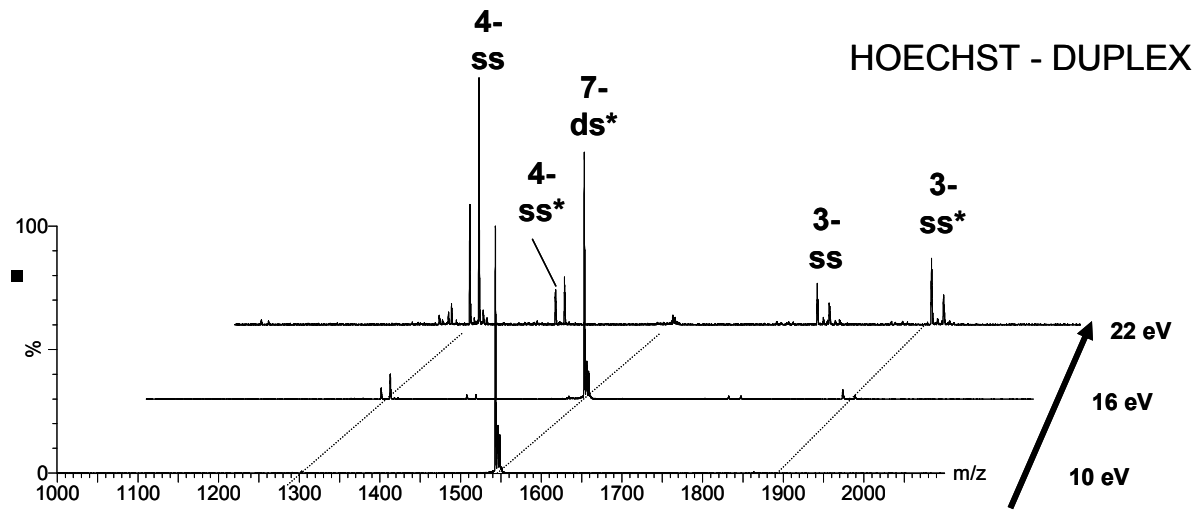

Figure 4.10 17-mer duplex complexes in a 1:1 ratio with Hoechst dye CID at increasing collisional energy

The CID of Hoechst dye with duplex DNA has been characterized extensively in the literature. As is the case with all known minor groove binders, the dissociation proceeds with strand separation with the drug being able to remain bound to either of the two strands. In the CID fragmentation of minor groove binders, the increase in the hexapole collision energy applied that is needed to fragment the complex, indicates that the complex is more stable than the free DNA alone.

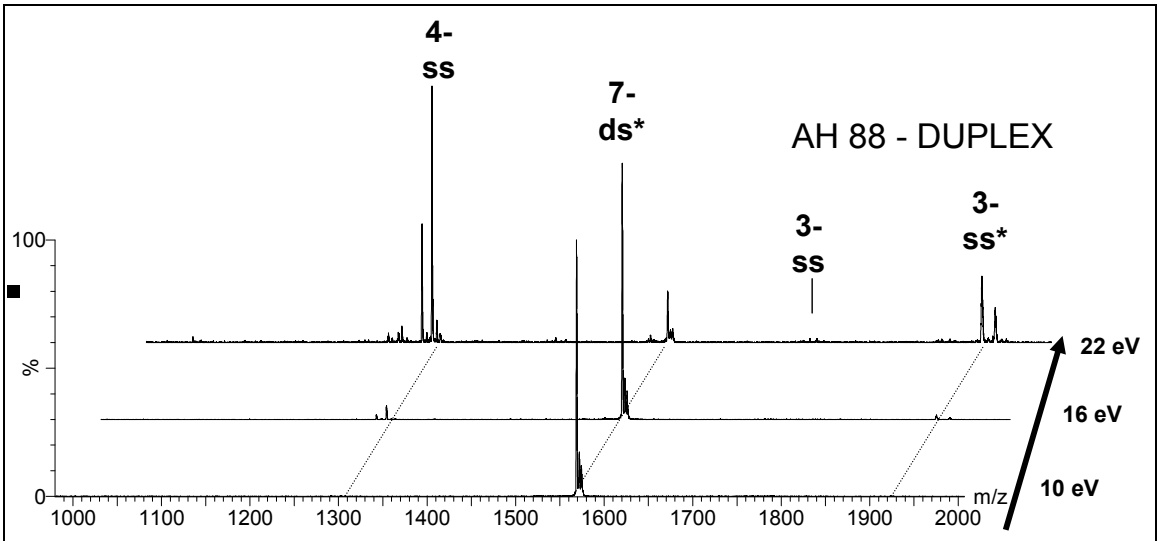

Figure 4.11 17-mer duplex with AH 88 in a 1:1 ratio CID at increasing collisional energy

The addition of hydrogen bonds between the two are thought to add to increased stabilization, but also the number of positive charges carried by the drug increases the electrostatic interactions.[5] Due to the small nature and low charge for the Hoechst dye, we can see the fragmentation pathway allows for the drug to be on both the lower and higher charged single strand formed after the CID experiment. As seen in Figure 4.10, the CID of the peak at 1543 m/z yields strand separation into both the free 3- and 4- single strand products as well as the 3- and 4- ss+Hoechst dye peaks. The additional hydrogen bonding provided by the Hoechst dye as well as the positive charge have been associated with an increase in the stabilization energies.[5]

The addition of the 4+ dinuclear platinum compound AH 88, reveals a slight increase in the overall duplex stability of the 17-mer over that of the Hoechst dye as seen in Figure 4.11. Given that the platinum compound has an increased positive charge over the Hoechst dye this may be the contributing factor. The complex with AH 88 is kinetically more stable as it forms more

hydrogen bonds with the DNA as well as having additional charge ~ 3+. The dissociation channel of the duplex when bound with the platinum compound is still representative of Figure 4.7, where single strand separation is the main dissociation pathway. The CID of 1568 m/z reveals that at the highest collisional energy used some free 3- ssDNA is starting to appear. As described above this is likely due to the neutral loss of the platinum compound. Since the platinum compound will still have some positive charge, the negative ion detection mode will not reveal the free platinum moiety.

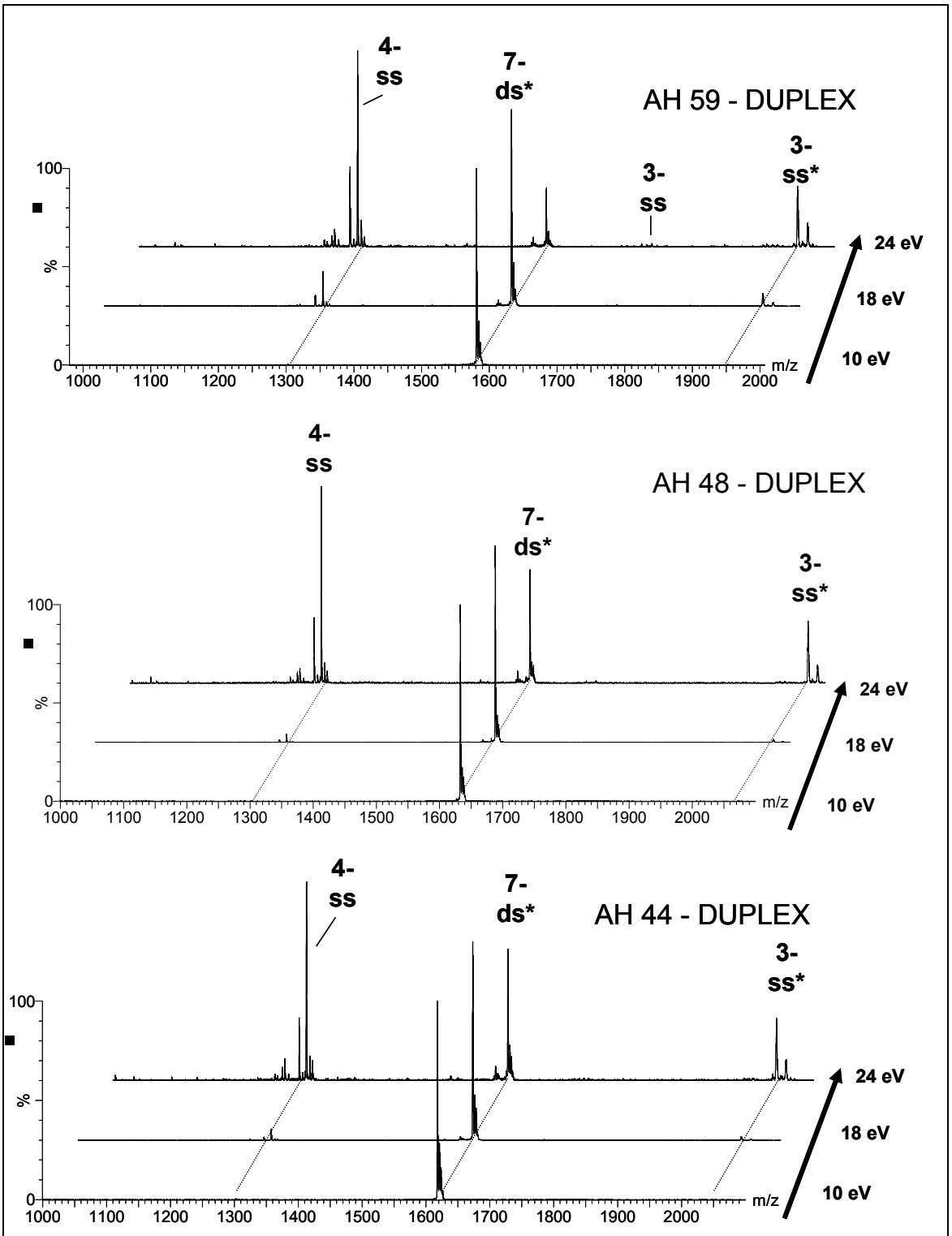

Figure 4.12 CID of 17-mer duplex with (A) AH 59, (B) AH 48, (C) AH 44 at increasing collisional energy

Charge state comparision

To investigate the effect that the size and hydrogen bonding ability have on the stability of duplex DNA three compounds: AH 59, AH 44, and AH 48 were investigated. Each of these compounds possesses a high charge with all being 6+, but they differ in the possible ways they may interact with the phosphate backbone of the DNA. AH 59 is a dinuclear compound that is separated by a spermine linker, AH 44 is a trinuclear compound, and AH 48 is a trinuclear compound that has a dien structure on the outer platinum centers. This addition of the dien structure should result in less ability to form the phosphate clamp binding motif and therefore, maybe the potential for a lower stabilizing effect. As mentioned earlier, the central platinum moiety is essential in making the pre-association contacts with DNA. Recently, the crystal structure of AH 59 with the Dickerson Drew Dodecomer (DDD) revealed that the AH 59 bridged the two duplex strands making hydrogen bond contacts through the terminal amine and the spermine NH_2. The comparison of the AH 44 with AH 59 reveals that the increased stability of the AH 44 over that of AH 59 is greatly enhanced, possibly by the stability added through the additional hydrogen bond contacts. As the charge and therefore electrostatic component of these two compounds are the same, the additional stability must be attributable to the central linker portion of the compound. Comparison of the stabilities between AH 44 and AH 48 reveal nearly identical $CE_{50\%}$ values. This may give some indication that the terminal platinum structures are involved, but to a lesser degree than the central portion of the compound. In the case for all three of these compounds, the stabilities and associations are strong enough that no free 3- ssDNA exists in the spectra.

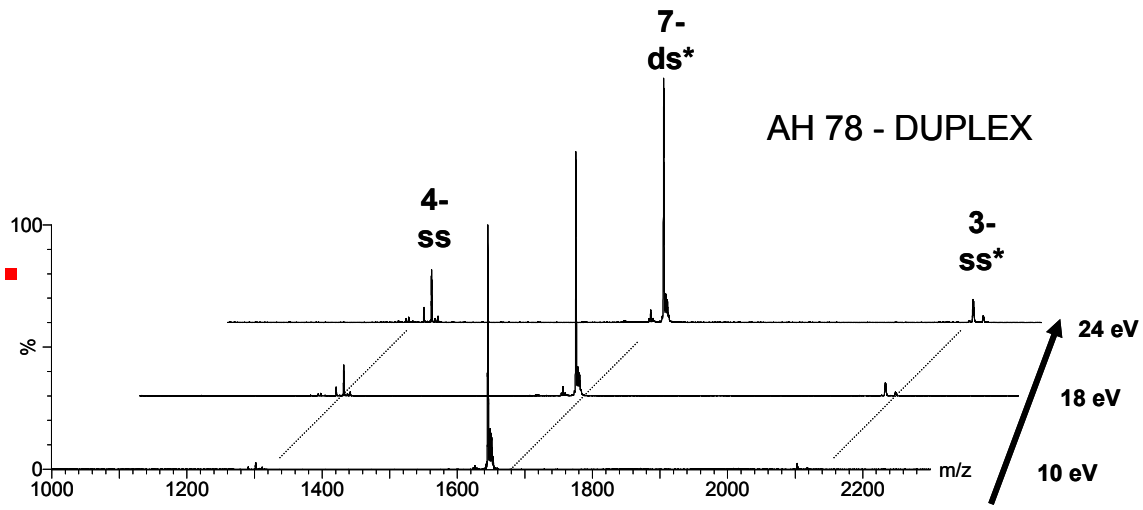

Figure 4.13. CID of 17-mer duplex with AH 78 at increasing collisional energy

When comparing the trinuclear compounds they both appear to be very similar in stabilizing potential. The addition of the dien structures does not appear to greatly alter the stabilizing effects of the compound. When compared with the dinuclear complex of the same charge, the addition of the central platinum moiety may play an essential role in the stabilizing effect. It was originally conceived that the dien structures would limit the phosphate clamp motif and therefore result in a lower $CE_{50\%}$ value, however, that has not proven to be the case. Based on crystal structure data of the trinuclear compounds, the central platinum moiety is involved in the phosphate clamp binding motif, adding strength to the argument. Additionally, NMR studies of the covalent trinuclear compound BBR 3464 shows that the central platinum makes an immediate association with the DNA.[2]

The greatest overall stability for these types of compounds was found to be exhibited by the large 8+ trinuclear compound AH78. Increasing the charge to 8+ and adding an aminohexane linker to the terminal platinum centers dramatically increases the overall duplex stability. The combined positive charge with the multiple hydrogen bonding ligands offers a profound effect

on the stabilization of duplex DNA. Seen in Figure 4.13, and illustrated in the dissociation energy plot in Figure 4.14, the $CE_{50\%}$ is extended over the other compounds to ~30V of collisional energy. Strand separation is still the preferred dissociation pathway for this compound as well, which may hint to a common characteristic for this type of new phosphate clamp binding motif.

A duplex dissociation curve is shown in Figure 4.14, comparing the gas phase duplex stability versus the applied hexapole collision energy. The plot reveals the trend of increasingly higher stabilities with increasing platinum compound size, charge, and hydrogen bonding ability. For the two compounds AH 44 and AH 48, the plot reveals very similar dissociation profiles. This was somewhat unexpected as the two should have different hydrogen bonding capabilities due to the presence of the dien ligand. Nevertheless, the stabilization effects are in line with the trends of charge and the existence of the central platinum moiety. It should be noted that there are several factors that affect the overall stability of noncovalent complexes in CID experiments: the binding energy, the size of the complex (degrees of freedom), internal energy, and charge state of the ion.

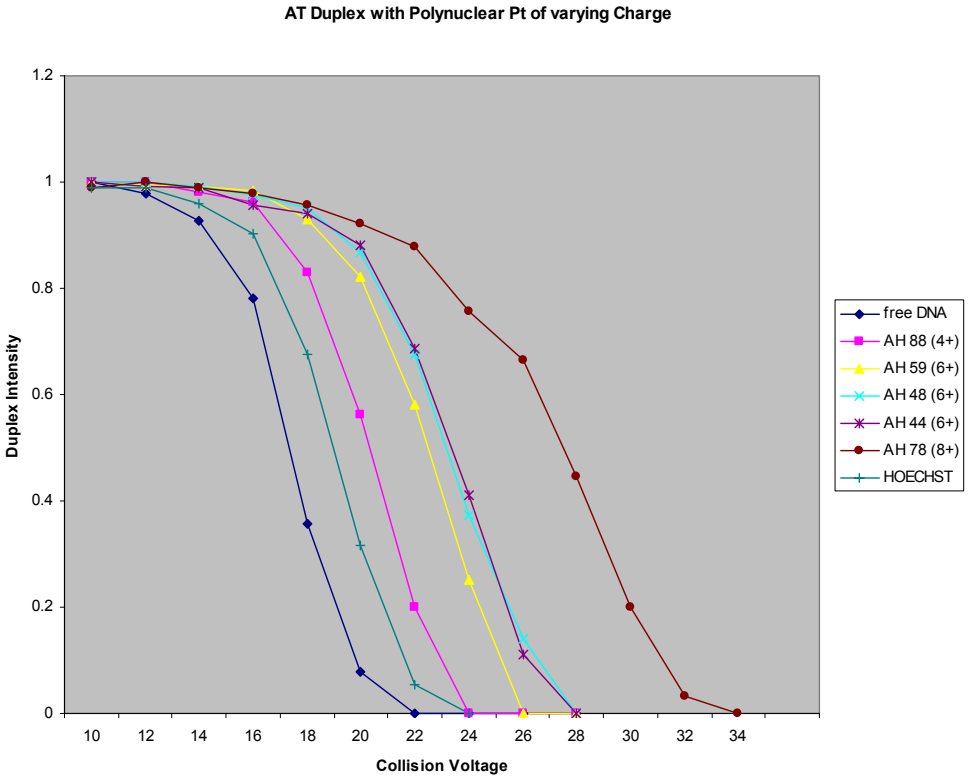

Figure 4.14. Duplex dissociation curve illustrating the increase in necessary applied collisional energy to achieve strand separation

For drug-DNA complexes an increase in hydrogen bonding character of the drug and the number of positive charges it carries has a dramatic effect on the overall stability of the complex in the gas phase. It was shown that when the duplex contains a high number of nucleobase pairs with low basicity the strand separation profile is generally preferred and the drug remains attached to one or both strands.[24, 25] The above results indicate an increase in overall stability with increasing size and charge of the platinum compound, but the increase in the vibrational degrees of freedom should also be considered.

4.8. Investigation of DNA length

19-mer Oligonucleotide

Additional experiments were conducted on two oligonucleotide duplexes of different lengths with the goal to see how strand length affects the dissociation pathway. Figure 4.15, shows the CID experiments carried out on the free (7-) 19-mer duplex (S1)5`-GGAAGGACAAACAGGAGAG-3` and (S2)3`- CTTCCTGTTTGTCCTCTCC -5`. This duplex contains the central A-T repeat region that is known to enhance the binding of cationic compounds. As is generally understood, cationic drugs have a strong propensity for the more negative potential regions associated with AT_n repeat units. The collisional energy at which 50% of the duplex remains ($CE_{50\%}$) was approximately 20 eV. It should be noted that CID in the QTOF-2 results in predominantly noncovalent dissociation of the duplex into single strands due to the fast heating conditions. As shown in Figure 4.16, the addition of the +6 trinuclear compound AH 44 to the duplex increases the $CE_{50\%}$ to approximately 27 eV. Much like minor groove binders, the trinuclear platinum compound remains noncovalently bound to one of the single strands, showing slight preference to the S1 strand. In addition, the presence of unbound single strand products indicates loss of the trinuclear platinum compound as a neutral, something common to intercalators. There does not appear to be any free duplex produced indicating that the loss of the phosphate clamp motif is a possible secondary fragmentation pathway that occurs after the noncovalent duplex dissociation. Increasing the overall charge of the platinum drug by the addition of the two hexane amines on AH 78 creates an opportunity to form two more phosphate clamp motifs. CID performed on the +8 trinuclear platinum compound AH 78, increases the $CE_{50\%}$ to approximately 30 eV. Similar to the +6 ligand, the +8 compound seems to show a preference for the S1 strand. As with these compounds, the formation of the phosphate

clamp binding motif allows the platinum compound to follow the curvature of the phosphate backbone, thus the propensity of the compound for the S1 strand with the AAA repeat may prove to warrant further investigations as possible unique binding sites.

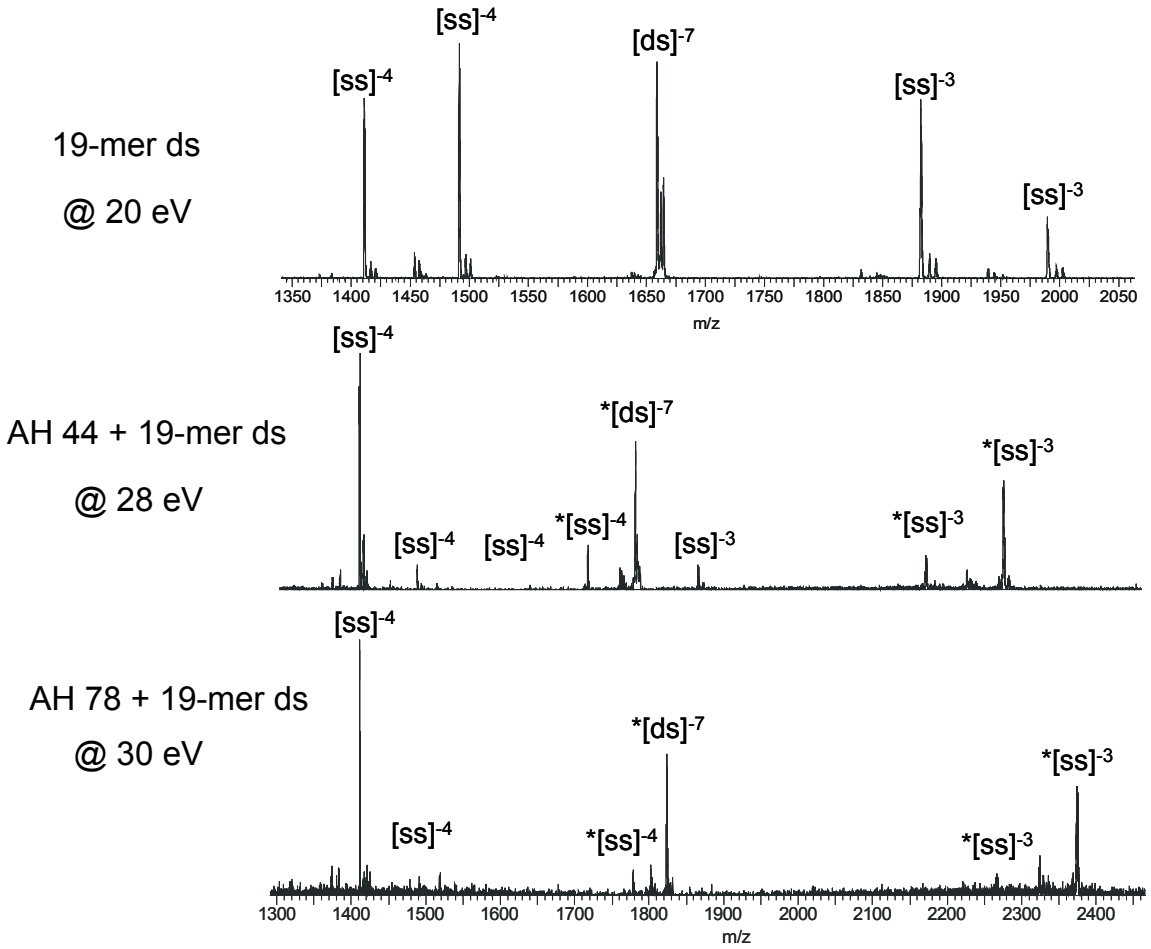

Figure 4.15 19-mer duplex with noncovalent platinum compounds at approximately $_{50\%}$CE

In efforts to determine what effect charge and hydrogen bonding character play on stability, a smaller dinuclear +4 platinum compound AH 88, was complexed with the 19-mer duplex. As expected the lower charged dinuclear compound with fewer opportunities for the phosphate clamp motif, exhibited a lower $CE_{50\%}$ of approximately 22 eV. The dissociation profile for the larger 19-mer oligonucleotide reveals a similar profile when comparing the three platinum compounds. It should be noted that due to the excessive covalent fragmentation of the phosphate backbone, the profile plots do not represent a full dissociation of the duplex and therefore the plot is not 100% dissociated.

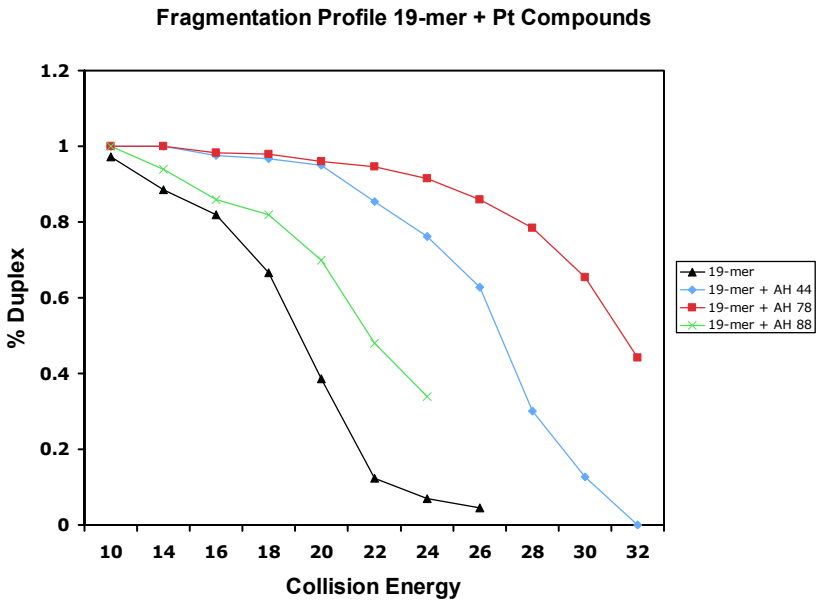

Figure 4.16. Duplex dissociation curve illustrating the effect of charge and size on the duplex gas phase stability

12-mer Dickerson-Drew Dodecamer

Dissociation of a 12-mer self-complementary duplex (5`- CGCGAATTCGCG -3`) when complexed with the 6+ AH 44 results in the covalent fragmentation of the duplex with subsequent phosphate backbone cleavage and base loss. Since this is a self-complementary sequence, no form of strand sequence preference can be made as the fragments from one strand would be same as the other. Given the low charge state of this complex (3-), the resultant covalent fragmentation, may be due to the lack of strand-strand repulsion in addition to the increase stability provided by the complex.

4.9 Conclusions

The dramatic effects that noncovalent polynuclear platinum compounds exhibit through the phosphate clamp binding motif is evident in the increased gas phase stabilities of the selected duplex DNA structures. The trend of increasing electrostatic charge rivals that of increasing the hydrogen bonding character as seen in the comparison of AH 44 with AH 48. The central platinum moiety appears to be crucial for the increased stability over similarly charged dinuclear complexes. Comparison of the binding mechanism through crystallographic data with the stability differences, may give an indication that the central platinum region of these types of phosphate clamp binding motifs is necessary for increased gas phase stability. In addition, the fragmentation pathway for all compounds appears to be the same regardless of the overall size and charge. The pathway for dissociation is predictable and comparisons can be drawn with known minor groove binding compounds. As this binding mechanism encompasses a phosphate tracking and groove spanning motif, a combination of single strand products with the intact platinum compound is identified and expected.

4.8. References

1. Hagan, N. A.; Fabris, D., Dissecting the Protein-RNA and RNA-RNA Interactions in the Nucleocapsid-mediated Dimerization and Isomerization of HIV-1 Stemloop 1. *Journal of Molecular Biology* **2007,** 365, (2), 396-410.

2. Hegmans, A.; Berners-Price, S. J.; Davies, M. S.; Thomas, D. S.; Humphreys, A. S.; Farrell, N., Long Range 1,4 and 1,6-Interstrand Cross-Links Formed by a Trinuclear Platinum Complex. Minor Groove Preassociation Affects Kinetics and Mechanism of Cross-Link Formation as Well as Adduct Structure. *J. Am. Chem. Soc.* **2004,** 126, (7), 2166-2180.

3. Hofstadler, S. A.; Sannes-Lowery, K. A., Applications of ESI-MS in drug discovery: interrogation of noncovalent complexes. *Nat Rev Drug Discov* **2006,** 5, (7), 585-95.

4. Valorie, G.; Edwin De, P., Comparison between solution-phase stability and gas-phase kinetic stability of oligodeoxynucleotide duplexes. *Journal of Mass Spectrometry* **2001,** 36, (4), 397-402.

5. Rosu, F.; Pirotte, S.; Pauw, E. D.; Gabelica, V., Positive and negative ion mode ESI-MS and MS/MS for studying drug-DNA complexes. *International Journal of Mass Spectrometry* **2006,** 253, (3), 156-171.

6. Kitova, E. N.; Bundle, D. R.; Klassen, J. S., Partitioning of solvent effects and intrinsic interactions in biological recognition. *Angew Chem Int Ed Engl* **2004,** 43, (32), 4183-6.

7. Ganem, B.; Li, Y. T.; Henion, J. D., Detection of noncovalent receptor-ligand complexes by mass spectrometry. *Journal of the American Chemical Society* **2002,** 113, (16), 6294-6296.

8. Jennifer L. Beck, M. L. C., Stephen F. Ralph, Margaret M. Sheil,, Electrospray ionization mass spectrometry of oligonucleotide complexes with drugs, metals, and proteins. *Mass Spectrometry Reviews* **2001,** 20, (2), 61-87.

9. Gabelica, V.; De Pauw, E.; Rosu, F., Interaction between antitumor drugs and a double-stranded oligonucleotide studied by electrospray ionization mass spectrometry. *J Mass Spectrom* **1999,** 34, (12), 1328-37.

10. Urathamakul, T.; Waller, D. J.; Beck, J. L.; Aldrich-Wright, J. R.; Ralph, S. F., Comparison of Mass Spectrometry and Other Techniques for Probing Interactions Between Metal Complexes and DNA. *Inorganic Chemistry* **2008,** 47, (15), 6621-6632.

11. Schug, K. A.; Lindner, W., Noncovalent binding between guanidinium and anionic groups: focus on biological- and synthetic-based arginine/guanidinium interactions with phosph[on]ate and sulf[on]ate residues. *Chem Rev* **2005,** 105, (1), 67-114.

12. Rosu, F.; Gabelica, V.; Houssier, C.; De Pauw, E., Determination of affinity, stoichiometry and sequence selectivity of minor groove binder complexes with double-stranded oligodeoxynucleotides by electrospray ionization mass spectrometry. *Nucleic Acids Res* **2002,** 30, (16), e82.

13. Farrell, N., In *Platinum Based Drugs in Cancer Therapy*, Kelland, L. R. F., N., Ed. Humana Press: Totawa, NJ, 2000; pp 321-328

.

14. Harris, A. L.; Yang, X.; Hegmans, A.; Povirk, L.; Ryan, J. J.; Kelland, L.; Farrell, N. P., Synthesis, Characterization, and Cytotoxicity of a Novel Highly Charged Trinuclear Platinum Compound. Enhancement of Cellular Uptake with Charge. *Inorg. Chem.* **2005,** 44, (26), 9598-9600.

15. Komeda, S.; Moulaei, T.; Woods, K. K.; Chikuma, M.; Farrell, N. P.; Williams, L. D., A Third Mode of DNA Binding: Phosphate Clamps by a Polynuclear Platinum Complex. *J. Am. Chem. Soc.* **2006,** 128, (50), 16092-16103.

16. Gabelica, V.; Rosu, F.; Houssier, C.; De Pauw, E., Gas phase thermal denaturation of an oligonucleotide duplex and its complexes with minor groove binders. *Rapid Commun Mass Spectrom* **2000,** 14, (6), 464-7.

17. Reyzer, M. L.; Brodbelt, J. S.; Kerwin, S. M.; Kumar, D., Evaluation of complexation of metal-mediated DNA-binding drugs to oligonucleotides via electrospray ionization mass spectrometry

10.1093/nar/29.21.e103. *Nucl. Acids Res.* **2001,** 29, (21), e103-.

18. Keller, K. M.; Zhang, J.; Oehlers, L.; Brodbelt, J. S., Influence of initial charge state on fragmentation patterns for noncovalent drug/DNA duplex complexes. *J Mass Spectrom* **2005,** 40, (10), 1362-71.

19. Alves, S.; Woods, A.; DelvolvΘ, A.; Tabet, J. C., Influence of salt bridge interactions on the gas-phase stability of DNA/peptide complexes. *International Journal of Mass Spectrometry* **2008,** 278, (2-3), 122-128.

20. Jackson, S. N.; Wang, H. Y.; Woods, A. S., Study of the fragmentation patterns of the phosphate-arginine noncovalent bond. *J Proteome Res* **2005,** 4, (6), 2360-3.

21. Woods, A. S.; Moyer, S. C.; Jackson, S. N., Amazing stability of phosphate-quaternary amine interactions. *J Proteome Res* **2008,** 7, (8), 3423-7.

22. Schug, K.; Lindner, W., Using electrospray ionization-mass spectrometry/tandem mass spectrometry and small molecules to study guanidinium-anion interactions. *International Journal of Mass Spectrometry* **2005,** 241, (1), 11-23.

23. Schug, K.; Lindner, W., Development of a screening technique for noncovalent complex formation between guanidinium- and phosphonate-functionalized amino acids by electrospray

ionization ion trap mass spectrometry: assessing ionization and functional group interaction. *International Journal of Mass Spectrometry* **2004,** 235, (3), 213-222.

24. Wilson, J. J.; Brodbelt, J. S., Infrared multiphoton dissociation of duplex DNA/drug complexes in a quadrupole ion trap. *Anal Chem* **2007,** 79, (5), 2067-77.

25. Xu, Y.; Afonso, C.; Wen, R.; Tabet, J. C., Investigation of double-stranded DNA/drug interaction by ESI/FT ICR: orientation of dissociations relates to stabilizing salt bridges. *J Mass Spectrom* **2008,** 43, (11), 1531-44.

Chapter 5:

Interaction of platinum compounds with model cell membrane structures

5.1 Introduction

Heparan sulfate proteoglycans (HSPGs) are multi-sulfated linear polysaccharides, found on the cell surface of most human cells and localized in mast cells, play an integral role in a variety of biological processes. These highly charged polysaccharides, are made up of repeating 1-4 linked polysulfated disaccharide units comprised of glucosamine and hexuronic acid, with up to three sulfate moieties per unit. Two structurally similar polysaccharides, heparin and heparan sulfate (HS) are the most complex members of the glycosaminoglycan (GAG) family, which also consists of chondrotin sulfate, dermatan sulfate, and keratin sulfate.[2] For the work herein we will only focus on HS. Heparan sulfate is biosynthesized as a proteoglycan and strategically located on the cell surface and in the extracellular matrix.[2] The role of HS has been shown to include a variety of biological processes ranging from cell adhesion, cell growth regulation, blood coagulation, binding of cell surface proteins, and tumor metastasis, just to name a few.[2] Heparan sulfate and heparin adopt a stiff helix conformation that positions clusters of sulfate groups at regularly spaced intervals of approximately 17 Å on either side of the helical axis.[3, 4] See Figure 5.1. The helical shape of heparin (Figure 5.1a) shows a close similarity to the helix formed in a duplex DNA molecule (figure 5.1b). The DNA crystal structure shows approximately 7-8 Å spacing between the phosphate clamp interactions between the amines of the AH 78 and the phosphate oxygen. A quick study of the heparin structure reveals that sulfate oxygen spacing on a disaccharide unit varies from approximately 5-7 Å. Given the fact that all the noncovalent

platinum compounds used in this research possess a flexible hexandiamine linker, favorable electrostatic or hydrogen bond interactions may also occur with the numerous sulfate groups.

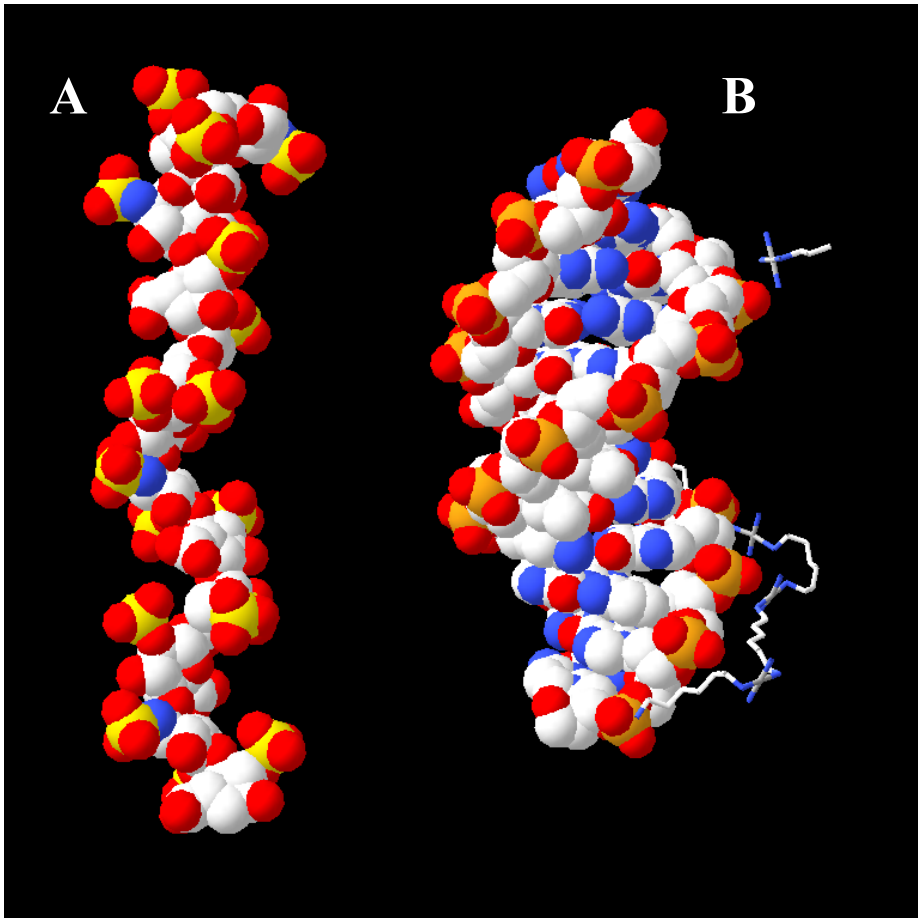

Figure 5.1 PDB database of heparin sulfate (A) and Dickerson-Drew Dodecamer with AH 78 (B). PDB reference (A) 3IRI (B) 2DYW

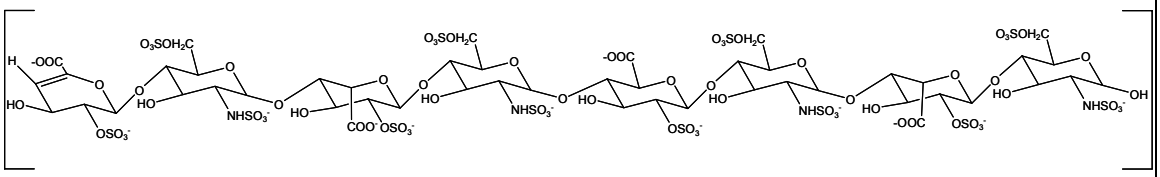

Figure 5.2 Structure of Heparan sulfate octasaccharide. 16 Na^+ counter ions ommited

5.2 Heparan sulfate internalization of cationic biomolecules

As mentioned earlier, one of the major requirements for the effectiveness of a platinum anticancer therapeutic is the successful cellular uptake of the compound. One of the most remarkable roles of the cell surface HS is the mediation of cellular internalization.[2]

Research of new drug delivery methods has focused on designing structures that utilize the endocytic pathway as a means to deliver the bioactive structure into the cell.[5] One of the most successful candidates has been cell penetrating peptides (CPPs), which consist of polycationic arginine rich oligopeptides, capable of migrating across the biological membrane of cell with a time range from seconds to minutes.[6-8] (For a review, see reference [8].) One of the remarkable characteristics of CPPs is the ability to assist other biomolecular compounds that may not readily migrate across the membrane. This requires that the CPPs not be covalently linked to the biomolecular cargo they are assisting, and also that the binding affinity between the two is sufficiently high to achieve a stabile transport.[9]

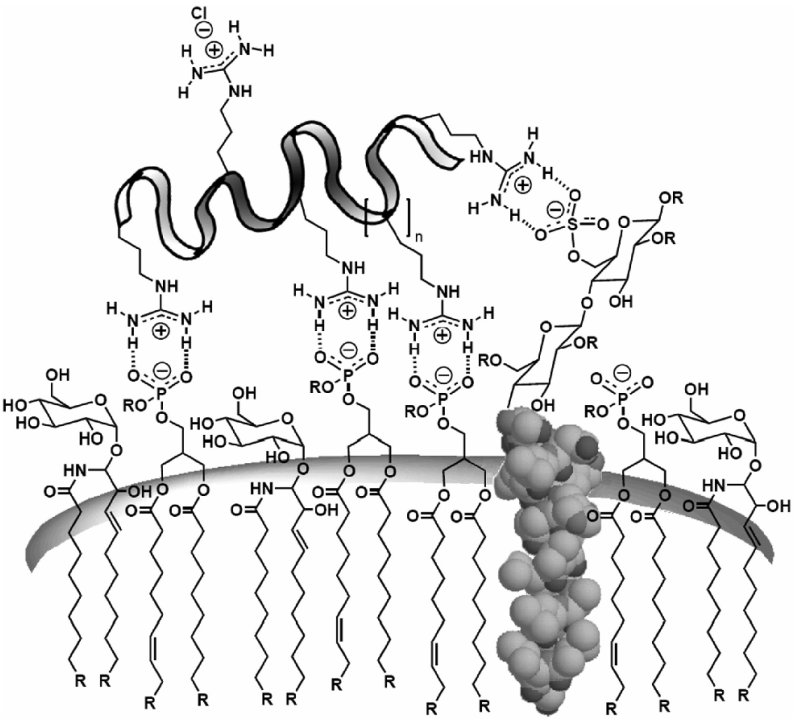

Figure 5.3 Cell surface guanidinium-anionic constituent interactions.[1]

For instance, fluorescently labeled CPPs are commonly identified within the cell nucleus which gives rise to the question: is the fluorescent signal due to the CPP binding strongly with DNA after the cellular uptake?[6] Using in vivo conditions, it has been shown that the binding of CPPs to DNA involves specific recognition sites and leads to the suggestion that the CPP interacts with the phosphate backbone of DNA.[6]

Common to all types of CPPs is the presence of a highly charged cationic region that is essential for the transport across the membrane.[10] This is in stark contrast to the fact that it is commonly accepted that charged molecules cannot pass through the lipid bilayer by passive diffusion.[10]

Two proposed mechanisms for this phenomemon are: (1) the formation of an electrically neutral complex formed between the cationic CPP and anionic heparan sulfate proteoglycans[11, 12], and (2) the binding of CPPs to the negatively charged lipids thus disrupting the lipid bilayer[13] and more recently, determined to show a strong electrostatic interaction followed by a weak hydrophobic adsorption/portioning.[10]

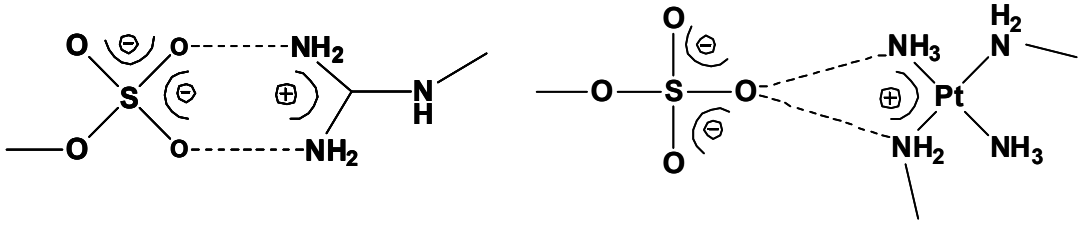

Figure 5.4 Structural comparison of possible sulfate clamp motif

Comparisons between short peptides with varying arginine and lysine content highlight the important fact that the overall charge of the CPP is important for uptake.[1] A similar charge-to-uptake correlation has been identified in the polynuclear platinum compounds highlighted in Chapter 2.[14]

The association of the positively charged guanidinium group with negatively charged cell surface structures such as carboxylates, phosphates and sulfates, occurs due to the rigid planar array of hydrogen bond donors that allow for bidentate bond formation.[1] These types of anionic structures are generally found on the cell membrane as the constituents of phospholipids, fatty acids, proteins, and heparan sulfate moieties.[1] This bidentate bond formation between the two charged groups provides a stronger interaction than the monodentate and thus, may provide some

rationalization to why arginines associate and cross the membrane at different levels than the lysines.[1, 15] In addition to the structural differences, it can also be hypothesized that charge is necessary for successful translocation, but as both polylysines and polyarginines carry a positive charge, other factors such as the degree of protonation may play a factor.[1] As such, the combination of a bidentate binding structure with a high positive charge in the functional group, results in the ideal moiety to interact with the phosphates, carboxylates, and sulfates located on the cell surface.[1] Just as the shape and charge are important, so is the effective length of the oligomer. For polyarginine CPPs, the effective range for cellular translocation was found to be greater than 6 arginine residues and shorter than 20 residues, with a maximal uptake of approximately 15 residues.[1, 16] The rationale for the decreased translocation of longer polyarginine structures, is that the increase in length increases the association to a level that is too high for the effective release of the structure from the membrane.[1]

As mentioned in Chapter 1, these types of polynuclear platinum compounds have a remarkable cellular uptake that appears to be based on the charge of the compounds.[14] Cellular uptake of biologically active compounds is a barrier that must be overcome in the development of new pharmaceutics.[17] The cellular surface contains an array of possible anionic binding sites, Figure 5.2 illustrates just the phospholipids and polysaccharide constituents. The interactions of the guanidinium unit of arginine rich peptides has been examined as a means for cellular translocation.[18] It has been well established that charged compounds do not readily cross the membrane without some sort of energetic assistance, which may come in the form of pumps or channels. Arginine rich peptides have been heavily studied because of their ability to translocate across the plasma membrane of living cells. One recent study predicted that arginine rich peptides like the TAT peptide float along the anionic phospholipid head group, strongly

interacting and thus reducing the peptides mobility.[19] Binding studies on the affinities of these cell penetrating peptides indicate a strong electrostatic interaction with anionic species located on the cell surface, such as lipid head groups, proteins, and proteoglycans, such as heparan sulfate.[17, 20, 21] While studies have shown that the TAT peptides bind to heparan sulfate with a higher affinity than anionic lipid vesicles, a direct method has yet to be identified.[17, 20, 21] As such, multiple mechanisms are possible and interaction of cell-penetrating peptides results in aggregation of both anionic lipids and proteoglycans.[17, 22, 23]

5.3 Mass spectrometry of guanidinium interactions:

Noncovalent interactions are numerous throughout biological systems. The gentle nature of ESI-MS ensures that such noncovalent interacting species are transferred from the solution to the gas phase. Polysulfated oligosaccharide chains are difficult to characterize because of their high polarity, structural diversity, and sulfate lability.[24] Schug and Linder have used ESI-MS to show that there is a significant difference in interaction strengths between guanidinium and phosphonate/sulfonates compared to carboxylates.[25] In addition, ESI-MS resulted in the phosphonate/sulfonates displaying a higher propensity to form complexes than the carboxylates.[25] Tandem mass spectrometry (MS/MS) of polysulfated oligosaccharides generally has four competing fragmentation pathways, (1) cleavage of the glycosidic bonds, (2) SO_3 loss from the isolated precursor ion, (3) charge reduction and equivalent loss of H_2SO_4, and (4) the loss of H^- from the precursor ion, thus reducing the overall charge.[26] It should be noted that pathway (2) typically dominates in the case of MS/MS analysis of lower charge state sulfated polysaccharides. The cleavage of the glycosidic bonds are generally preferred when a proton or another cation are interacting with the glycosidic oxygen.[26, 27] For the GAG ions, the overall

charge state is always lower than the available number of mobile protons, thus increasing the potential for the protons to be available to destabilize the glycosidic bonds.[26] The cases involving the loss of SO_3, generally occur when the available protons are associated with the sulfate groups, thus rendering the ion with a lower overall charge state.[26] However, for these experiments, the ion of lower charge state is preferred to study the stabilizing effects these new noncovalent polynuclear complexes induce on the anion GAGs. In addition, the higher charge state GAG ions result in increased charge-charge repulsion which stress the glycosidic bonds, making for a competing fragmentation pathway with the loss of sulfate moieties.[26] The addition of ion-pairing molecules, such as ammonium counter ions, displaces sodium adducts, prevents the loss of sulfate groups, and greatly simplifies the resulting mass spectra.[26]

5.4 Experimental

Mass spectra were acquired on a Micromass-Waters Qtof-2 mass spectrometer (Milford, MA) equipped with a custom built microspray source. Samples were introduced by flow injection at flow rates of 0.5-0.7 μL/min using a syringe pump (Harvard Apparatus). Electrospray source conditions were kept constant with a source temperature of 120°C and spray voltage of 2.0 kV. In tandem mass spectrometry (MS/MS) experiments, collisional energy was varied from 10 eV to 40 eV. Heparan sulfate octasaccharide was purchased from V-Labs (Covington, LA) and reconstituted in 18 MΩ water to form a 375 μM stock solution. Platinum compounds were reconstituted in 18 MΩ water to a stock concentration of 500 μM. Samples were mixed at a 1:2 molar ratio in 18 MΩ water with a final concentration of 10mM NH4OAc. Mixtures were incubated at 37°C for 20 minutes then dialyzed in a custom flow through micro dialysis chamber at 3 μL/min using 13,000 molecular weight cut off (MWCO) hollow cellulose fibers from

SpectraPor, (Rancho Dominguez, CA) and recollected. DPPS and DPPA phospholipids were purchased from Avanti Inc, (Alabaster, AL). Samples were mixed in chloride free pipes buffer (pH = 7.4) at a molar ratio of 1:2. Following incubation at 37 °C suspensions were extracted using chloroform. The extract was then lyophilized to dryness and reconstituted in ESI solution.

5.5 Results and discussion

In this study, gas-phase interactions between heparan sulfate (HS) octasaccharides and noncovalent polynuclear platinum compounds of varying size (dinuclear and trinuclear) and charge (4+ to 8+) were investigated using ESI-MS. This is the first such experiment investigating the interaction of a noncovalent platinum compound with a sulfated polysaccharide.

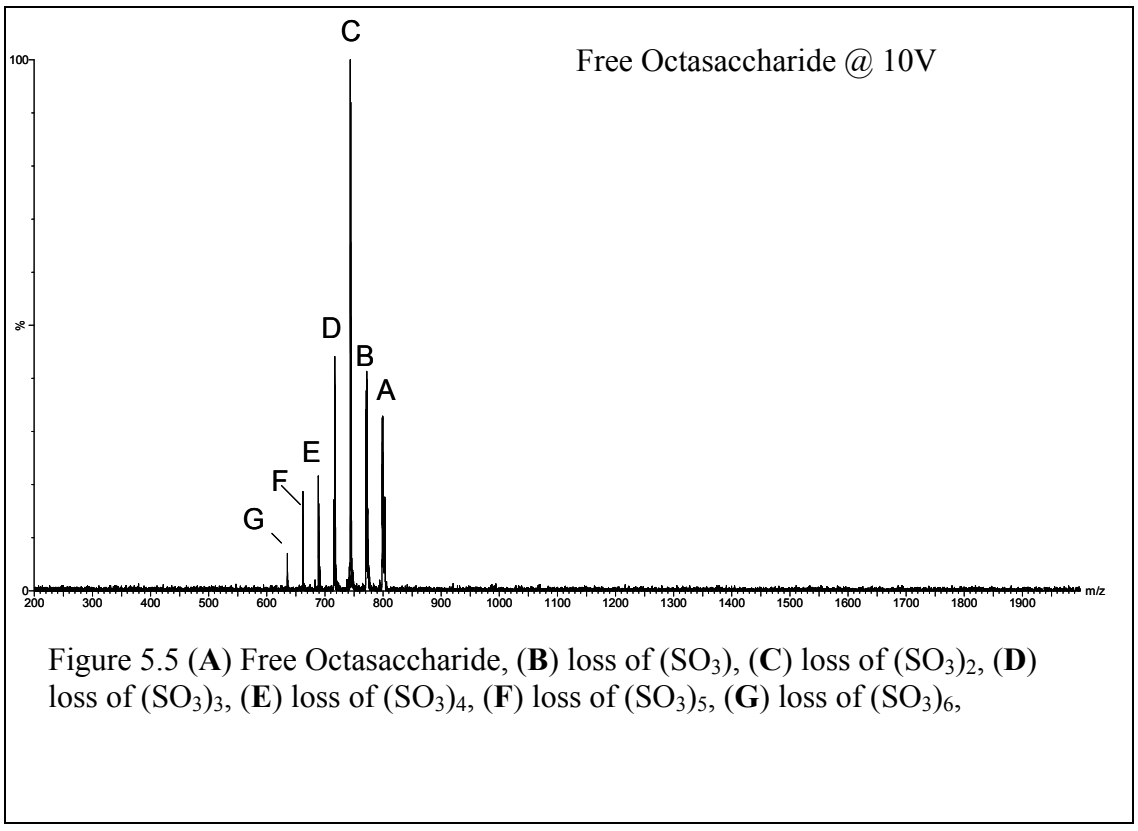

Figure 5.5 (**A**) Free Octasaccharide, (**B**) loss of (SO_3), (**C**) loss of $(SO_3)_2$, (**D**) loss of $(SO_3)_3$, (**E**) loss of $(SO_3)_4$, (**F**) loss of $(SO_3)_5$, (**G**) loss of $(SO_3)_6$,

The HS octasaccharide was chosen to serves as a model system for the HS found on the surface of cells and to represent a possible means of cellular internalization of these types of platinum compounds. Figure 5.5 shows the free 3- charge state of a HS octasaccharide, designated (A) 799 *m/z*, at 10V of collisional energy. Under these ESI-MS/MS conditions the sulfates are extremely labile, as expected during the negative mode acquisition. The addition of ammonium acetate to the ESI solution results in ammonium salt NH_4^+ binding to the sulfates which, during the ESI desolvation process release as ammonium NH_3. The resultant protonated HSO_3 is less stable than $NaSO_3$ and easily fragments from the oligosaccahride.

The 10V of collision energy, which is usually a starting point for all MS/MS experiments in this laboratory, as it provides efficient ion cooling and aids in the transfer of the ion packets, results in the sequential loss of sulfates. It should be noted that the low charge state (3-) used for these experiments typically favors the loss of sulfates from the glycosidic backbone. Higher charge states for these types of complexes have been difficult to obtain. This is most likely due to the energetics applied to the ions associated with the QTOF-2. This has been illustrated by Naggar et. al where they point out that the lack of higher charge states in the ESI-MS of GAG molecules may be due to the high energetic penalty of desolvation on an orthogonal time of flight instrument.[26] As illustrated in Figure 5.5, it is evident that HS octasaccharide loses up to six sulfates upon "gentle" collision settings, again, owing to the labile nature of the sulfates in the gas-phase. As the collision energy is increased from 10 to 20V, the extent of the sulfate loss increases to eight total sulfates. Of the 12 total sulfates associated with this octasaccharide, 8 are of the HSO_3 structure and 4 are found as H_2SO_4 structures. (see Figure 5.2) The collision voltage of 30V results in a loss of a total 9 sulfates without any detectible glycosidic bond cleavages, or change in the overall charge state. Figure 5.6. The identification of the preferred dissociation

pathway for this HS octamer being the sequential loss of sulfate rather than cleavage of the glycosidic bonds, makes this system amenable for studying the noncovalent interactions of the platinum compounds with sulfates.

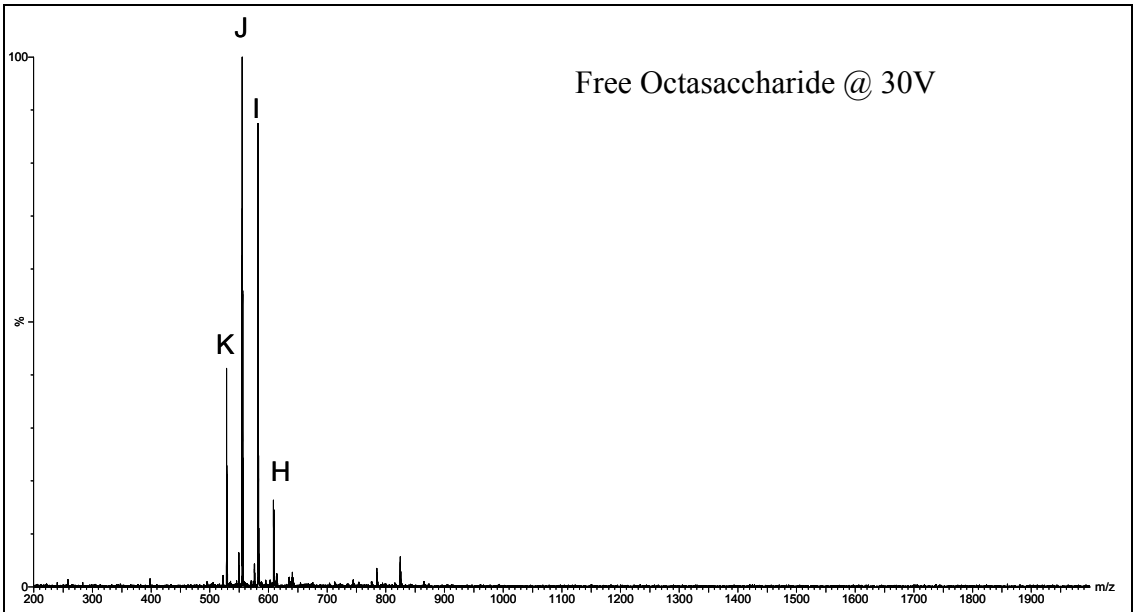

Figure 5.6 (**A**) Free Octasaccharide, (**B**) loss of (SO_3), (**C**) loss of $(SO_3)_2$, (**D**) loss of $(SO_3)_3$, (**E**) loss of $(SO_3)_4$, (**F**) loss of $(SO_3)_5$, (**G**) loss of $(SO_3)_6$, (H) loss of $(SO_3)_7$ (I) loss of $(SO_3)_8$, (**J**) loss of $(SO_3)_9$, (**K**) loss of $(SO_3)_{10}$,H_2SO_4

ESI-MS/MS studies of Heparan Sulfate Octasaccharide with Noncovalent Polynuclear Platinum Compounds

To investigate the fragmentation pathway for the complexation of HS and noncovalent platinum compounds (AH 88, AH 44, and AH 78), ESI-MS/MS studies were conducted see Figure 3.2. The $[HS\text{-}Pt]^{3-}$ ion was fragmented at varying collision energies 10, 20, and 30 V. Figure 5.7 shows the fragmentation profile at 10V of collisional energy. The fragments observed are characteristic of the same sulfate loss pathway seen in the free octasaccharide.

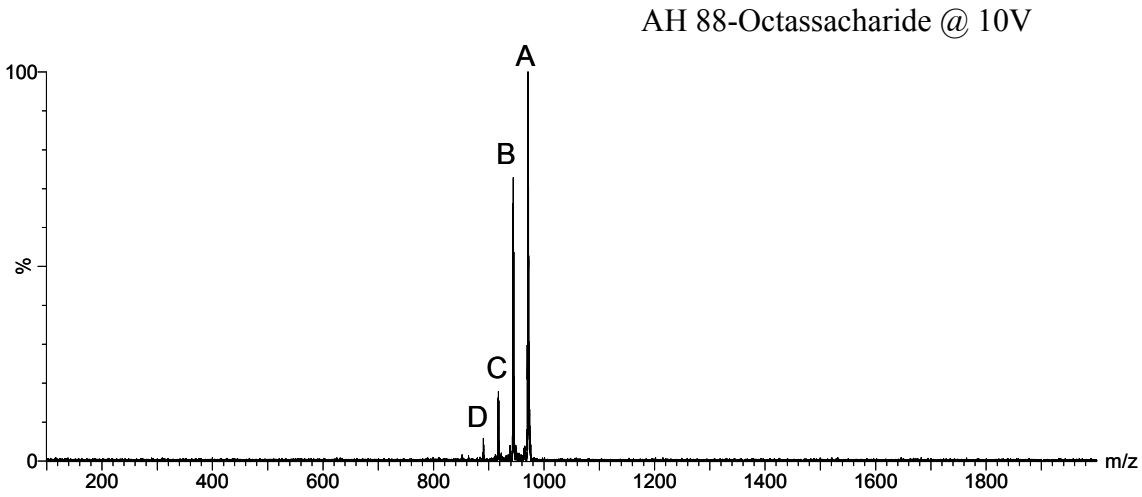

Figure 5.7 (**A**) AH88- Octasaccharide, (**B**) loss of (SO_3), (**C**) loss of $(SO_3)_2$, (**D**) loss of $(SO_3)_3$,

However, it is clear that the addition of the 4^+ charged dinuclear platinum compound AH 88, results in an increased stabilization of the sulfate moieties.Figures 5.8 shows the resultant fragmentation products from 30 V of collisional energy, respectively. The dominant peaks correspond to the loss of five and six sulfates, 832m/z and 805 m/z, shown as (F) and (G) in Figure 5.8, respectively. Careful identification of the spectra shows that as the collision energy is increased, there is a new series of peaks that begin to appear, corresponding to the loss of a H^+ and the attachment of a Na^+ ion, 837 m/z and 810 m/z. The binding between HS and AH 88 is strong, as there is not direct evidence of free HS in the ESI-MS/MS spectra. The subsequent loss of up to six sulfate moieties does not deter the interaction between the two complexes.

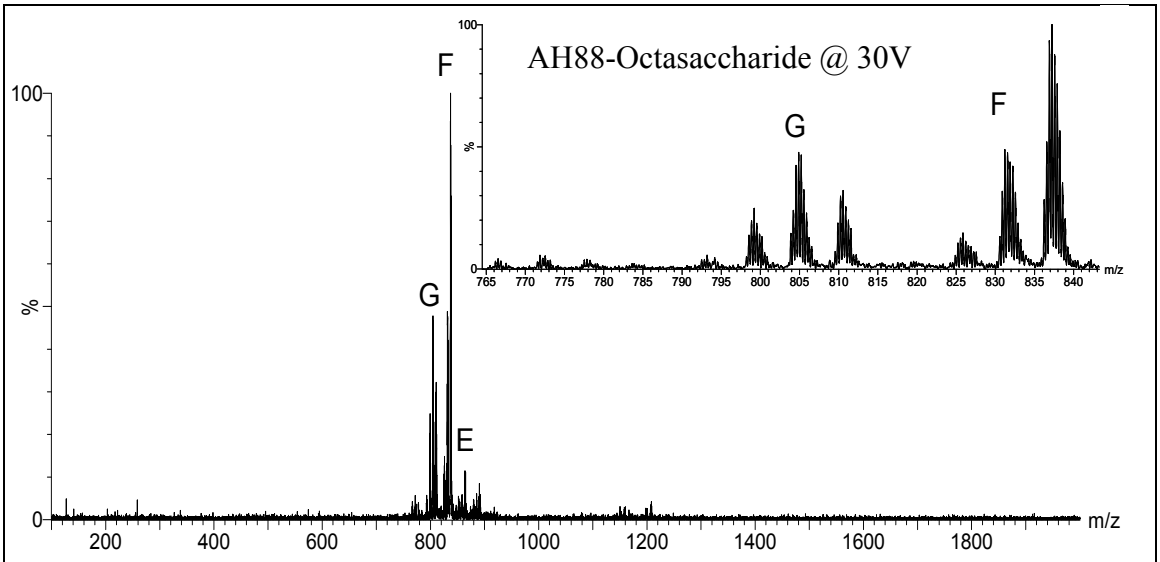

Figure 5.8 (**E**) loss of $(SO_3)_4$, (**F**) loss of $(SO_3)_5$, (**G**) loss of $(SO_3)_6$,

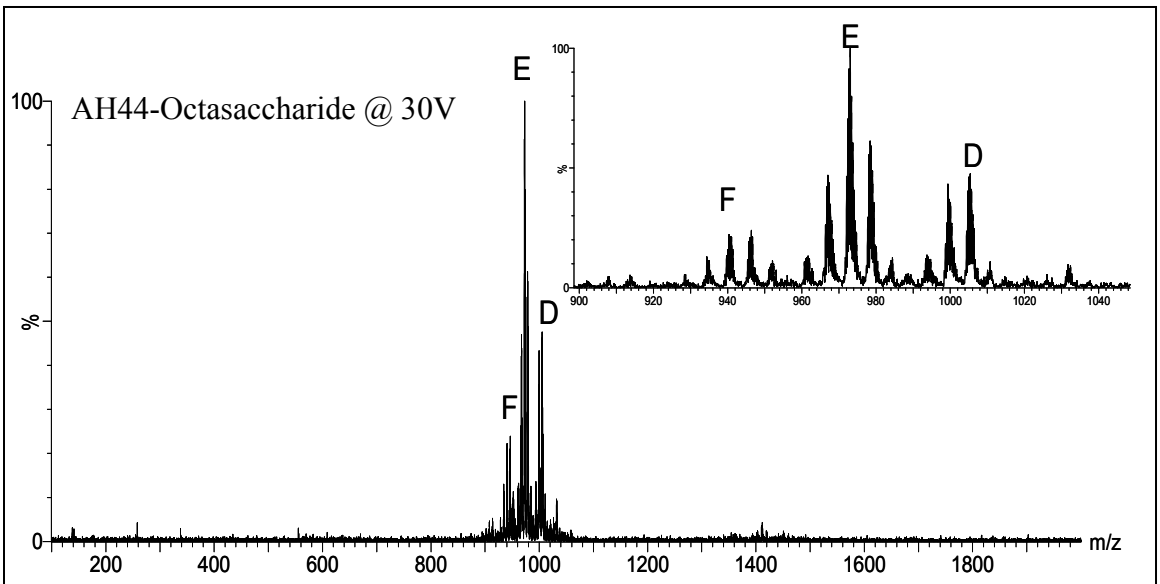

Figure 5.9 (**A**) AH44 - Octasaccharide, (**B**) loss of (SO_3), (**C**) loss of $(SO_3)_2$, (**D**) loss of $(SO_3)_3$, (**E**) loss of $(SO_3)_4$, (**F**) loss of $(SO_3)_5$,

Figure 5.9 illustrates the ESI-MS/MS spectra of the 3- charge state of the noncovalent trinuclear compound AH 44 with HS, (peak A), at 10 V of collision energy.

Figure 5.10 shows the isolation and fragmentation of the 3- charge state of the 8+ AH 78 with HS, (peak A). The loss of sulfate from the intact structure still occurs, but is only representative of approximately 10% of the relative abundance of the intact species. Increasing the voltage from 20 to 30 V, as depicted in Figure 5.10, yields a maximum of three sulfate moieties lost during the MS/MS.

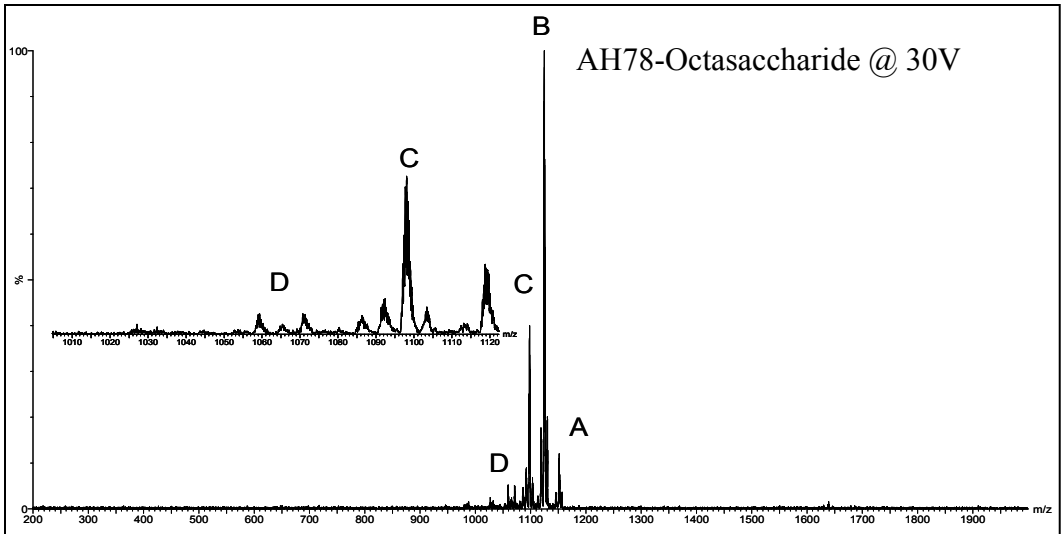

Figure 5.10 (**A**) AH78-Octasaccharide, (**B**) loss of (SO_3), (**C**) loss of $(SO_3)_2$, (**D**) loss of $(SO_3)_3$,

Interaction of Noncovalent Polynuclear Compounds with Phospholipids

In efforts to look at the possible interactions of these compounds with anionic cell surface structures, namely phospholipids, an ESI-MS study was done. Previous work has been accomplished using ESI-MS and NMR as a means to study these polynuclear platinum compounds interacting with lipid structures.[30] In those studies, the covalent platinum compound BBR 3464 was found to exhibit a slight electrostatic association with negative phospholipids head groups. Additionally, a comparison of the binding affinity showed that the DPPA (mw 647 Da) had a slightly higher binding affinity than DPPS (mw 734 Da), which was attributed to the smaller phosphate head group of DPPA having more electronic density.[30] For the work done here, a liposome-Pt extract was reconstituted in ESI spray solution consisting of 80% MEOH, 15% $CHCl_3$, and 5% 10mM ammonium acetate.

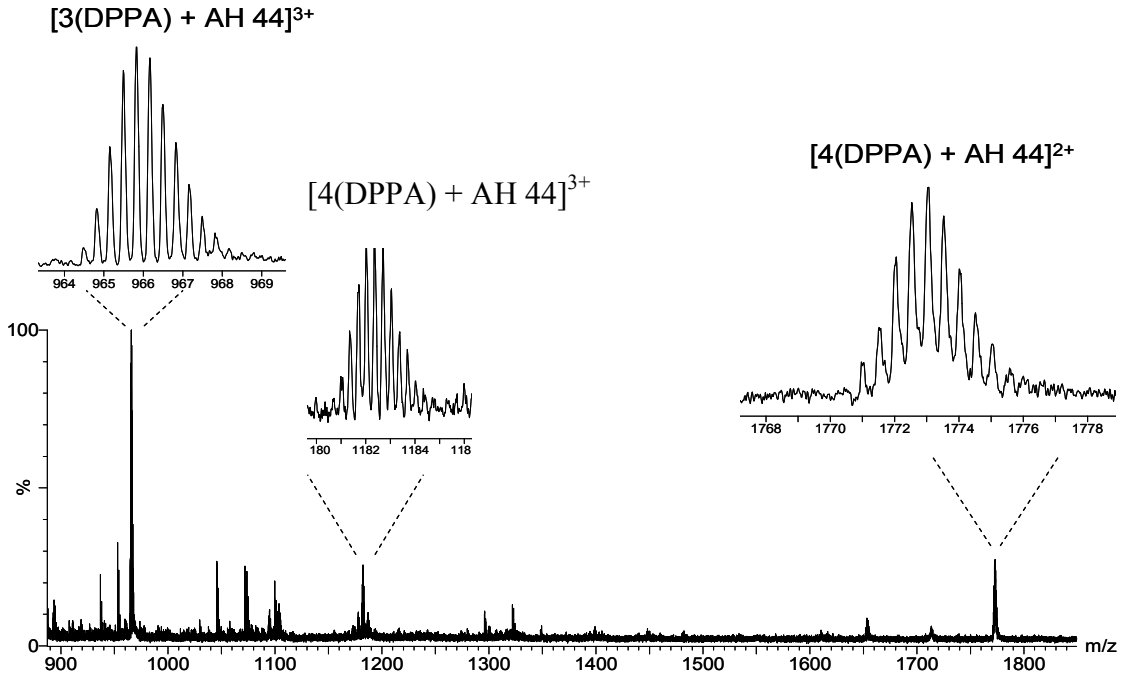

Figure 5.11 Positive ESI-MS of phospholipid DPPA with AH 44. The electrostatic binding is seen for up to four DPPA groups per one platinum compound.

Figure 5.11 shows the resultant positive ESI-MS spectra of the liposome-Pt extract. The dominant peak in the spectra corresponds to the 3+ ion and electrostatic interaction of three intact DPPA lipids with one AH 44 trinuclear platinum compound at 966 m/z. Additionally, the presence of peaks with four DDPA lipids electrostatically bound to AH 44 is also detected at 1182 and 1773 m/z respectively.

Figure 5.12 shows the ESI-MS spectra of the phospholopid DPPS with AH 44. The phospholipid DPPS contains a phosphatidyl-serine head group that presents multiple sites for formation of the "clamp" type binding motif. The notable peaks are 1053 m/z, 1298 m/z, and the 1544 m/z, these correspond to the electrostatic association of three, four, and five intact DPPS lipids, respectively. Also, careful examination of the peak located at 1023 m/z reveals a loss of 87 Da, which would correspond to the loss of one serine head group moiety from the lipid structure. Additionally, this is also evident for the 4DDPS gas phase structure, as noted by the peak at 1269 m/z.

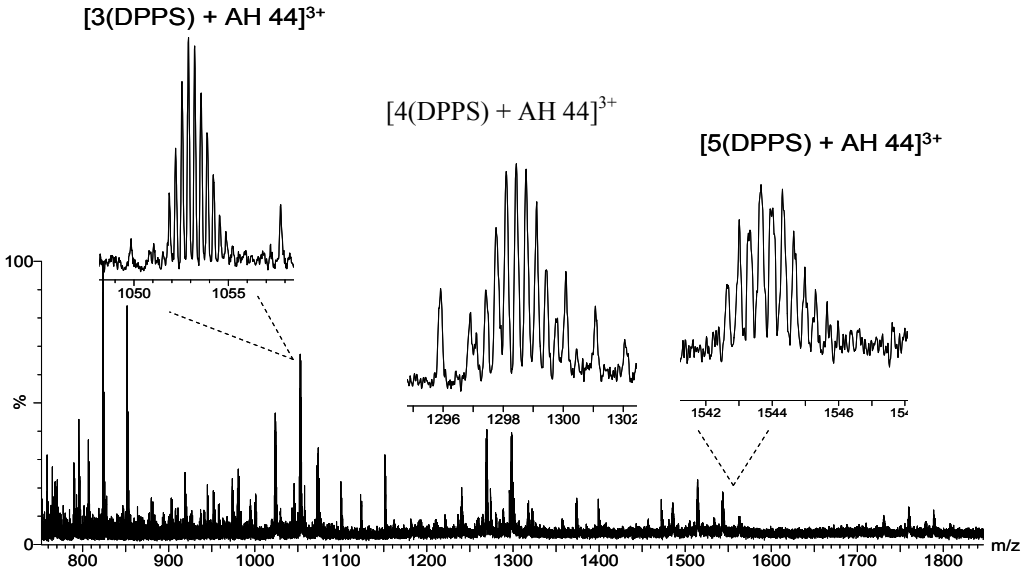

Figure 5.12 Positive ESI-MS of DPPS and AH 44

While only a marginal conclusion can be drawn, this may give some indication that the preferred binding site is the phosphate portion of the lipid headgroup. It is undetermined weather the product of the cleavage is the result of the electrospray process or some other event prior to the electrostatic association with the AH 44.

The ESI-MS of the DPPA and DPPS with the trinuclear 8+ compound AH 78 reveal a similar type binding profile. Figure 5.13 shows the peaks obtained from the samples extracted from the mixture of DPPA with AH 78. The interaction appears to be more favorable than that observed for the AH 44. As the case of AH 44, a distribution of electrostatic associations range from 3-6 DPPA intact lipid structures. The most intense peaks correspond to the distribution of three, four, and five DPPA moieties.

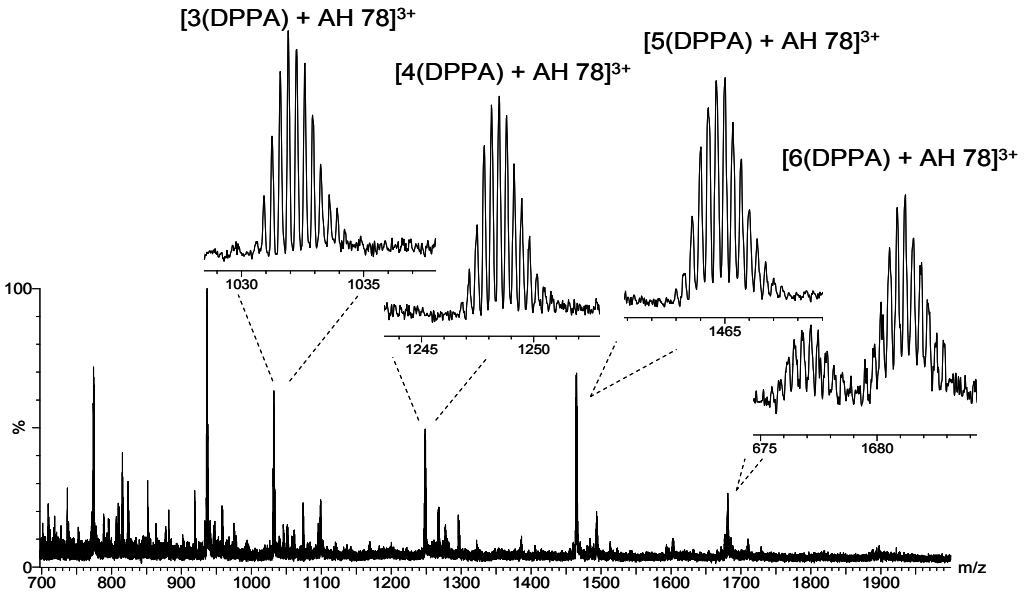

Figure 5.13Positive ESI-MS of DPPA with AH 78. Increasing the overall charge of the platinum compound results in a larger number of electrostatic interactions ranging from 3-6 DPPA lipids.

The binding profile of AH 78 with DPPS is less complicated than that of AH 44 for reasons undetermined. Examination of Figure 5.14 reveals the noncovalent association of up to six DPPS lipids per AH 78 compound. However, unlike before, there appears little to no fragmentation of the phosphatidyl-serine head group. The major species present in the spectra corresponds to the 3+ charge state of three DPPS lipids with one AH 78 at 1119 m/z. An unresolved peak shift of 57 Da is seen for all species present in solution. At this time, no attempt has been made to provide an explanation and further purification of the sample before ESI-MS may be necessary. The ion intensity for the four and five DPPS-Pt structures appears equivalent at 1365 and 1610 m/z, respectfully.

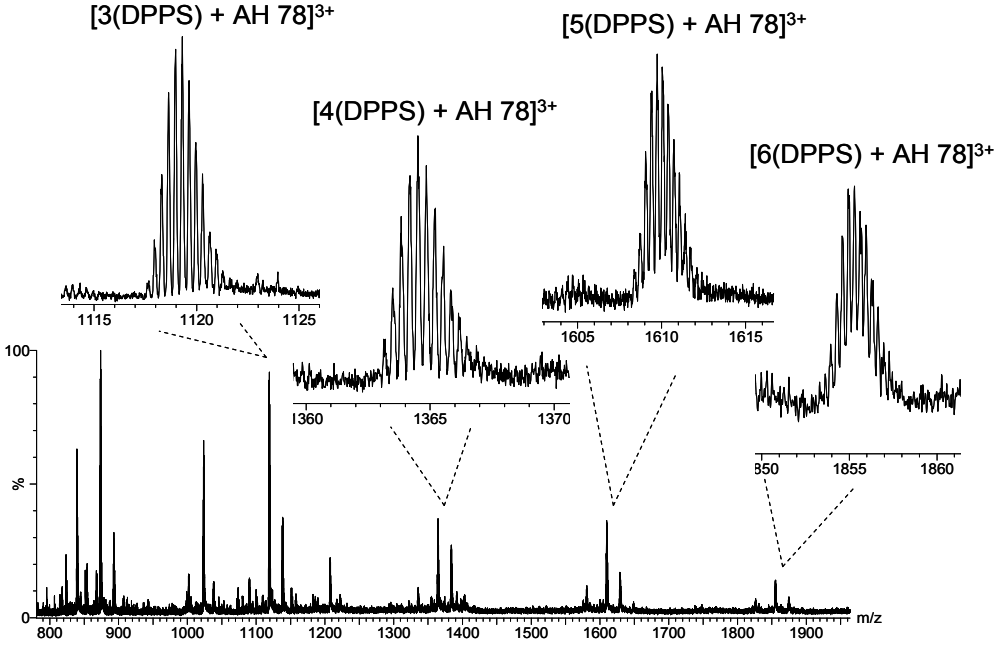

Figure 5.14 ESI-MS of DPPS with AH 78 showing up to six DPPS intact lipid structures binding through electrostatic associations.

No evidence for any higher number structures exists in the spectra. This may be the result of the square planar geometry of the Pt centers and the fact that two "phosphate clamps" are able to form on either side of the platinum compound. A proposed structure of this binding arrangement is seen in Figure 5.15. Based on the phosphate clamp motif with DNA, as shown by crystal structure, one platinum center is cable of forming the clamping motif with multiple anionic structures. Such is the case presented here with all available sites occupied with phosophate clamp motifs.

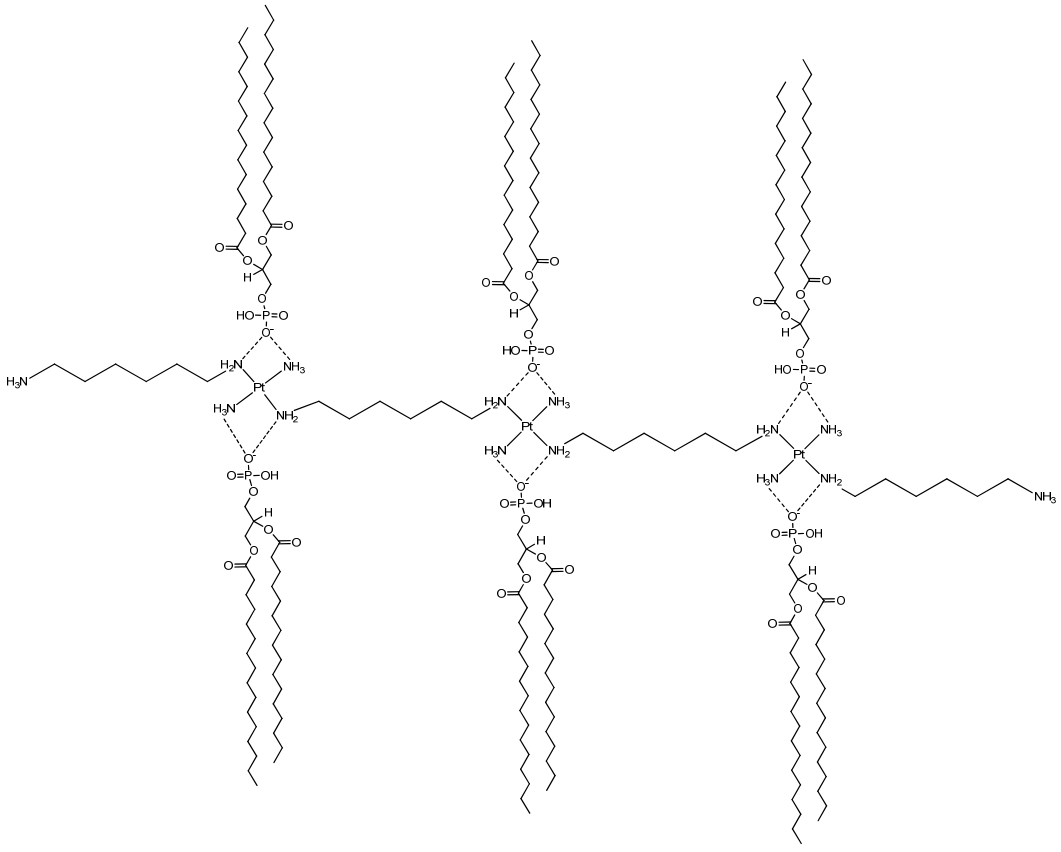

Figure 5.15 Proposed binding scheme of up to six DPPA lipids with AH 78

5.6 Conclusions

The results obtained from the ESI-MS/MS of the HS octasaccharide electrostatically bound with a noncovalent polynuclear platinum compound suggest the main dissociation pathway is cleavage of the labile sulfate moieties. While the quantitative measure of the binding energies cannot be accessed, the strength of the interaction between the HS and "sulfate" clamps is remarkable. It should be mentioned that the strength of electrostatic interactions is actually strengthened in the gas phase compared to solution phase.[28 1&6] This added association strength comes from the dielectric constant of the solvents used in the experiment as they tend to weaken the electrostatic interactions.[28] At the higher voltages used, 30V, there are some fragmentations of the HS polysaccharide structure. However, these are negligible when compared to the intensity of the ions from sulfate loss and is less than 3% of the base peak intensity. Increasing the size and charge of the noncovalent platinum compound results in an increased overall stability of the complex and fewer sulfate moieties lost during the MS/MS experiment. As mentioned earlier, the higher the charge state or more deprotonated a GAG is, the higher the propensity is for glycosidic bond cleavage. In the case with the noncovalent polynuclear compounds, the ability to form a "sulfate clamp" binding motif limits the available number of sulfates that are able to become deprotonated and therefore the major fragmentation pathway is loss of sulfate moieties. It has been observed that for gas-phase dissociations, the lability of sulfate groups tend to follow the order of $SO_3H > SO_3 > SO_3Na$.[29] Therefore as the number of sodium adducts increases that amount of sulfate loss decreases. This is the similar trend for the noncovalent platinum complexes. As such, this example of increased stability serves as a method for verifying the complexation with sulfate moieties and not elsewhere on the glycosidic backbone. To reiterate, the perceived increase in stability and therefore lack of sulfate loss

exhibited by these complexations follows the existing methodology that cations binding to the anionic sulfate help stabilize the structure from sulfate loss. This helps strengthen the argument that these noncovalent platinum complexes are able to bind sulfate moieties in a similar fashion as the phosphate clamp binding motif. Analogous to the studies of the gas-phase stabilities with utilizing the phosphate clamp binding motif on DNA, these results with sulfate indicate a very strong interaction. The MS/MS studies reveal a preferred dissociation pathway of sulfate loss with no dissociation of the noncovalent platinum compound from the heparan sulfate polysaccharide.

In addition, the ESI-MS results of the DPPS and DPPA with AH 44 and AH 78, help illustrate a possible phospholipid association. Based on the observed peaks in the ESI-MS experiments with up to six phospholipids bound to one platinum compound, it is conceivable to think that the structure represented in Figure 5.14 could represent the movement of a noncovalent platinum compound through the lipid bilayer as a means of cellular uptake. As charged compounds do not readily permeate the membrane, the neutralization via the phosphate head groups may assist in the migration. Additional experiments with different lipid head group structures needs to be addressed as a way to identify the binding affinity for model cell surface structures.

5.7 References

1. Wender, P. A.; Galliher, W. C.; Goun, E. A.; Jones, L. R.; Pillow, T. H., The design of guanidinium-rich transporters and their internalization mechanisms. *Advanced Drug Delivery Reviews* **2008,** 60, (4-5), 452-472.

2. Rabenstein, D. L., Heparin and heparan sulfate: structure and function. *Nat Prod Rep* **2002,** 19, (3), 312-31.

3. Vlodavsky, I.; Ilan, N.; Nadir, Y.; Brenner, B.; Katz, B. Z.; Naggi, A.; Torri, G.; Casu, B.; Sasisekharan, R., Heparanase, heparin and the coagulation system in cancer progression. *Thromb Res* **2007,** 120 Suppl 2, S112-20.

4. Mulloy, B.; Forster, M. J.; Jones, C.; Davies, D. B., N.M.R. and molecular-modelling studies of the solution conformation of heparin. *Biochem. J.* **1993,** 293, (3), 849-858.

5. Jones, A. T., Gateways and tools for drug delivery: Endocytic pathways and the cellular dynamics of cell penetrating peptides. *International Journal of Pharmaceutics* **2008,** 354, (1-2), 34-38.

6. Ziegler, A.; Seelig, J., High Affinity of the Cell-Penetrating Peptide HIV-1 Tat-PTD for DNA. *Biochemistry* **2007,** 46, (27), 8138-8145.

7. Schwarze, S. R.; Hruska, K. A.; Dowdy, S. F., Protein transduction: unrestricted delivery into all cells? *Trends Cell Biol* **2000,** 10, (7), 290-5.

8. Lindgren, M.; Hallbrink, M.; Prochiantz, A.; Langel, U., Cell-penetrating peptides. *Trends Pharmacol Sci* **2000,** 21, (3), 99-103.

9. Choosakoonkriang, S.; Lobo, B. A.; Koe, G. S.; Koe, J. G.; Middaugh, C. R., Biophysical characterization of PEI/DNA complexes. *J Pharm Sci* **2003,** 92, (8), 1710-22.

10. Ziegler, A.; LiBlatter, X.; Seelig, A.; Seelig, J., Protein Transduction Domains of HIV-1 and SIV TAT Interact with Charged Lipid Vesicles. Binding Mechanism and Thermodynamic Analysis. *Biochemistry* **2003,** 42, (30), 9185-9194.

11. Frankel, A. D.; Pabo, C. O., Cellular uptake of the tat protein from human immunodeficiency virus. *Cell* **1988,** 55, (6), 1189-93.

12. Tyagi, M.; Rusnati, M.; Presta, M.; Giacca, M., Internalization of HIV-1 tat requires cell surface heparan sulfate proteoglycans. *J Biol Chem* **2001,** 276, (5), 3254-61.

13. Prochiantz, A., Messenger proteins: homeoproteins, TAT and others. *Curr Opin Cell Biol* **2000,** 12, (4), 400-6.

14. Harris, A. L.; Yang, X.; Hegmans, A.; Povirk, L.; Ryan, J. J.; Kelland, L.; Farrell, N. P., Synthesis, Characterization, and Cytotoxicity of a Novel Highly Charged Trinuclear Platinum Compound. Enhancement of Cellular Uptake with Charge. *Inorg. Chem.* **2005,** 44, (26), 9598-9600.

15. Mitchell, D. J.; Kim, D. T.; Steinman, L.; Fathman, C. G.; Rothbard, J. B., Polyarginine enters cells more efficiently than other polycationic homopolymers. *J Pept Res* **2000,** 56, (5), 318-25.

16. Wender, P. A.; Mitchell, D. J.; Pattabiraman, K.; Pelkey, E. T.; Steinman, L.; Rothbard, J. B., The design, synthesis, and evaluation of molecules that enable or enhance cellular uptake: peptoid molecular transporters. *Proc Natl Acad Sci U S A* **2000,** 97, (24), 13003-8.

17. Schmidt, N.; Mishra, A.; Lai, G. H.; Wong, G. C., Arginine-rich cell-penetrating peptides. *FEBS Lett* **2009**.

18. Tang, M.; Waring, A. J.; Hong, M., Phosphate-Mediated Arginine Insertion into Lipid Membranes and Pore Formation by a Cationic Membrane Peptide from Solid-State NMR. *Journal of the American Chemical Society* **2007,** 129, (37), 11438-11446.

19. Ciobanasu, C.; Harms, E.; Tunnemann, G.; Cardoso, M. C.; Kubitscheck, U., Cell-penetrating HIV1 TAT peptides float on model lipid bilayers. *Biochemistry* **2009,** 48, (22), 4728-37.

20. Ziegler, A.; Blatter, X. L.; Seelig, A.; Seelig, J., Protein transduction domains of HIV-1 and SIV TAT interact with charged lipid vesicles. Binding mechanism and thermodynamic analysis. *Biochemistry* **2003,** 42, (30), 9185-94.

21. Goncalves, E.; Kitas, E.; Seelig, J., Binding of oligoarginine to membrane lipids and heparan sulfate: structural and thermodynamic characterization of a cell-penetrating peptide. *Biochemistry* **2005,** 44, (7), 2692-702.

22. Tiriveedhi, V.; Butko, P., A fluorescence spectroscopy study on the interactions of the TAT-PTD peptide with model lipid membranes. *Biochemistry* **2007,** 46, (12), 3888-95.

23. Ziegler, A.; Seelig, J., Binding and clustering of glycosaminoglycans: a common property of mono- and multivalent cell-penetrating compounds. *Biophys J* **2008,** 94, (6), 2142-9.

24. Chai, W. G.; Luo, J. L.; Lim, C. K.; Lawson, A. M., Characterization of heparin oligosaccharide mixtures as ammonium salts using electrospray mass spectrometry. *Analytical Chemistry* **1998,** 70, (10), 2060-2066.

25. Schug, K. A.; Lindner, W., Noncovalent binding between guanidinium and anionic groups: focus on biological- and synthetic-based arginine/guanidinium interactions with phosph[on]ate and sulf[on]ate residues. *Chem Rev* **2005,** 105, (1), 67-114.

26. Naggar, E. F.; Costello, C. E.; Zaia, J., Competing fragmentation processes in tandem mass spectra of heparin-like glycosaminoglycans. *J Am Soc Mass Spectrom* **2004,** 15, (11), 1534-44.

27. Hofmeister, G. E.; Zhou, Z.; Leary, J. A., Linkage position determination in lithium-cationized disaccharides: tandem mass spectrometry and semiempirical calculations. *Journal of the American Chemical Society* **1991,** 113, (16), 5964-5970.

28. Jackson, S. N.; Wang, H. Y.; Woods, A. S., Study of the fragmentation patterns of the phosphate-arginine noncovalent bond. *J Proteome Res* **2005,** 4, (6), 2360-3.

29. Yagami, T.; Kitagawa, K.; Aida, C.; Fujiwara, H.; Futaki, S., Stabilization of a tyrosine O-sulfate residue by a cationic functional group: formation of a conjugate acid-base pair. *J Pept Res* **2000,** 56, (4), 239-49.

30. Liu, Q.; Qu, Y.; Van Antwerpen, R.; Farrell, N., Mechanism of the Membrane Interaction of Polynuclear Platinum Anticancer Agents. Implications for Cellular Uptake. Biochemistry 2006, 45, 4248-4256.

Chapter 6

Solution Composition and Thermal Denaturation for the Production of Single-Stranded PCR Amplicons: Piperidine-Induced Destabilization of the DNA Duplex?

John B. Mangrum, Jason W. Flora, and David C. Muddiman
Department of Chemistry, Virginia Commonwealth University, Richmond, Virginia, USA
Journal of the American Society for Mass Spectrometry, 13(3); **2002**, 232-240

6.1 Introduction

The precise determination of DNA sequence variations requires methodologies that are sensitive, accurate, and have high throughput efficiency. Electrospray ionization[1]Fourier transform ion cyclotron resonance mass spectrometry[2] (ESI-FTICR-MS) has proven to be an ideal method for genotyping length polymorphisms, such as, short tandem repeats (STRs).[3, 4] In determining sequence variations for use as genetic markers, these STRs are invaluable as they are highly polymorphic[5, 6], have an occurrence approximately every 10-20 kilo bases (kb) in the genome[7-9], and can be easily isolated using polymerase chain reaction (PCR) methods[7, 8, 10] ESI-MS typically results in the observation of duplex PCR amplicons.[3, 4, 11-20], as the Watson-Crick base pairing[21] is retained in the gas phase.

ESI when paired with FTICR has the advantage of being able to detect large molecules[22] with the measurement of large PCR amplicons up to 500 bp in length.[16] In addition, the ESI-FTICR method has allowed a single acquisition mass spectra to be collected from 5nM solutions of PCR amplicons.[20] The fitting of a modified dual electrospray source[23] has allowed for the mass accuracies approaching the theoretical limit ±10 ppm for large

biomolecules (>10 kDa).[24] However, the challenge to acquire mass accuracies high enough to accurately genotype length polymorphisms derived from complex STRs, which contain multiple repeat units, base insertions, and deletions, is still hampered.[25] This difficulty in obtaining accurate mass measurements of duplex PCR amplicons occurs because a base substitution, such as an A→T transversion, cannot be resolved by mass spectrometry because the complementary strand would also have a T→A transversion resulting in a zero mass difference. Therefore, it is necessary to be able to routinely generate single-stranded (ss) PCR amplicons for accurate characterization of base substitutions within STRs.[3, 15]

A survey through the literature reveals several strategies for the routine production of single stranded PCR products using mass spectrometry such as, nozzle skimmer dissociation [26], biotin-streptavidin chemistry[27-33], and the use of a DNA repair enzyme, lambda exonuclease.[3, 15] Gabelica et al. have used nozzle skimmer dissociation on ad 16-mer oligonucleotide with a G-C content approaching 75% to achieve complete dissociation with no sign of covalent backbone cleavage.[26] Research from this group on the nozzle skimmer dissociation of a 20-mer oligonucleotide with a G-C content of approximately 70% yield single stranded species, but a majority of the duplex structure remained and a significant amount of backbone cleavage was evident. The use of biotin-streptavidin magnetic beads has been shown to be effective, but sufficient sample loss has been shown to occur when trying to remove the strands form the bead surfaces.[3, 15] The use of lambda exonuclease to selectively digest the 5' phosphorylated strand of the duplex structure leaving only the complementary strand remaining has been shown to be effective[3, 15], but this method requires an additional enzymatic digestion step and in the

event of incomplete phosphorylation of the PCR primers, the amplicons are resistant to degradation.[3, 15]

Efforts to generate single stranded amplicons prior to entering the mass spectrometer have been shown by Williams and co-workers using thermal denaturation with the use of a resistively heated wire[34] This method is advantageous because it eliminates the probability of sample contamination since sample handling is reduced. This research focuses on the manipulation of solution compositions and thermal denaturation during the ESI process to control the stability of DNA duplexes in efforts to routinely generate single stranded species. The experimental conditions allow for the tailoring of the solutions to promote either single-stranded or double-stranded on the fly prior to the entrance into the mass spectrometer.

6.2 Experimental

Materials and Sample Preparation

Synthetic complementary 20-mer oligonucleotides 5'-CAGCGTGCGCCATCCTTCCC-3' and 5'-GGGAAGGATGGCGCACGCTG-3' were purchased from Midland Certified Reagent Company (Midland, TX). The oligonucleotides were desalted prior to ESI-MS using a microdialysis setup utilizing a hollow microdialysis membrane with 18,000 MWCO.[17, 35] The complementary 20-mers were annealed at a 1:1 molar ratio at 90°C for 2 minutes in their ESI solutions (vide infra) and slowly cooled back to room temperature. The final concentration of duplex was 4μM when prepared in ESI solutions. The 20-mer

duplex (MW = 12237.9) has an estimated melting temperature (T_m) of 71.6°C, which was calculated using the following equation[36]:

$T_m = 22 + 1.46(I_n)$ where I_n = 2 x (#GC base pairs) + (#AT base pairs) (Eq. 1)

The T_m is defined as the temperature at which one half of the duplex structure is in a denatured state. All other reagents were purchased from Sigma-Aldrich (St. Louis, MO); and used without further purification.

Mass Spectrometry

All spectra were obtained using a modified IonSpec Corporation (Irvine, CA) FTICR mass spectrometer with a 4.7 tesla superconducting magnet (Cryomagnetics, Inc. Oak Ridge TN). The ESI source (Analytica of Brandford Inc, Branford, CT) was modified with a heated metal capillary[37] applying a constant temperature (allowing for routine detection of noncovalent complexes with exception) for all experiments, and micro-electrospray emitter tips. The tips were hand pulled from a fused-silica capillary 50μm to 10μm i.d.[38] All samples were directly infused using a Harvard syringe pump, (South Natick, MA) at an infusion rate of 0.4 μL/min. All spectra were single acquisitions using 512 k of data for 20-mer oligonucleotides and 32 k of data for 82-bp HUMTHO1 PCR amplicons, acquired at 500 kHz ADC rate. Acquistions involved two 1-sec hexapole accumulations followd by gated trapping.[39] The unapodized data were zero filled two times and Fourier transformed prior to spectral analysis. Figure 1. shows a schematic of the heated transfer line used for thermal denaturation experiments. The transfer line was

constructed using as 24V DC power supply (Springboro, OH) to apply a DC voltage to the monochrome wire coiled around high temperature insulation. Real time temperature measurements were acquired using a thermocouple attached between the transfer line and insulation. Temperatures were displayed on an Omega CN9000A readout (Stamford, CT).

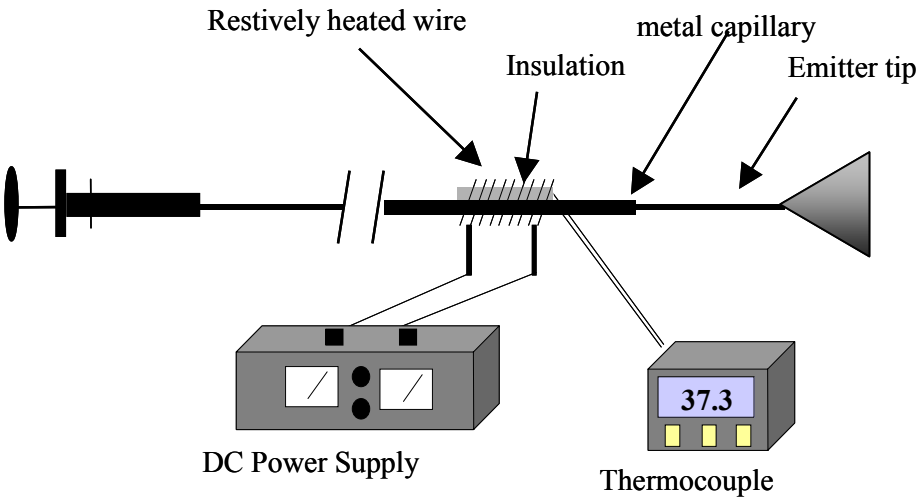

Figure 6.1: Schematic of ESI source with resistively heated transfer line.

6.3 Results and Discussion

The ESI-FTICR mass spectrum shown in Figure 6.2a is a double-stranded 20-mer oligonucleoide with a T_m = 71.6 ºC using the current electrospray solution of 60% acetonitrile, 20% isopropyl alchohol, 20% acqueous phase with at final concentration of 2 mM ammonium acetate, and 20 mM piperdine and imidazole.[3, 4 3, 15-20]

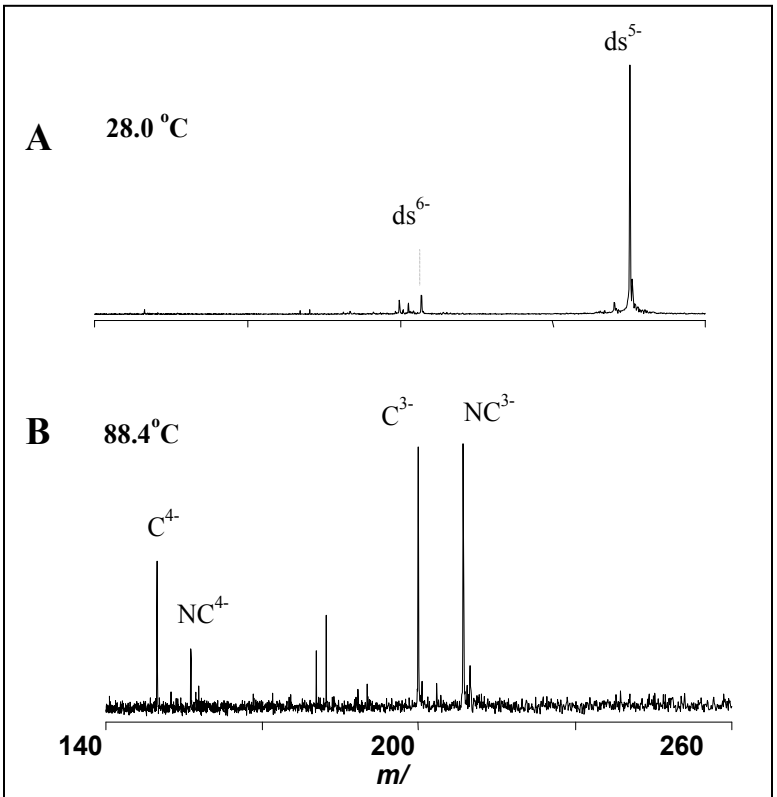

Figure 6.2: ESI-FTICR mass spectra of 20-mer oligonucleotides using original ESI solution consisting of 60% acetonirile, 20% isopropyl alcohol, 20% 10 mM ammonium acetate with final concentration of 20 mM Piperidine and Imidazole. A) dsDNA is observed at ambient temperature (28° C). B) Only ssDNA is observed when temperature of the heated metal transfer line is significantly above its T_m (88.4° C). All charge states and coding (C) and noncoding (NC) strands are labeled.

The spectrum in Figure 6.2b shows the result of using a resistively heated transfer line providing thermal denaturation of the 20-mer duplex as it was introduced into the entrance of the mass spectrometer. The elevated temperature that was required to destabilize the large number of hydrogen bonds between the nucleobases resulted in a highly unstable electrospray, which caused ion intensity issues and lack or reproducible results. In efforts to circumvent the instability and low signal to noise during the thermal denaturation, modifications to the electrospray solutions were examined and increases to the aqueous content were made. As the proportion of aqueous content of the electrospray solutions was increased the dsDNA became denatured and single stranded DNA ssDNA was detected. Figure 6.3 shows the ESI-FTICR mass spectra of the 20-mer dsDNA at ambient temperature with various aqueous content percentages as a plot of relative ion intensity of the single stranded species I_{ss}, divided by the total ion intensity, $I_{ss} + I_{ds}$, versus the percentage of aqueous content. The ESI solutions with 25% of aqueous content contained all duplex structure. As the percentage is increase to 40%, the spectra now contains the 20-mer DNA in both the duplex and single stranded forms. As the content surpassed 50-60%, only single stranded DNA remained in the spectra.

It should be noted that the signal to noise ratio shown in Figures 6.2b and 6.3 appears slightly compromised by the higher than normal aqueous content used in the solutions. This may be attributed to the following scenarios: (1) the total ion intensity is distributed among four species (C^{4-},NC^{4-},C^{3-}, and NC^{3-}) at the higher 55% aqueous content rather than just two species (ds^{6-}, and ds^{5-}) at the lower content, 25%; (2) increasing the aqueous content results in a higher surface tension of the dropets, yet the heated metal capillary was maintained at a constant temperature, so incomplete desolvation and lower ion

production may be related; (3) The FTICR signals scales linearly with charge, so for lower charge states (i.e. single strands) they induce less of an image current than the duplex species. Also of note, the average charge state for the duplex species increases with the increase in aqueous content, (Figure 6.3). This may be due to: (1) the higher aqueous content droplets accommodate a higher charge density, and therefore impart more charge onto the oligonucleotide structure, and (2) the apparent pH of the solution increases slightly with increasing the aqueous content. The increase in pH decreases the relative proportion of protonated piperdine which is known to reduce charge states when in the protonated form.[40]

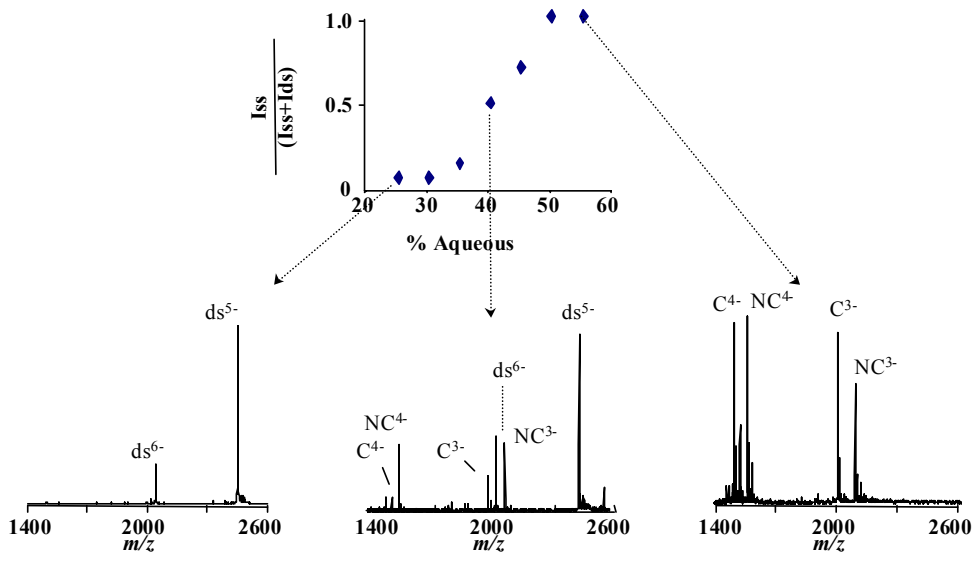

Figure 6.3 Dissociation plot of 20-mer duplex at varying aqueous content

The single stranded products in Figure 6.3 show no sign of backbone fragmentation and represent the individual intact single stranded species. This is consistent with the work by Gabelica et al. in which they used a higher proportion of aqueous content for the nozzle skimmer dissociation of the 16-mer duplexes.[26] The nozzle skimmer dissociations from this research was done using an ESI solution that was conducive for duplex stabilization (ie, 20% aqueous) and therefore the higher amounts of backbone fragmentation resulted.

Based on the positive results with the 20-mer model system, attention was directed to an 82-bp PCR amplicon that was electrosprayed from solutions with 50-70% aqueous content. The higher percentatages were chosen based on the higher number of hydrogen bond associated with the greater number or base pairs. The estimated T_m for the PCR amplicon was determined using the following equation[36]:

$$T_m = 81.5 + [16.6(\log[X^+])] + [0.41(\%GC)] - [500 / \#\text{ of base pairs}] \quad \text{(Eq.2)}$$

This equation is only valid for monovalent cation concentrations, represented by $[X^+]$, in the range of 0.01-0.4M and the DNA duplex of interests must contain a GC percentage between 30-75%.[36] The sodium concentration was assumed to be zero since all samples were thoroughly dialyzed to remove salt adduction. However, the solutions also contain ammonium ions and protonated piperidine. The T_m was calculated using protonated piperidine concentrations determined by α-values for a given pH. Figure 6.4a illustrates the ESI-FTICR mass spectrum of a stable DNA duplex at 50% aqueous ESI solution (pH

= 11.1; T_m = 58.5 °C). Figure 6.4b shows the same 82-bp PCR amplicon now at 60% aqueous content, which shows only a marginal amount of single stranded product(pH = 11.2; T_m = 57.6 °C). Figure 6.4c shows a completely denatured 82-bp PCR product at 70% aqueous phase(pH = 11.3; T_m = 56.9 °C). The increase in aqueous character of the solution increased the pH also, which decreased the amount of protonated piperidine and therefore decreased the ionic strength of the solution. However, the range of ionic strengths is very narrow, and the melting temperatures only changed by 1.6 °C which suggest that additional factors play a role in the DNA duplex stability such as the degree of hydration and the hydrogen bonding capability of neutral piperidine.

Experiments were then done to thermally control the state of the species (ssDNA or dsDNA) observed in the spectrum. A resistive heating of the transfer line was conducted using 60% aqueous solution (pH = 11.2; T_m = 57.6 °C) as it appears to be right on the threshold of dsDNA stability, shown in Figure 6.4b. The 82-bp PCR product in 60% aqueous solution with increasing capillary temperature is shown in Figure 6.5. This method of analysis allows for the simultaneous detection of both ssDNA and dsDNA in the same ESI experimental run. Figure 6.5 shows a plot of the relative ion intensity versus the temperature of the heated transfer line measured at the insulating jacket. At a temperature of 28 °C, the 82-bp product is detected as mainly dsDNA. As the temperature of the surrounding heating jacket is increased to 42 °C, the PCR product is observed as both dsDNA and ssDNA states. Increasing the temperature of the capillary to 53 °C, results in the production of predominantly ssDNA species. The observation of dsDNA destabilization at 53 °C is below our calculated T_m 57.6°C, which is consistent with the observations in Figures 6.3 and 6.4, that higher aqueous phase in the ESI

solution decreases T_m. It was found that an increase in aqueous content increases the apparent pH of each solution. This indicated that the pH of ESI solution might play a critical role in the DNA duplex stability. In the ESI solution is piperidine, a strong base (pKa = 11.1), which raises the pH of the solutions as well as reduces the alkali metal adduction[40] Based on aqueous phase α-plot for piperidine, at pH values below its pKa, piperidine is in its protonated form in the solution. At pH values above the pKa, piperidine resides primarily in a neutral state. In accord with the α-plot, $\alpha_0 = 0.61$ for the protonated form and $\alpha_1 = 0.39$ for the neutral piperidine in the 20 % aqueous solution, which has an apparent pH = 10.9. The corresponding values for the 55% aqueous solution with an apparent pH of 11.3, is $\alpha_0 = 0.43$ for the protonated form and $\alpha_1 = 0.57$. For the 20-mer oligonucleotide, these two aqueous percentages and their corresponding α-values illustrate that the percentage of protontated and neutral piperdine in solution seem to play a crucial role in the state of the DNA.

Figure 6.6 shows an ESI-FTICR mass spectra of the 20-mer oligonucleotide from solutions without imidazole. This was chosen to simplify the ESI mixtures. Figure 6.6a shows a mass spectrum of the 20-mer in 20% aqueous solution in which the dsDNA is observed as expected for this pH. Figure 6.6b shows the same 20-mer in 55% aqueous solution, which induces the production of ssDNA.

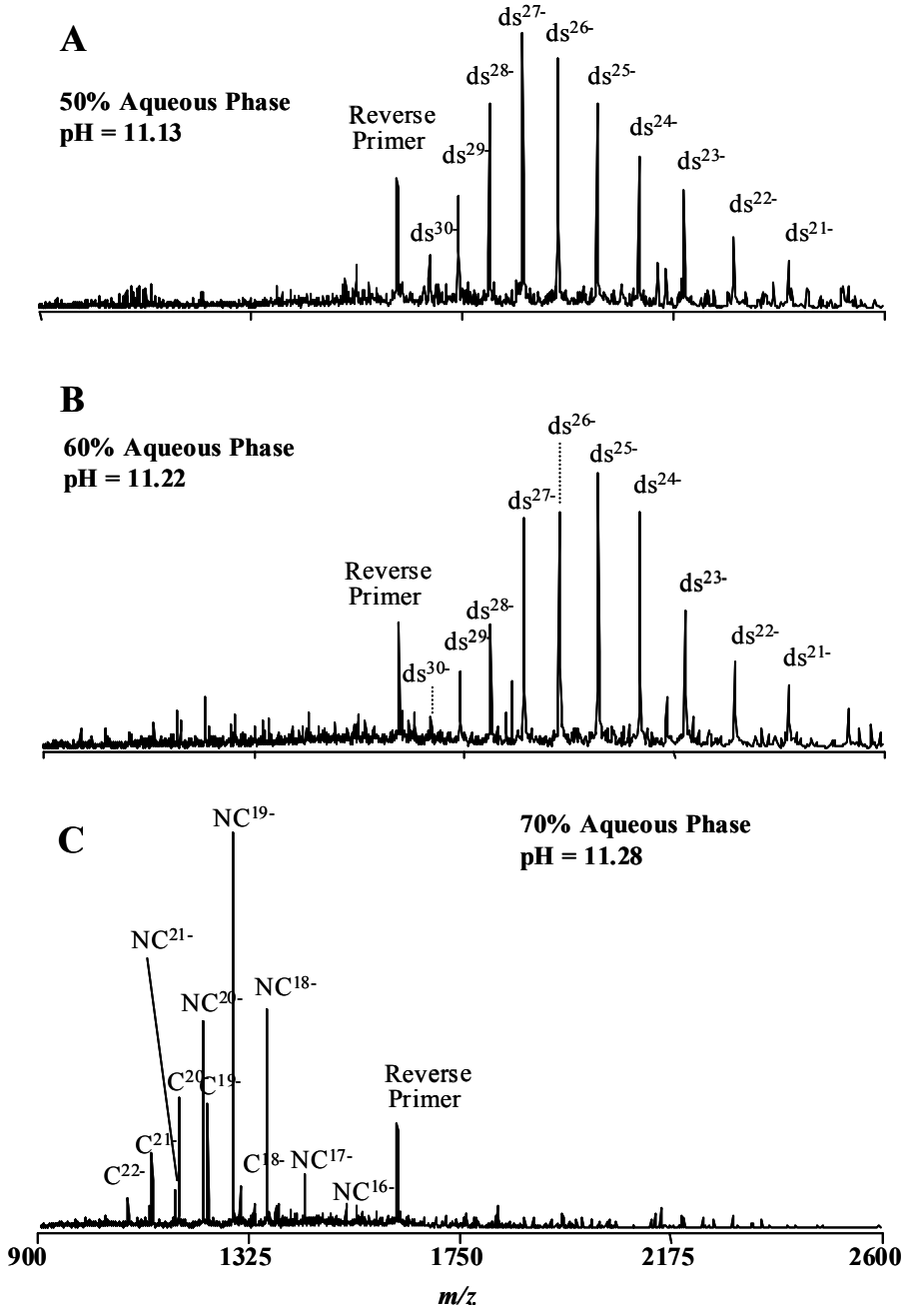

Figure 6.4: ESI solutions consisted of 20 mM piperidine, 20 mM imidazole, and 2 mM ammonium acetate with A) 50% aqueous (pH = 11.1), B) 60% aqueous (pH = 11.3), C) 70% aqueous (pH = 11.3).

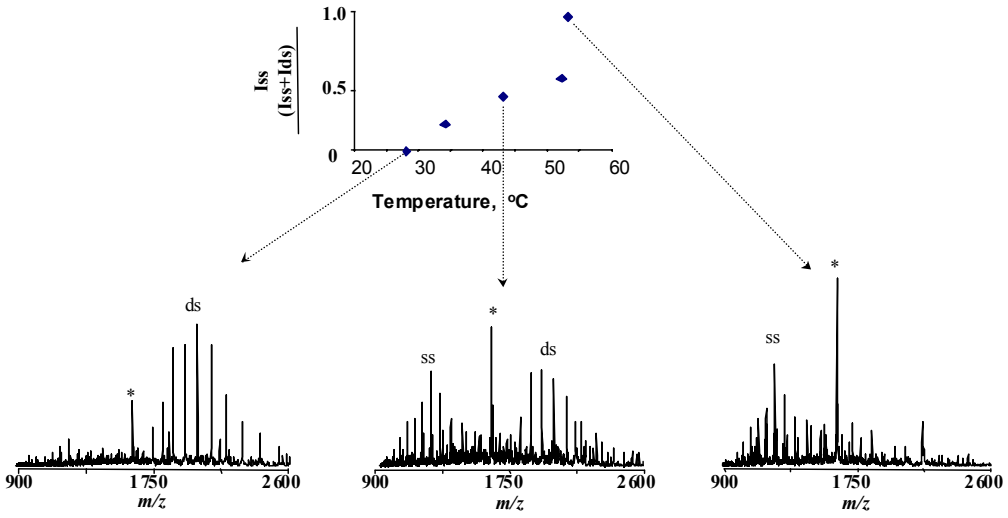

Figure 6.5: PCR product in 60% aqueous ESI solution using with resistively heated metal transfer line to induce the production of single-stranded species.

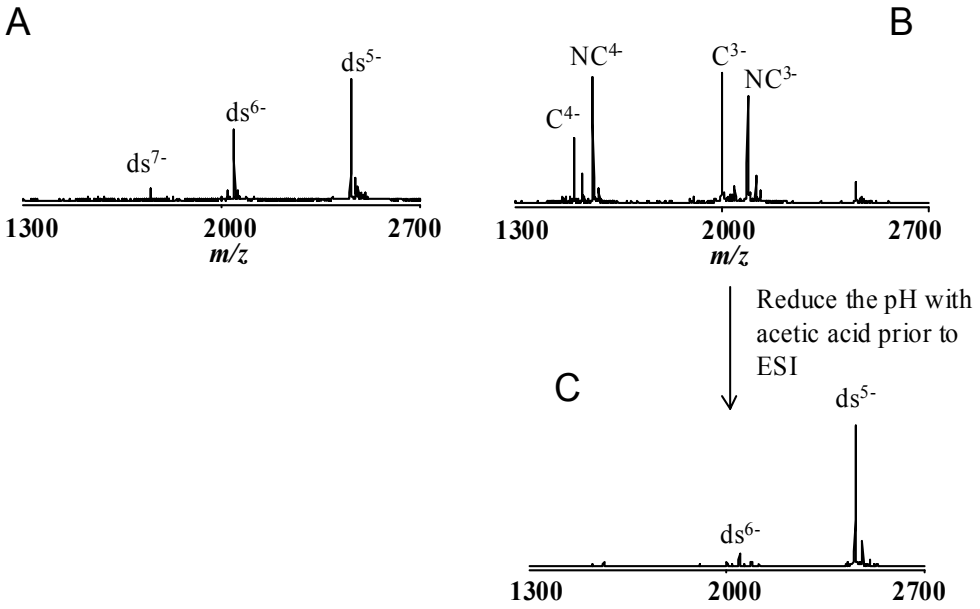

Figure 6.6: ESI-FTICR mass spectra of 20-mer oligonucleotide at A) 20% aqueous with an apparent pH of 10.9, B) 55% aqueous with an apparent pH of 11.3, C) 55% aqueous where the apparent pH has been adjusted to 11.0 with the addition of acetic acid.

Figure 6.6c shows that by lowering the pH of the 55% solution with acetic acid to less than 11.0 the ssDNA is resorts back to the dsDNA conformation. When the apparent pH is above the pKa of piperidine, the DNA is destabilized and produces single stranded products. As the apparent pH is reduced below the pKa of piperidine, the DNA in solution is of the duplex form. It should be noted that there is a small decrease in the average charge state of the duplexes shown in Figure 6.6a and 6.6c, to roughly 5.6 and 5.1, respectively. This decrease in average charge state is due to the approximately 6% increase in the protonated form of piperidine, which is known to reduce charge states.[40]

Scheme 1, illustrates the proposed mechanism for piperidine interaction based upon the experimental data and the α-plot values for piperidine. At pH values below the pKa, the excess of protonated piperidine acts like a cation and electrostatically binds to the phosphate backbone thus neutralizing the strand-strand repulsion of the negatively charged backbone. This creates a similar structure such as peptide nucleic acids (PNAs) where there is no negative-negative repulsions and increased duplex stability exists.[41] At pH values that are above the pKa of piperidine, the excess of neutral piperidine can hydrogen bond with the nucleabases of the double helix and thus act in an analogous fashion as the known denaturant formamide.[42]

To further investigate this possible mechanism, a study of melting temperature of the 20-mer duplex in two different ESI solutions with different pH values was undertaken. Figure 6.7 is a plot of the relative intensity of the ssDNA versus the temperature of the resistively heated transfer line at 30% aqueous solution. The pH values are 10.9 and 10.7 respectivley, adjusted with acetic acid. When the 10.9 solution is electrosprayed at room temperature (28 °C), the mass spectrum shows the dsDNA conformation.

Heating the transfer line to 58 °C, results in almost complete denaturation of the 20-mer. However, for the ESI solution with the lower pH value, 10.7, increased duplex stability is observed. Temperatures of over 100 °C were necessary to achieve dissociation of the dsDNA. Analogous to PNA-PNA duplex stability[43], the oligonucletide in the lower pH solution and thus more protonated piperdine, stabilizes the anionic phosphate backbone of the double helix. The result is an increase in the melting temperature that is roughly twice the value of the higher pH solution 20-mer. The decrease in pH from 10.9 to 10.7 is reflected in the charge-states observed for the dsDNA at ambient temperatures. When the concentration of protonated piperidine increase by 9%, the average charge state of the dsDNA decreases.

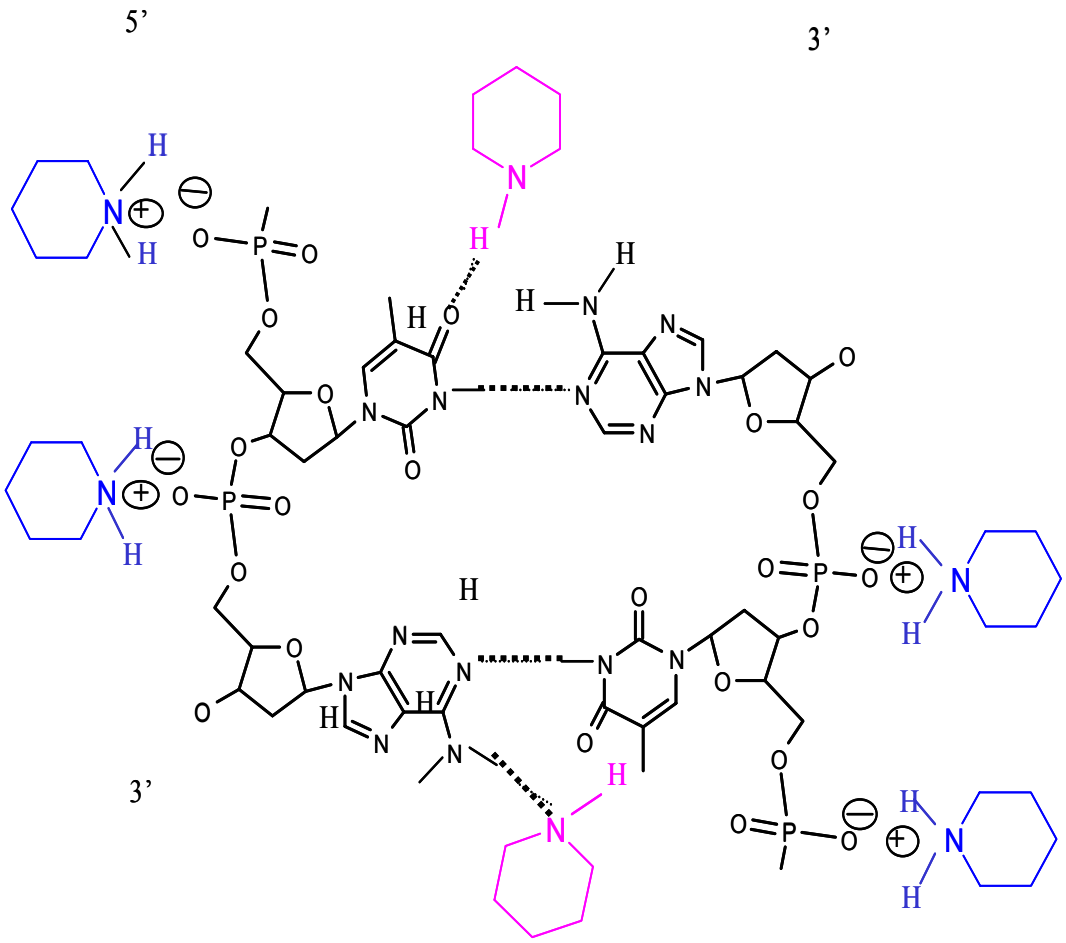

Scheme 1: Piperidine interaction with DNA double helix. Protonated piperidine acts as a counter-cation for the anionic phosphate backbone stabilizing the double helix. Neutral piperidine can hydrogen bond with the nucleobases destabilizing the double helix analogous to the denaturant formamide.

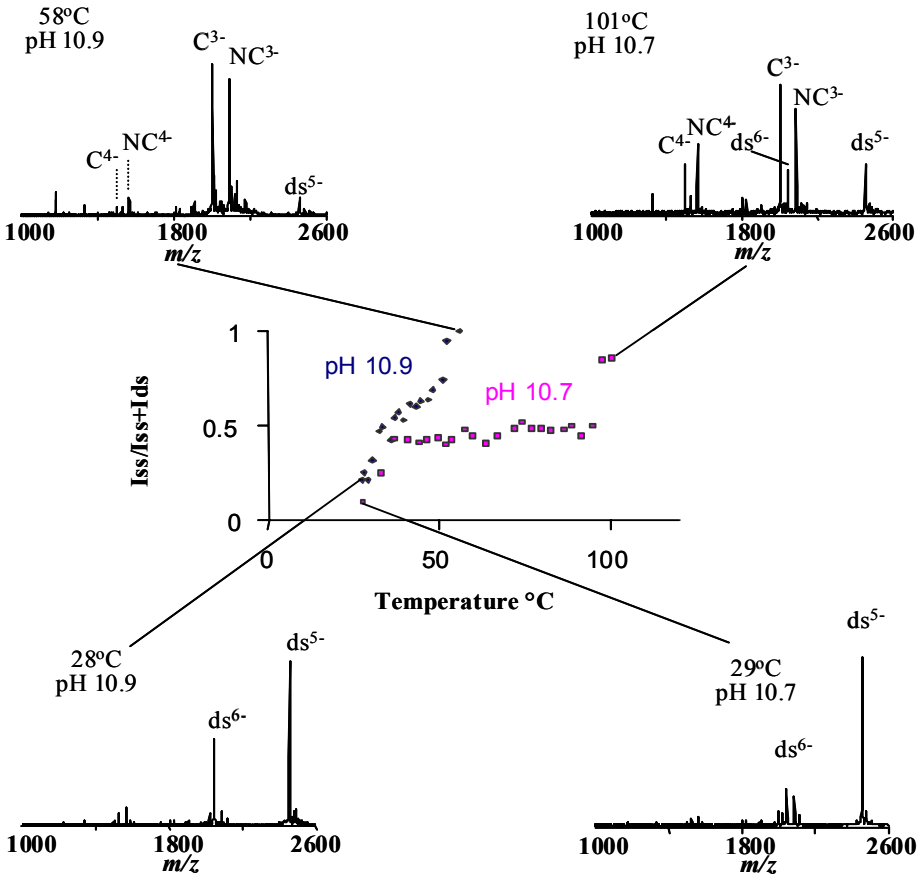

Figure 6.7: Relative ion intensity of single-stranded 20-mer versus heated electrospray transfer line temperature at 30% aqueous ESI solution with apparent pH of 10.9 and 10.7.

6.4 Conclusions

The ESI solutions are relatively complex and numerous factors play a role in the DNA stability(e.g., ionic strength which is pH dependent, aqueous content, and temperature). A higher detailed study of these factors is warranted to fully understand the role in the processes observed. Conductivity measurements were done, but results were inconclusive and also warrant further investigations. Never the less, single stranded moieties can be routinely generated from double stranded PCR products using a combination of aqueous solution modifications and restively heated electrospray sources.

6.5 References

1. Fenn, J. B.; Mann, M.; Meng, C. K.; Wong, S. F.; Whitehouse, C. M., Electrospray ionization for mass spectrometry of large biomolecules. *Science* **1989,** 246, (4926), 64-71.

2. Comisarow, M. B.; Marshall, A. G., Fourier transform ion cyclotron resonance spectroscopy. *Chemical Physics Letters* **1974,** 25, (2), 282-283.

3. Null, A. P.; Hannis, J. C.; Muddiman, D. C., Genotyping of simple and compound short tandem repeat loci using electrospray ionization Fourier transform ion cyclotron resonance mass spectrometry. *Anal Chem* **2001,** 73, (18), 4514-21.

4. Null, A. P.; Muddiman, D. C., Perspectives on the use of electrospray ionization Fourier transform ion cyclotron resonance mass spectrometry for short tandem repeat genotyping in the post-genome era. *J Mass Spectrom* **2001,** 36, (6), 589-606.

5. Weber, J. L., Human DNA polymorphisms and methods of analysis. *Curr Opin Biotechnol* **1990,** 1, (2), 166-71.

6. Weber, J. L.; Wong, C., Mutation of human short tandem repeats. *Hum Mol Genet* **1993,** 2, (8), 1123-8.

7. Weber, J. L.; May, P. E., Abundant class of human DNA polymorphisms which can be typed using the polymerase chain reaction. *Am J Hum Genet* **1989,** 44, (3), 388-96.

8. Litt, M.; Luty, J. A., A hypervariable microsatellite revealed by in vitro amplification of a dinucleotide repeat within the cardiac muscle actin gene. *Am J Hum Genet* **1989,** 44, (3), 397-401.

9. Edwards, A.; Civitello, A.; Hammond, H. A.; Caskey, C. T., DNA typing and genetic mapping with trimeric and tetrameric tandem repeats. *Am J Hum Genet* **1991,** 49, (4), 746-56.

10. Mullis, K. B.; Faloona, F. A., Specific synthesis of DNA in vitro via a polymerase-catalyzed chain reaction. *Methods Enzymol* **1987,** 155, 335-50.

11. Bayer, E.; Bauer, T.; Schmeer, K.; Bleicher, K.; Maier, M.; Gaus, H. J., Analysis of double-stranded oligonucleotides by electrospray mass spectrometry. *Anal Chem* **1994,** 66, (22), 3858-63.

12. Doktycz, M. J.; Habibi-Goudarzi, S.; McLuckey, S. A., Accumulation and storage of ionized duplex DNA molecules in a quadrupole ion trap. *Anal Chem* **1994,** 66, (20), 3416-22.

13. Aaserud, D. J. K., N.L.; Little, D.P.; McLafferty, F.W., Accurate Base Composition of Double-Strand DNA by Mass Spectrometry. *J. Am. Soc. Mass. Spectrom* **1996,** 7, 1266-1269.

14. Greig, M. J.; Gaus, H. J.; Griffey, R. H., Negative ionization micro electrospray mass spectrometry of oligonucleotides and their complexes. *Rapid Commun Mass Spectrom* **1996,** 10, (1), 47-50.

15. Null, A. P.; Hannis, J. C.; Muddiman, D. C., Preparation of single-stranded PCR products for electrospray ionization mass spectrometry using the DNA repair enzyme lambda exonuclease. *Analyst* **2000,** 125, (4), 619-26.

16. Muddiman, D. C.; Null, A. P.; Hannis, J. C., Precise mass measurement of a double-stranded 500 base-pair (309 kDa) polymerase chain reaction product by negative

ion electrospray ionization Fourier transform ion cyclotron resonance mass spectrometry. *Rapid Commun Mass Spectrom* **1999,** 13, (12), 1201-1204.

17. Hannis, J. C.; Muddiman, D. C., Characterization of a microdialysis approach to prepare polymerase chain reaction products for electrospray ionization mass spectrometry using on-line ultraviolet absorbance measurements and inductively coupled plasma-atomic emission spectroscopy. *Rapid Communications in Mass Spectrometry* **1999,** 13, (5), 323-330.

18. Hannis, J. C.; Muddiman, D. C., Accurate characterization of the tyrosine hydroxylase forensic allele 9.3 through development of electrospray ionization Fourier transform ion cyclotron resonance mass spectrometry. *Rapid Commun Mass Spectrom* **1999,** 13, (10), 954-62.

19. Hannis, J. C.; Muddiman, D. C., A dual electrospray ionization source combined with hexapole accumulation to achieve high mass accuracy of biopolymers in Fourier transform ion cyclotron resonance mass spectrometry. *J Am Soc Mass Spectrom* **2000,** 11, (10), 876-83.

20. Hannis, J. C.; Muddiman, D. C., Detection of double-stranded PCR amplicons at the attomole level electrosprayed from low nanomolar solutions using FT-ICR mass spectrometry. *Fresenius J Anal Chem* **2001,** 369, (3-4), 246-51.

21. Watson, J. D.; Crick, F. H., Molecular structure of nucleic acids; a structure for deoxyribose nucleic acid. *Nature* **1953,** 171, (4356), 737-8.

22. Henry, K. D.; Williams, E. R.; Wang, B. H.; McLafferty, F. W.; Shabanowitz, J.; Hunt, D. F., Fourier-transform mass spectrometry of large molecules by electrospray ionization. *Proc Natl Acad Sci U S A* **1989,** 86, (23), 9075-8.

23. Flora, J. W.; Hannis, J. C.; Muddiman, D. C., High-mass accuracy of product ions produced by SORI-CID using a dual electrospray ionization source coupled with FTICR mass spectrometry. *Anal Chem* **2001,** 73, (6), 1247-51.

24. Beavis, R. C., Chemical mass of carbon in proteins. *Analytical Chemistry* **1993,** 65, (4), 496-497.

25. Urquhart, A.; Kimpton, C. P.; Downes, T. J.; Gill, P., Variation in short tandem repeat sequences--a survey of twelve microsatellite loci for use as forensic identification markers. *Int J Legal Med* **1994,** 107, (1), 13-20.

26. Valorie, G.; Edwin De, P., Comparison between solution-phase stability and gas-phase kinetic stability of oligodeoxynucleotide duplexes. *Journal of Mass Spectrometry* **2001,** 36, (4), 397-402.

27. Ross, P. L.; Lee, K.; Belgrader, P., Discrimination of single-nucleotide polymorphisms in human DNA using peptide nucleic acid probes detected by MALDI-TOF mass spectrometry. *Anal Chem* **1997,** 69, (20), 4197-202.

28. Uhlen, M., Magnetic separation of DNA. *Nature* **1989,** 340, (6236), 733-4.

29. Tang, K.; Fu, D.; Kotter, S.; Cotter, R. J.; Cantor, C. R.; Koster, H., Matrix-assisted laser desorption/ionization mass spectrometry of immobilized duplex DNA probes. *Nucleic Acids Res* **1995,** 23, (16), 3126-31.

30. Chou, C. W.; Bingham, S. E.; Williams, P., Affinity methods for purification of DNA sequencing reaction products for mass spectrometric analysis. *Rapid Commun Mass Spectrom* **1996,** 10, (11), 1410-4.

31. Koster, H.; Tang, K.; Fu, D. J.; Braun, A.; van den Boom, D.; Smith, C. L.; Cotter, R. J.; Cantor, C. R., A strategy for rapid and efficient DNA sequencing by mass spectrometry. *Nat Biotechnol* **1996,** 14, (9), 1123-8.

32. Jurinke, C.; van den Boom, D.; Jacob, A.; Tang, K.; Worl, R.; Koster, H., Analysis of ligase chain reaction products via matrix-assisted laser desorption/ionization time-of-flight-mass spectrometry. *Anal Biochem* **1996,** 237, (2), 174-81.

33. Jurinke, C.; van den Boom, D.; Collazo, V.; Luchow, A.; Jacob, A.; Koster, H., Recovery of nucleic acids from immobilized biotin-streptavidin complexes using ammonium hydroxide and applications in MALDI-TOF mass spectrometry. *Anal Chem* **1997,** 69, (5), 904-10.

34. Jurchen, J. C. R.-C., S.E.; Williams, E.R.; In *A Comparison of the Thermal Stability of High Order DNA Structures in Solution and in the Gas-Phase*, Proceedings of the 47th Annual ASMS Conference on Mass Spectrometry and Allied Topics, Dallas, TX 1999; Dallas, TX 1999; pp 2599-2600.

35. Liu, C.; Wu, Q.; Harms, A. C.; Smith, R. D., On-line microdialysis sample cleanup for electrospray ionization mass spectrometry of nucleic acid samples. *Anal Chem* **1996,** 68, (18), 3295-9.

36. Strachan, T. R., A.P., *Human Molecular Genetics 2*. John Wiley & Sons, Inc.: New York, 1999.

37. Chowdhury, S. K.; Katta, V.; Chait, B. T., An electrospray-ionization mass spectrometer with new features. *Rapid Commun Mass Spectrom* **1990,** 4, (3), 81-7.

38. James, C. H.; David, C. M., Nanoelectrospray mass spectrometry using non-metalized, tapered (50 rarr 10á&mgr;m) fused-silica capillaries. *Rapid Communications in Mass Spectrometry* **1998,** 12, (8), 443-448.

39. Senko, M. W.; Hendrickson, C. L.; Emmett, M. R.; Shi, S. D. H.; Marshall, A. G., External Accumulation of Ions for Enhanced Electrospray Ionization Fourier Transform Ion Cyclotron Resonance Mass Spectrometry. *Journal of the American Society for Mass Spectrometry* **1997,** 8, (9), 970-976.

40. Muddiman, D. C.; Cheng, X.; Udseth, H. R.; Smith, R. D., Charge-state reduction with improved signal intensity of oligonucleotides in electrospray ionization mass spectrometry. *Journal of the American Society for Mass Spectrometry* **1996,** 7, (8), 697-706.

41. Hillen, W.; Goodman, T. C.; Wells, R. D., Salt dependence and thermodynamic interpretation of the thermal denaturation of small DNA restriction fragments. *Nucleic Acids Res* **1981,** 9, (2), 415-36.

42. Blake, R. D.; Delcourt, S. G., Thermodynamic effects of formamide on DNA stability. *Nucleic Acids Res* **1996,** 24, (11), 2095-103.

43. Eugen, U.; Anusch, P.; Gerhard, B.; David, W. W., PNA: Synthetic Polyamide Nucleic Acids with Unusual Binding Properties. *Angewandte Chemie International Edition* **1998,** 37, (20), 2796-2823.

Appendix A

Investigation into Mulinuclear Ruthenium Compund Binding with DNA

Work used in the publication of:
Mendoza-Ferri, M. G.; Hartinger, C. G.; Mendoza, M. A.; Groessl, M.; Egger, A. E.; Eichinger, R. E.; **Mangrum, J. B.**; Farrell, N. P.; Maruszak, M.; Bednarski, P. J.; Klein, F.; Jakupec, M. A.; Nazarov, A. A.; Severin, K.; Keppler, B. K., Transferring the Concept of Multinuclearity to Ruthenium Complexes for Improvement of Anticancer Activity.
Journal of Medicinal Chemistry 2009, 52, (4), 916-925.

A.1 Introduction

Ruthenium(II) arene complexes represent a new class of anticancer compounds that have shown cytotoxicity in cells displaying cisplatin-resistance.[1-3] In fact, two Ru(III) compounds have made it into clinical evaluations.[4-6] Ruthenium compounds have attracted considerable attention due to the fact their tumor-inhibiting effects are different from platinum compounds.[7, 8] However, similar to cisplatin anticancer complexes, Ru(II) complexes show a preferred binding target at the guanine N7 site of DNA.[1, 9, 10] As mentioned in Chapter 1, the toxicity, side effects, and developed resistance has led to the development of platinum compounds with multiple metal centers, such as the polynuclear platinum compounds described therein. Polynuclear Ru compounds are relatively new and therefore have rarely been studied for their anticancer properties.[6, 11, 12] The few studies performed on their anticancer activity showed a level of cyctoxicity lower than that of a mononuclear ruthenium compound. [6, 11, 12] This is remarkably different in the case of platinum compounds, where the introduction of polynuclear platinum centers actually increases the cytoxicity and leads to overcoming cisplatin resistance.[13]

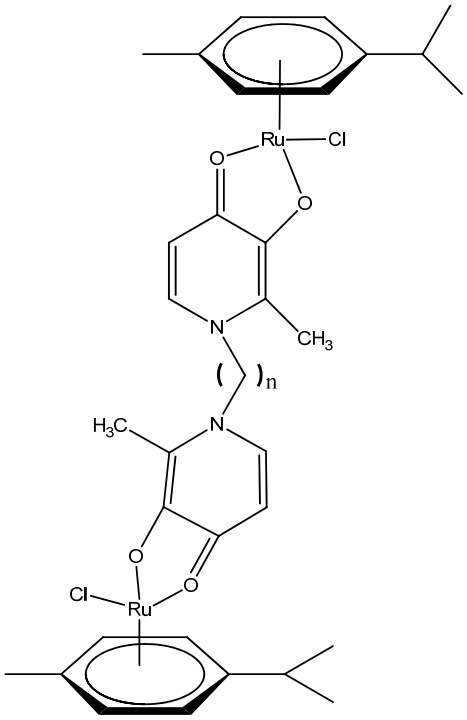

Figure A.1 Structure of Dinuclear Ru(II)-arene complex with (n) = alkyl chain length

Expanding on the recent success of multinuclear platinum complexes, like the clinically relevant BBR 3464, a multicentered Ru(II) compound was synthesized by our collaborators see Figure A.1.[6, 14] The concept behind these compounds was to have alkyl chains of varying lengths. The most potent of these compounds in A2780 cell lines was when the alkyl spacer was n=6.[7] As such, the n=6 alkyl chain spaced compound was chosen to study its binding to DNA.

A.2 Experimental

For the MS studies, the non-self complementary DNA 13-mer 5'-ATC TGT TTG TCT T-3' (3921 Da; Midland Certified Reagents, Midland TX) was incubated with **Ru(II)** in

H_2O at DNA : complex ratios ranging from 5 : 1 (r_B 0.015) to 1 : 5 (r_B 1.5). Before use, the purified 13-mer was further desalted using a custom built dialysis chamber equipped with a hollow micro dialysis fiber with a 13 000 molecular weight cut off (MWCO) from Spectrum Laboratories (Rancho Dominguez, CA) in 25 mM ammonium acetate solution. The desalted oligonucleotide was lyophilized to dryness and reconstituted in 18 MΩ water.

The sample mixtures were analyzed immediately after mixing and after 30 min and 24 h of incubation on a Waters/Micromass Qtof-2 (Manchester, UK) instrument equipped with a custom built micro-spray source operated in negative ion mode over a mass range of 500–2000 *m/z*. Samples were introduced into the inlet at 1.0 μL/min with a capillary voltage of –1.9 kV and a cone voltage of 36 V. The source temperature was maintained constant at 110 ºC throughout the experiments. A 1: 1 mixture of methanol : water (with 25 mM ammonium acetate) was used as the spray solvent. Data were collected and processed using the Mass Lynx 4.0 software and the deconvolution to molecular mass scale was performed using the maximum entropy (Max Ent) software supplied with the instrument.

A.3 Results and Discussion

In efforts to determine the affinity of the dinuclear Ru(II) compound in Figure A1., the binding with a 13-mer single stranded oligonucleotide was undertaken. Different DNA : complex ratios were prepared and the amount of bound ruthenium increased with the r_B. For example, at $r_B = 0.15$ the 13-mer and an adduct assignable to 13-mer + [**Ru(II)** – 2Cl] (4721 Da) were observed at a relative intensity of ca. 1:1.When increasing

the r_B = 0.46, there is a significant decrease in the free oligonucletide resulting in approximately 40% free oligonucleotide. Incubation of the complexes at an r_B = 1.0, results in the formation of a bisadduct, attained (13-mer + [2 **Ru(II)** – 4 Cl], 5521 Da), and at r_B = 1.5 the ratio between these two adducts was found to be 1 : 1 with no unruthenated 13-mer being detectable. The reactivity of Ru(II) for the available binding sits of nucleobases follows the order: G(N7) > T(N3) > C(N3) > A(N7), A(N1).[15] Given the number of thymine nucleobases present in the sequence, it is plausible for the single strand to contain multiple covalently bonded Ru(II) compounds. It is not possible to further increase the concentration of **Ru(II)** since this induces the precipitation of the 13-mer. Furthermore, precipitation was observed in all samples with r_B > 1 and when incubating the mixtures for 24 hr. It should be noted that free 13-mer ion intensity was much lower at the higher r_B values and in overnight incubations. The covalent binding under these conditions is extremely rapid and no significant changes were scene at incubation times of longer than 1hr. Given the presence of two available guanines in the 13-mer sequence, it was also considered that the dinuclear complex could cross-link two 13-mer single strands: however, such species were not observed in the mass spectra but their presence cannot be excluded from the precipitate found after longer incubation times and higher r_B values. The complexation of Ru(II) dinuclear complexes with single stranded DNA displayed rapid covalent binding event with no detectable aquo species present.

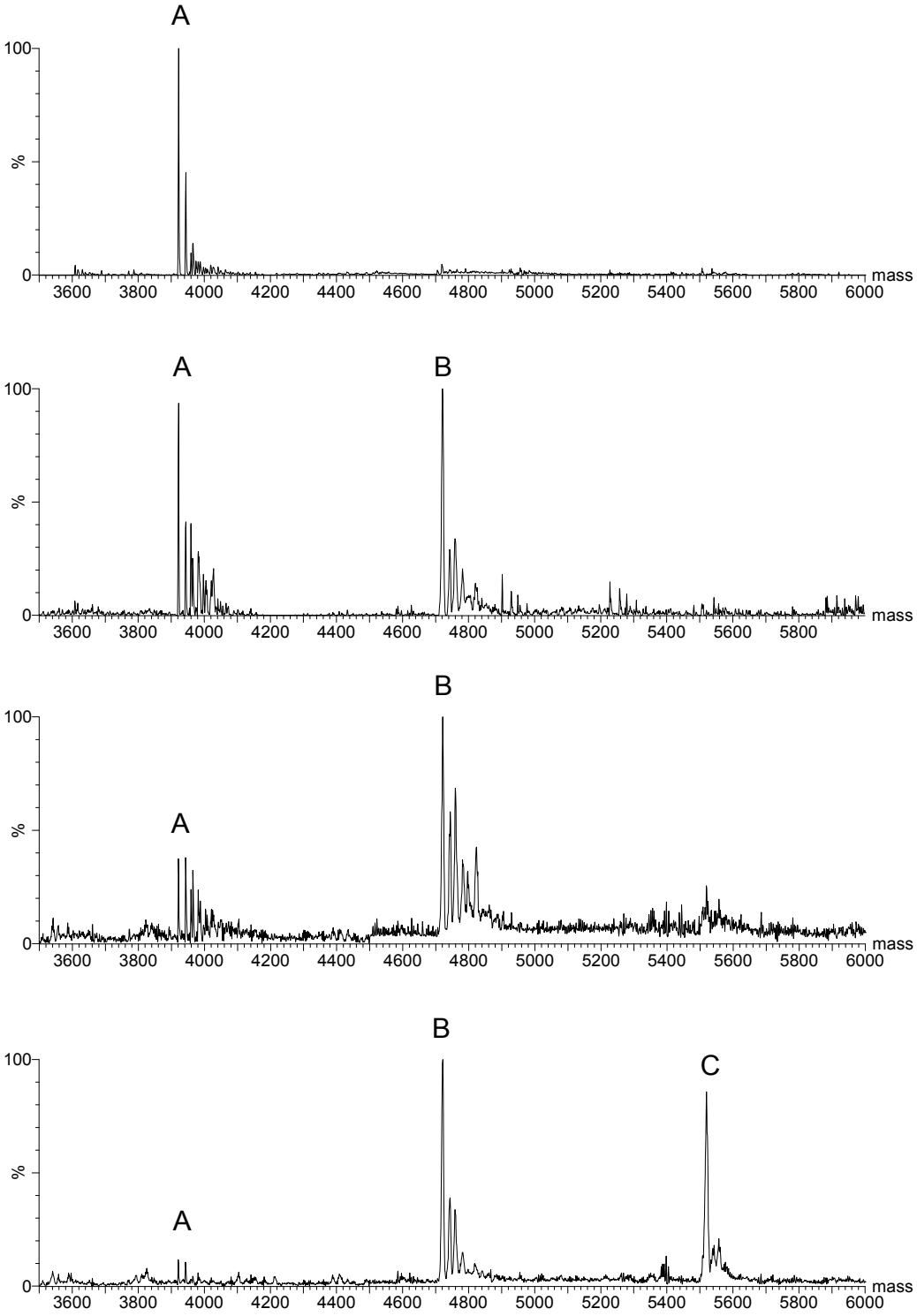

Figure A.2. Deconvoluted ESI-MS of 13-mer single strand DNA with Ru(II) compound at varying r_B values. (1) free 13-mer, (2) 1:1 mixture, $r_B = 0.15$ (3) 1:3 mixture, $r_B = 0.46$ (4) 1:7 mixture, $r_B = 1.07$ (**A**) free 13-mer, (**B**) 1:1 Ru:Oligo, (**C**)2:1 Ru:Oligo

A.4 Conclusions

The influence of coupling two Ru(II) moieties together via an alkyl chain was investigated with regard to binding ratios on a single stranded 13-mer oligonucleotide sequence. As DNA is the ultimate target for platinum anticancer agents, the results described show that dinucler Ru(II) complexes also exhibit a strong interaction with nucleotides. Rapid and favorable complexation between the Ru(II) compound and oligonucleotide was identified. The amount of "ruthenation" increased with the r_B values. While higher r_B values could have been investigated, the level of precipitation in the solution led to inconclusive results when electrosprayed. A more detailed examination of the binding mechanism is needed and expansion into duplex oligonucletides is also warranted.

A.5 References

1. Wang, F.; Bella, J.; Parkinson, J. A.; Sadler, P. J., Competitive reactions of a ruthenium arene anticancer complex with histidine, cytochrome c and an oligonucleotide. *J Biol Inorg Chem* 2005, 10, (2), 147-55.

2. Aird, R. E.; Cummings, J.; Ritchie, A. A.; Muir, M.; Morris, R. E.; Chen, H.; Sadler, P. J.; Jodrell, D. I., In vitro and in vivo activity and cross resistance profiles of novel ruthenium (II) organometallic arene complexes in human ovarian cancer. *Br J Cancer* 2002, 86, (10), 1652-7.

3. Morris, R. E.; Aird, R. E.; Murdoch Pdel, S.; Chen, H.; Cummings, J.; Hughes, N. D.; Parsons, S.; Parkin, A.; Boyd, G.; Jodrell, D. I.; Sadler, P. J., Inhibition of cancer cell growth by ruthenium(II) arene complexes. *J Med Chem* 2001, 44, (22), 3616-21.

4. Rademaker-Lakhai, J. M.; van den Bongard, D.; Pluim, D.; Beijnen, J. H.; Schellens, J. H., A Phase I and pharmacological study with imidazolium-trans-DMSO-imidazole-tetrachlororuthenate, a novel ruthenium anticancer agent. *Clin Cancer Res* 2004, 10, (11), 3717-27.

5. Hartinger, C. G.; Zorbas-Seifried, S.; Jakupec, M. A.; Kynast, B.; Zorbas, H.; Keppler, B. K., From bench to bedside--preclinical and early clinical development of the anticancer agent indazolium trans-[tetrachlorobis(1H-indazole)ruthenate(III)] (KP1019 or FFC14A). *J Inorg Biochem* 2006, 100, (5-6), 891-904.

6. Mendoza-Ferri, M. G.; Hartinger, C. G.; Nazarov, A. A.; Eichinger, R. E.; Jakupec, M. A.; Severin, K.; Keppler, B. K., Influence of the Arene Ligand, the Number

and Type of Metal Centers, and the Leaving Group on the in Vitro Antitumor Activity of Polynuclear Organometallic Compounds. *Organometallics* 2009, 28, (21), 6260-6265.

7. Mendoza-Ferri, M. G.; Hartinger, C. G.; Eichinger, R. E.; Stolyarova, N.; Severin, K.; Jakupec, M. A.; Nazarov, A. A.; Keppler, B. K., Influence of the spacer length on the in vitro anticancer activity of dinuclear ruthenium-arene compounds. *Organometallics* 2008, 27, (11), 2405-2407.

8. Clarke, M. J.; Zhu, F.; Frasca, D. R., Non-platinum chemotherapeutic metallopharmaceuticals. *Chem Rev* 1999, 99, (9), 2511-34.

9. Chen, H.; Parkinson, J. A.; Parsons, S.; Coxall, R. A.; Gould, R. O.; Sadler, P. J., Organometallic ruthenium(II) diamine anticancer complexes: arene-nucleobase stacking and stereospecific hydrogen-bonding in guanine adducts. *J Am Chem Soc* 2002, 124, (12), 3064-82.

10. Chen, H.; Parkinson, J. A.; Morris, R. E.; Sadler, P. J., Highly selective binding of organometallic ruthenium ethylenediamine complexes to nucleic acids: novel recognition mechanisms. *J Am Chem Soc* 2003, 125, (1), 173-86.

11. Chen, H.; Parkinson, J. A.; Novakova, O.; Bella, J.; Wang, F.; Dawson, A.; Gould, R.; Parsons, S.; Brabec, V.; Sadler, P. J., Induced-fit recognition of DNA by organometallic complexes with dynamic stereogenic centers. *Proc Natl Acad Sci U S A* 2003, 100, (25), 14623-8.

12. Huxham, L. A.; Cheu, E. L. S.; Patrick, B. O.; James, B. R., The synthesis, structural characterization, and in vitro anti-cancer activity of chloro(p-cymene) complexes of ruthenium(II) containing a disulfoxide ligand. *Inorganica Chimica Acta* 2003, 352, 238-246.

13. Farrell, N., *Met Ions Biol Syst* 2004, 42, 251-296.

14. Mendoza-Ferri, M. G.; Hartinger, C. G.; Mendoza, M. A.; Groessl, M.; Egger, A. E.; Eichinger, R. E.; Mangrum, J. B.; Farrell, N. P.; Maruszak, M.; Bednarski, P. J.; Klein, F.; Jakupec, M. A.; Nazarov, A. A.; Severin, K.; Keppler, B. K., Transferring the Concept of Multinuclearity to Ruthenium Complexes for Improvement of Anticancer Activity. *Journal of Medicinal Chemistry* 2009, 52, (4), 916-925.

15. Pizarro, A. M.; Sadler, P. J., Unusual DNA binding modes for metal anticancer complexes. *Biochimie* 2009, 91, (10), 1198-211.

Appendix B.

Interaction of Covalent Polynuclear Compounds with a Zinc Finger Model

B.1. Introduction

The nucleocapsid NCp7 protein represents a very attractive target for antiviral drug compounds.[1] Nucleocapsid proteins characteristically contain a conserved region of CCHC sequence, Cys-X_2-Cys- X_4-His- Cys (X= variable sequence).[2, 3] The NCp7 nucleocapsid protein for human immunodeficiency virus type 1 (HIV-1) has two highly conserved zinc finger domains necessary for successful viral replication,[3-5] NCp7 have a high affinity for single stranded nucleic acids [3, 6, 7], has been shown to act as a chaperone nucleic acid folding/unfolding events and are generally involved in numerous events in the viral replication.[8]

Efforts to disrupt the function of the NCp7 proteins have involved covalent modification of the protein through the use of strong electrophiles that modify the zinc binding site.[9] The end result of this modification is the cleavage of the Zn-S bond and eventual zinc ion release resulting in inactivity via the loss of the important tertiary structure.[3] Our group has successfully modified zinc finger models with mononuclear platinum compounds (trans-$[PtCl(9\text{-}EtGH)(py)_2]^{2+}$), resulting in covalent modification, zinc ejection, and changes in protein conformation.[3, 10]

B.2. Experimental

Dinuclear platinum compounds were synthesized in house as previously described.[11, 12] The peptide (KGCWKCGKQEHQMKDCTER) was purchased from GeneScript and used as purified. To prepare the zinc finger, the previously described protocol was followed.[10] Briefly, zinc acetate and the peptide were dissolved in an ~ 1.2:1.0 equimolar ratio in water with the final pH adjusted to 7.0 using ammonium hydroxide. The zinc finger peptide was incubated

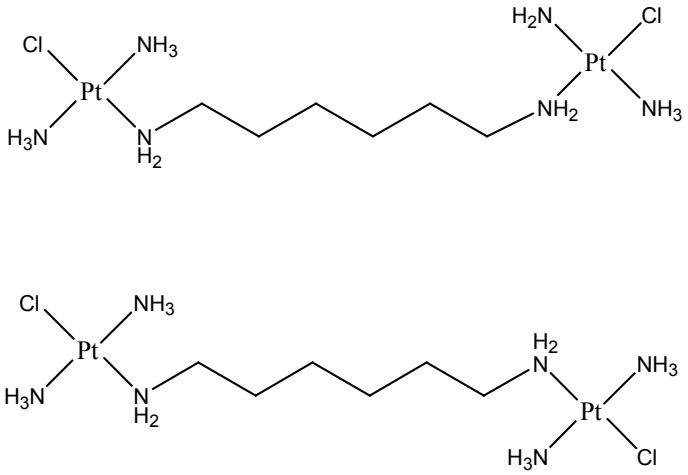

Figure B.1 Structures of the dinuclear platinum compounds 1,1/cc (upper) and 1,1/tt (lower)

for 2 hrs at 37 °C. Formation of the zinc finger peptide was confirmed with ESI-MS and circular dichroism. The sample mixtures were analyzed on a Waters/Micromass Qtof-2 (Manchester, UK) instrument equipped with a custom built micro-spray source operated in positive ion mode over a mass range of 200–2000 *m/z*. Samples were introduced into the inlet at 1.0 μL/min with a capillary voltage of 1.8 kV and a cone voltage of 30 V. The source temperature was maintained constant at 120 ºC throughout the experiments. Collision gas was introduced into the hexapole to aid in ion cooling. Data were collected and processed using the Mass Lynx 4.0 software.

B.3. Results and Discussion

The reaction of dinuclear platinum compounds can be monitored by ESI-MS to give an approximate identification of the species formed over time. Figure B.2. shows the ESI-MS spectra of the reaction between 1,1/cc and ZF at a 1:1 ratio at T= 0 and T= 4hrs. Figure B.2.A corresponds to the 2+ free zinc finger at 1144 m/z and B.2.B represents the 3+ zinc finger-Pt complex (922 m/z) in which the 1,1/cc is bound covalently with a bidentate coordination on both platinum centers. Additionally, this type of binding structure results in the loss of the essential zinc ion. Incubation of the solution at longer time periods reveals an increase in the 922 m/z ion. Under these reaction conditions, there does not appear to be any appreciable monodentate binding of the platinum centers as would be expected.

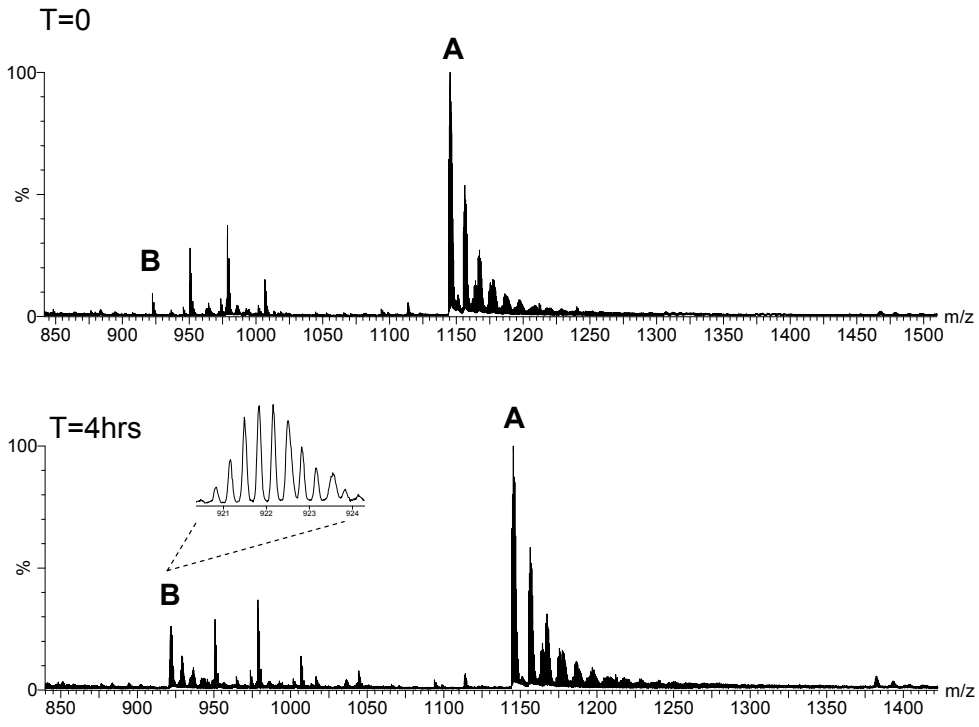

Figure B.2. ESI-MS of 1,1/cc with intact zinc finger at t = 0 and t = 4hrs. (A) in both plots is free intact zinc finger and (B) is a bidentate coordination of 1,1/cc with subsequent zinc ejection

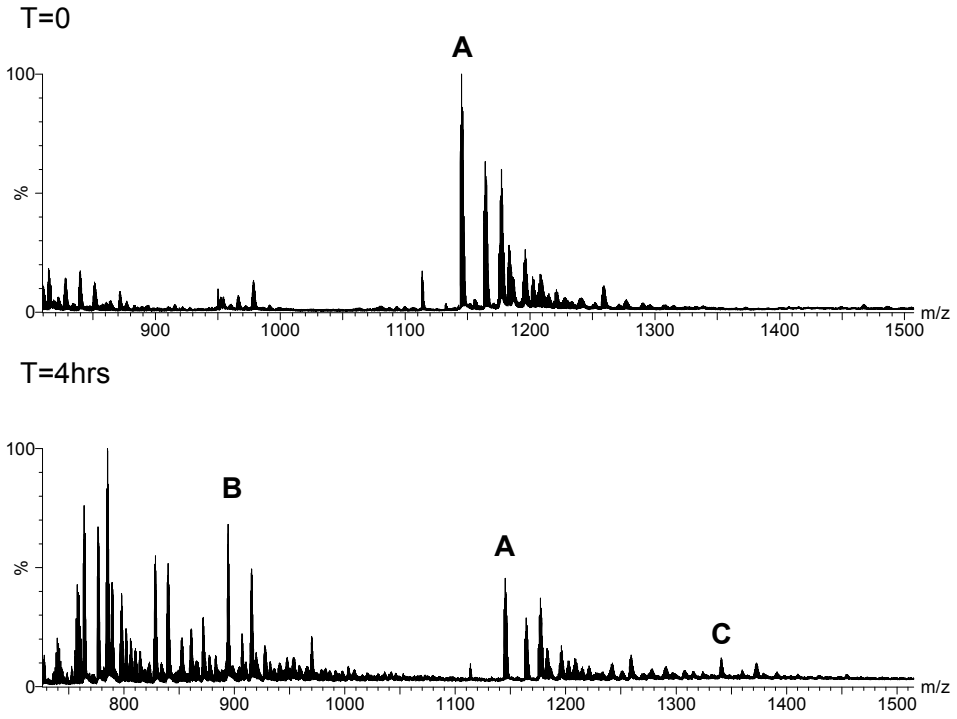

Figure B.3. ESI-MS of 1,1/tt with intact zinc finger at t = 0 and t = 4hrs. (A) in both plots is free intact zinc finger and (B) is a bidentate coordination of 1,1/tt with a cleavage of the –KG- amino acids from the intact peptide.

Switching to the 1,1/tt trans dinuclear compound reveals a slightly more reactive interaction in the fact that multiple ion peaks are present throughout the spectra. Figure B.3.A again shows the free 2+ zinc finger peptide at 1144 m/z. At the first initial time point t = 0, there does not appear to be any interaction between the two species. However, after 4 hrs of incubation, a substantial peak appears at 894 m/z corresponding to the 3+ charge state of the peptide/Pt interaction. However, upon closer inspection, the mass of an intact 1,1,/tt complex with the peptide would result in a higher mass to charge ratio. The corresponding mass of the 3+ ions reveals that a cleavage of the KG- amino acids from the intact peptide may have occurred. Platinum compounds have been shown to induce a hydrolytic cleavage of peptides, but generally at very

low pH, ~2. This reaction was down initially at pH= 7.0, but may have lowered due to the reaction.

While structural assignments are difficult to determine, an ms/ms of the 894 m/z peak Figure B.4., reveals fragmentation products relating to the y_1, y_2, y_3, y_4, $y_{8,}$ and y_{13}^{2+}. This would give a remaining peptide sequence of -CWKC- which is a probable binding site due to the thiols of the cysteine residues. The dominant fragment ions in the ms/ms spectra are those of the y-type ions. As such, no discernible fragment ions are identified for the N-terminus ions with or without platinum adducts.

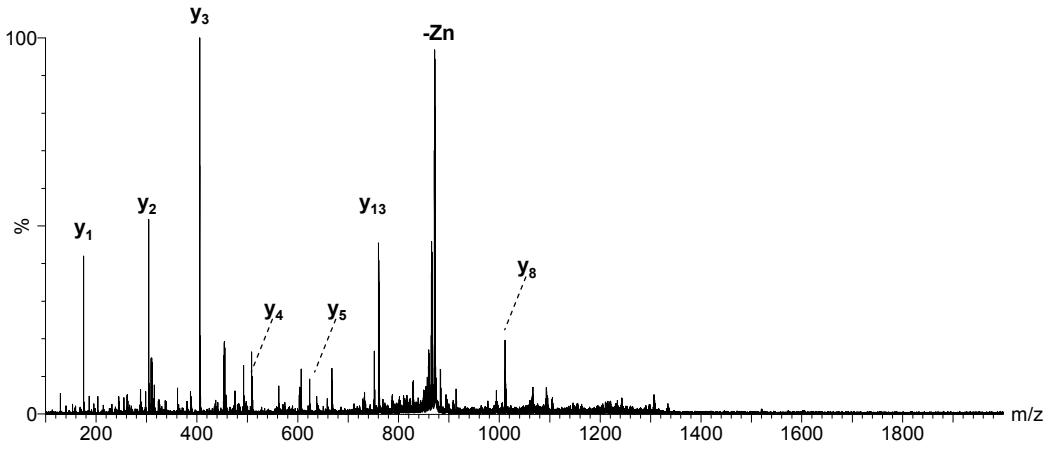

B.4. ESI-MS/MS of the 3+ 894m/z peak. Fragmentation products yield primarily y-type ions. The region of CWKC is absent from the spectra and may indicate the binding site of the 1,1/tt.

Under gentle conditions it was also noticed that an electrostatic association occurred during the early time points. The association of intact 1,1/tt with the zinc finger was identified as a 3+ peak at 978 m/z. This peak was confirmed to be an electrostatic association by performing ms/ms at increasing collisional energies. Figure B.5 shows the resultant ms/ms of the electrostatic association at peak 978 m/z. Peak A produced from the ms/ms represents the intact zinc finger at 1144 m/z and the peak labeled B represents the intact 1,1/tt compound at 644m/z. Also,

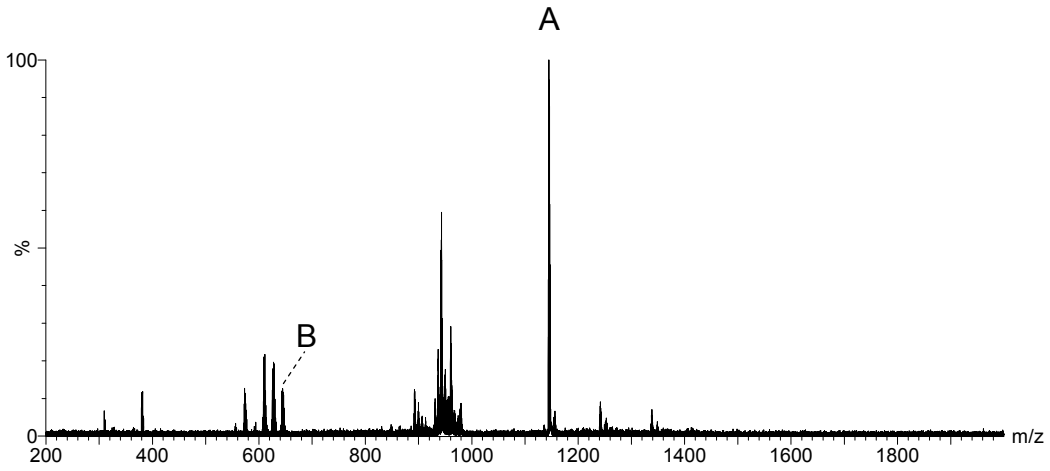

B.5 ESI-MS/MS of the electrostatic association of 1,1/tt or 1,1/cc with the intact zinc finger m/z = 978. (A) is the free intact zinc finger. (B) is the intact dinuclear platinum compound. Additional peaks left of (B) are the subsequent loss of the chloro ligands from the platinum moiety.

identifiable are the peaks corresponding to the sequential loss of the two Cl^- produced during the collision event, at 609 and 574 m/z respectively.

B.4. Conclusions

The reaction of dinuclear platinum compounds with a model zinc finger peptide reveal subtle differences in the cis and trans geometries. While a reaction scheme cannot be ascertained at the present time, what can be determined is that the cis geometry provides the most stable (in terms of few species) complex. The downside of the trans geometry is the reaction with sulfur groups often results in the trans effect breakdown of the compound. Not shown in the presented spectra, but evident throughout the 1,1/tt experiments, were the platinum fragments commonly associated with trans effect.

The reaction of these covalent dinuclear platinum compounds with zinc finger models is difficult to characterize due to the abundance of species present. Further work is necessary to accurately determine the species present in solution. Nevertheless, covalent modification of zinc finger complexes with platinum moieties results in loss of zinc ions and therefore may eventually find a niche in treatment as an antiviral therapeutic.

B.5. References

1. Anzellotti, A. I.; Liu, Q.; Bloemink, M. J.; Scarsdale, J. N.; Farrell, N., Targeting Retroviral Zn Finger-DNA Interactions: A Small-Molecule Approach Using the Electrophilic Nature of trans-Platinum-Nucleobase Compounds. *Chemistry & Biology* **2006,** 13, (5), 539-548.

2. Summers, M. F.; Henderson, L. E.; Chance, M. R.; Bess, J. W., Jr.; South, T. L.; Blake, P. R.; Sagi, I.; Perez-Alvarado, G.; Sowder, R. C., 3rd; Hare, D. R.; et al., Nucleocapsid zinc fingers detected in retroviruses: EXAFS studies of intact viruses and the solution-state structure of the nucleocapsid protein from HIV-1. *Protein Sci* **1992,** 1, (5), 563-74.

3. Anzellotti, A. I.; Liu, Q.; Bloemink, M. J.; Scarsdale, J. N.; Farrell, N., Targeting retroviral Zn finger-DNA interactions: a small-molecule approach using the electrophilic nature of trans-platinum-nucleobase compounds. *Chem Biol* **2006,** 13, (5), 539-48.

4. Bess, J. W., Jr.; Powell, P. J.; Issaq, H. J.; Schumack, L. J.; Grimes, M. K.; Henderson, L. E.; Arthur, L. O., Tightly bound zinc in human immunodeficiency virus type 1, human T-cell leukemia virus type I, and other retroviruses. *J Virol* **1992,** 66, (2), 840-7.

5. Gorelick, R. J.; Nigida, S. M., Jr.; Bess, J. W., Jr.; Arthur, L. O.; Henderson, L. E.; Rein, A., Noninfectious human immunodeficiency virus type 1 mutants deficient in genomic RNA. *J Virol* **1990,** 64, (7), 3207-11.

6. Mely, Y.; de Rocquigny, H.; Sorinas-Jimeno, M.; Keith, G.; Roques, B. P.; Marquet, R.; Gerard, D., Binding of the HIV-1 nucleocapsid protein to the primer tRNA(3Lys), in vitro, is essentially not specific. *J Biol Chem* **1995,** 270, (4), 1650-6.

7. Khan, R.; Giedroc, D. P., Nucleic acid binding properties of recombinant Zn2 HIV-1 nucleocapsid protein are modulated by COOH-terminal processing. *J Biol Chem* **1994,** 269, (36), 22538-46.

8. Herschlag, D., RNA chaperones and the RNA folding problem. *J Biol Chem* **1995,** 270, (36), 20871-4.

9. Musah, R. A., The HIV-1 nucleocapsid zinc finger protein as a target of antiretroviral therapy. *Curr Top Med Chem* **2004,** 4, (15), 1605-22.

10. de Paula, Q. A.; Mangrum, J. B.; Farrell, N. P., Zinc finger proteins as templates for metal ion exchange: Substitution effects on the C-finger of HIV nucleocapsid NCp7 using M(chelate) species (M=Pt, Pd, Au). *J Inorg Biochem* **2009,** 103, (10), 1347-54.

11. Harris, A. L.; Yang, X.; Hegmans, A.; Povirk, L.; Ryan, J. J.; Kelland, L.; Farrell, N. P., Synthesis, Characterization, and Cytotoxicity of a Novel Highly Charged Trinuclear Platinum Compound. Enhancement of Cellular Uptake with Charge. *Inorg. Chem.* **2005,** 44, (26), 9598-9600.

12. Qu, Y.; Harris, A.; Hegmans, A.; Petz, A.; Kabolizadeh, P.; Penazova, H.; Farrell, N., Synthesis and DNA conformational changes of non-covalent polynuclear platinum complexes. *Journal of Inorganic Biochemistry*

The Ninth International Symposium on Platinum Compounds in Cancer Chemotherapy **2004,** 98, (10), 1591-1598.

Curriculum Vitae

NAME	POSITION:TITLE
John B. Mangrum	Graduate Student Department of Chemistry Virginia Commonwealth University
Telephone 804.828.7487 (work) 804.432.1069 (mobile) Facsimile 804.827.8599 Electronic Mail jbmangrum@vcu.edu Citizenship United States	

EDUCATION/TRAINING

INSTITUTION AND LOCATION	DEGREE *(if applicable)*	MM/YY	FIELD OF STUDY
Longwood University, Farmville, VA	B.S.	05/2000	Chemistry & Biology
Virginia Commonwealth University, Richmond, VA	Ph.D.	05/2010	Chemistry

Dissertation Title: "*Electrospray Ionization Mass Spectrometry for the Characterization of Covalent and Noncovalent Polynuclear Platinum Compounds Interacting with Bio-molecules*"	Ph.D. Director Nicholas P. Farrell

A. Current Research Interests

My current research focuses on the use of mass spectrometry as a tool for characterization of novel polynuclear platinum compounds interacting with bio-molecules. Through the comparison of fragmentation data, I have been able to accurately determine the binding site location of a noncovalent polynuclear platinum compound associating with the phosphate backbone of DNA. Concurrently, I have examined the stabilization effects of a series of noncovalent polynuclear platinum compounds on duplex DNA. In addition to the research involving anticancer therapeutics, I also have a strong interest in the development and/or modification of new ionization methods. To aid in my research, I constructed a dual μ-electrospray ionization (ESI) source that enabled the accurate characterization of a platinum compounds covalent modifications to DNA.

B. Professional Experience

2005-2009 Interim Manager of the Mass Spectrometry Center for the Study of Biocomplexity, Virginia Commonwealth University, Richmond, VA. Responsibilities included operation and fiscal oversight of the facility, instrument service contract negotiations, and the running and maintenance of instrumentation. I also worked with method development and interpretation of data for facility users.

2003-2005 Graduate research assistant for the Mass Spectrometry Center for the Study of Biocomplexity. This position involved instrument maintenance, running samples, and data interpretation for facility users.

2000-2001 Graduate teaching assistant in the Department of Chemistry

C. Instrumentation Skills of Interest

Quadrupole Time of Flight	(QTOF-2, LCT)	Micromass/ Waters
Ion Trap	(LCQ-DECA-XP)	ThermoFinnigan
nanoLC	(Paradigm MS4)	Michrom
HPLC	(Waters 2795)	Waters
FTICR-MS	(4.7, 7, & 9.4T)	IonSpec/Varian
Ionization interfaces (ESI, nano-ESI, DESI)		
Vacuum Pump Systems		Edwards
Gel-Electrophoresis		
Knowledgeable of Microarray Technology		
Knowledgeable of Class 1000 Cleanroom Etiquette		
Microsoft and Apple Computing Systems		

D. Awards & Service

-Mass Spectrometry Resource for the Study of Biological Complexity (MSRBC) director search committee

-2010 Department of Chemistry Mary E. Kapp Distinguished Service Award

E. Peer-reviewed Publications (in reverse chronological order)

1. Determination of binding site location of polynuclear platinum complexes along the polyanionic phosphate backbone of DNA
   John B. Mangrum and Nicholas P. Farrell. Chemical Communications invited article *manuscript in preparation*

2. Influence of polynuclear platinum phosphate clamps on gas-phase DNA duplex stabilization
   John B. Mangrum and Nicholas P. Farrell. *Manuscript in preparation*

3. Reactions of palladium and gold complexes with zinc-thiolate chelates using electrospray mass spectrometry and X-ray diffraction: molecular identification of [Pd(bme-dach)], [Au(bme-dach]+ and [ZnCl(bme-dach)]2Pd
   Queite A. de Paula, Qin Liu, Elky Almaraz, Jason A. Denny, **John B. Mangrum**, Nattamai Bhuvanesh, Marcetta Y. Darensbourg and Nicholas P. Farrell, *Dalton Transactions*., **2009**, 10896-10903.

4. Zinc finger proteins as templates for metal ion exchange: Substitution effects on the C-finger of HIV nucleocapsid NCp7 using M(chelate) species (M=Pt, Pd, Au)
   de Paula, Queite A.; **Mangrum, John B**.; Farrell, Nicholas P. *Journal of Inorganic Biochemistry* **2009**, 103(10), 1347-1354.

5. Transferring the Concept of Multinuclearity to Ruthenium Complexes for Improvement of Anticancer Activity
   Mendoza-Ferri, Maria G.; Hartinger, Christian G.; Mendoza, Marco A.; Groessl, Michael; Egger, Alexander E.; Eichinger, Rene E.; **Mangrum, John B.**; Farrell, Nicholas P.; Maruszak, Magdalena; Bednarski, Patrick J.; et al *Journal of Medicinal Chemistry* **2009**, 52(4), 916-925.

6. Interaction of trivalent antimony with a CCHC zinc finger domain: potential relevance to the mechanism of action of antimonial drugs
   Demicheli, Cynthia; Frezard, Frederic; **Mangrum, John B**.; Farrell, Nicholas P. *Chemical Communications* (Cambridge, United Kingdom) **2008**, (39), 4828-4830.

7. New insights into the chemical structure and composition of the pentavalent antimonial drugs, meglumine antimonate and sodium stibogluconate
   Frezard, Frederic; Martins, Patricia S.; Barbosa, Millen C. M.; Pimenta, Adriano M. C.; Ferreira, Weverson A.; de Melo, Juliane E.; **Mangrum, John B.**; Demicheli, Cynthia
   Journal of Inorganic Biochemistry **2008**, 102(4), 656-665.

8. Pre-association of polynuclear platinum anticancer agents on a protein, human serum albumin. Implications for drug design Eva I. Montero, Brad T. Benedetti, **John B. Mangrum**, Michael J. Oehlsen, Yun Qu and Nicholas P. Farrell, *Dalton Transactions,* (43) **2007**, 4938-4942

9. Selective N1-Alkylation of 2′-Deoxyguanosine with a Quinolinyl Quinone Methide
   Qibing Zhou, Ting Xu, and **John B. Mangrum,** *Chemical Research in Toxicology*, **2007**, 20 (8), 1069–1074

10. Studies of the Interaction of Platinum Drugs with DNA Using Oligonucleotide Microarrays
    Anthony Guiseppi-Elie**,** Scott Taylor, Louise Lingerfelt, Chris Nixon, Ryan Georgiana, Joy Kim, Stephanie Smith, **Brad Mangrum** and Nicholas Farrell, *Macromolecular Symposia* **2006** 235(1), 115-120

11. Complexation of Gas-Phase Metal Ions with Furan: Experimental and Quantum Chemical Binding Energies *Grimm, R.L.; Mangrum, J.B.; Dunbar, R.C., Journal of Physical Chemistry A. 2004; 108 (49); 10897-10905*

12. Solution composition and thermal denaturation for the production of single-stranded PCR amplicons: piperidine-induced destabilization of the DNA duplex?
    John B. Mangrum, Jason W. Flora and David C. Muddiman, *Journal of the American Society for Mass Spectrometry*, 13(3); **2002**, 232-240

F. Scientific Conference Presentations(in reverse chronological order)

2007: "DNA Stabilization by Polynuclear Platinum Phosphate Clamps"
John B. Mangrum and Nicholas P. Farrell
American Society for Mass Spectrometry, Indianapolis, Indiana.

2007: "Use of a QCM to Monitor the Interaction of Multinuclear Platinum Complexes to Biologically Relevant Molecules"
Shuford, Christopher M; Rhoten, Melissa C.; Mangrum, John B. and Farrell, Nicholas P. American Chemical Society National Meeting, Chicago, Illinois.

2006: "Real-time Monitoring of Multinuclear Platinum Drug Binding to Electrode-Immobilized DNA Using a Quartz Crystal Microbalance"
Shuford, Christopher M; Rhoten, Melissa C.; Mangrum, John B. and Farrell, Nicholas P. American Chemical Society National Meeting, Atlanta, Georgia.

2005: "Investigation of Non-covalent Complexation Between Biomolecules and Polynuclear Platinum Drugs: A Study by ESI Ion-Trap Mass Spectrometry"
John B. Mangrum and Nicholas P. Farrell
International Conference on Biological Inorganic Chemistry, Ann Arbor, Michigan.

2004: "Shining a High Resolving Power Spin on Biological Macromolecules"
Muddiman, David C.; Null, Allison, P.; Gordon, Eric, F.; Flora, Jason, W.;Nepomuceno, Angelito, I.; Mangrum, John, B.; Frahm, Jennifer, L.; Hawkridge, Adam, M.; Johnson, Kenneth, L.; Mason, Christopher, J.; Bergen, H. Robert, III; Hannis, James, C.
American Chemical Society National Meeting, Philadelphia, Pennsylvania.

2004: "Interactions of High Affinity Polynuclear Platinum Complexes with DNA Investigated by Oligonucleotide Microarrays and Quartz Crystal Microbalance" John B. Mangrum, Anthony Guiseppi-Elie, and Nicholas P. Farrell
21st Annual Daniel T. Watts Research Symposium, Richmond, Virginia.

2001: "Preparation of Single-Stranded PCR Amplicons by Physical and Enzymatic Methods for Determination by ESI-FT-ICR-MS"
John B. Mangrum, A.P. Null, J.W. Flora, and D.C. Muddiman
American Society for Mass Spectrometry, Chicago, Illinois.

G. Patents

β-O4 and β-O5 Trimer and Tetramers as Anti-coagulation and Anti-inflammation Agents.
UR Desai, BL Henry, A Liang, J Thakkar, **JB Mangrum**, I Torres Filho, BD Spiess, B Saluja, M Sakagami
International patent application filed on August 8, 2009 with the USPTO

H. Professional Memberships

American Society for Mass Spectrometry (ASMS)

I. References

Nicholas P. Farrell, Ph.D.
Professor
Department of Chemistry
Virginia Commonwealth University
1001 West Main St.
Richmond, VA 23284
Phone: (804) 828-6320
npfarrell@vcu.edu

Kristina T. Nelson, Ph.D.
Director of Mass Spectrometry Facility
Department of Chemistry
Virginia Commonwealth University
1001 West Main St.
Richmond, VA 23284
Phone: (804) 828- 7804
ktnelson@vcu.edu

David C. Muddiman, Ph.D.
Professor
Department of Chemistry
North Carolina State University
208 Dabney Hall
2620 Yarbrough Drive
Raleigh, NC 27695
Phone: (919) 513-0084
DavidMuddiman@ncsu.edu